International Journal of Modern Physics B, Vol. 6, Nos. 9 & 10 (1992) 1863–1884
© World Scientific Publishing Company

NUMBER-PHASE SQUEEZED STATES AND PHOTON FRACTIONING

G. M. D'ARIANO
Dipartimento di Fisica 'Alessandro Volta', Università di Pavia, via Bassi 6, I-27100 Pavia, Italy

Received 12 January 1992

The number-phase squeezing mechanisms related to the multiphoton and photon-fractioning procedures are analyzed. The main ingredients in these approaches are nonlinear multimode realizations of group-theoretical states and nonunitary subdynamics of the field modes. The states which are squeezed in the number of photons are suited to optical communications in local area networks; the states squeezed in the phase of the field optimize high-sensitive interferometry.

Corresponding to the different kinds of squeezing and to the pertaining group-theoretical states one has different types of amplifying devices with the same dynamical group of the states. In particular, two recently proposed devices – the photon-number amplifier (PNA) and the photon-number duplicator (PND) – attain both the multiphoton and photon-fractioning transformations. The PNA amplifies the field without degrading the direct-detection signal-to-noise ratio and thus can be used to produce number-squeezed states; the PND provides two copies of the same input number-state and, therefore, can connect two-mode states with one-mode states. Both the PNA and PND allow the realization of virtually lossless optical taps, which are essential in designing highly transparent local area networks. The PND can also be used in series with a conventional phase-insensitive amplifier to produce phase-squeezed states.

1. Introduction

The statistical description of optical systems is ultimately a quantum-mechanical one: it is specified by the quantum state of the field and the quantum measurement performed on it. In all existing optical applications the available quantum states are coherent states (CS) or random-phase mixtures of CS: these are obtained from conventional laser sources and light-emitting diodes. The detection schemes are either the direct detection or the homodyne and heterodyne detections: they correspond to the quantum measurement of the number of photons $\hat{n} = a^\dagger a$, single field quadrature $\hat{a}_\phi$, and both field quadratures $(\hat{a}_\phi, \hat{a}_{\phi+\pi/2})$, respectively[1] (the quadrature of the field at the locked-in phase ϕ is defined as $\hat{a}_\phi = (e^{i\phi}a + e^{-i\phi}a^\dagger)/2$). In these conventional systems a quantum noise at optical wavelengths is quantitatively equivalent to black-body fluctuations of thousands of kelvin degrees: this leads to a serious need for control over quantum statistics when designing highly-sensitive or very-transparent optical devices, as in all such critical situations encountered in

interferometric gravitational-waves detection[2] or in quantum-optical communications and computers.[3]

Since the early 1970's considerable effort has been spent on the problem of reducing the quantum noise of the CS. In a pictorial way, this quantum noise reduction is commonly referred to as 'squeezing the state' (extensive reviews are given in Refs. 4–6).

There are different kinds of squeezing, depending on the application and on the detection scheme. Reduction of quantum noise in the detected observable $\hat{O}_1$ affects the statistics of any noncommuting observable $\hat{O}_2$ according to the Heisenberg uncertainty principle

$$\langle \Delta\hat{O}_1^2 \rangle \langle \Delta\hat{O}_2^2 \rangle \geq \frac{1}{4} \langle \hat{O}_3 \rangle^2 \ , \tag{1.1}$$

where $[\hat{O}_1, \hat{O}_2] = i\hat{O}_3$ and $\Delta\hat{O} = \hat{O} - \langle \hat{O} \rangle$. The technique of squeezing needs to maintaining the detected field in a minimum-uncertainty state, while simultaneously reducing $\langle \Delta\hat{O}_1^2 \rangle$ and increasing $\langle \Delta\hat{O}_2^2 \rangle$ by the same factor. The latter is generally written in terms of the squeezing parameter ρ as follows

$$\langle \Delta\hat{O}_{1,2}^2 \rangle \to e^{\mp 2\rho} \langle \Delta\hat{O}_{1,2}^2 \rangle \ . \tag{1.2}$$

Highly-sensitive interferometry and optical communications are the two major classes of quantum-optical applications. Interferometric detection essentially is equivalent to the measurement of a field phase-shift, which in turn is obtained through homodyne or heterodyne detection. Optical communications, on the other hand, are usually performed in the direct-detection mode, but also homodyne or heterodyne schemes have been recently suggested.

Depending on the detection mode, one can use different kinds of squeezing to improve sensitivity and signal-to-noise ratio (SNR). Quadrature-squeezed states (QSS), for example, are suited to homodyning when they are squeezed in the detected quadrature $\hat{a}_\phi$ and noisy in the conjugated one $\hat{a}_{\phi+\pi/2}$. In the same fashion the phase-squeezed states (PSS) — which exhibit improved statistics in the phase and wide distributions in the photon number — optimize interferometry, whereas the number-squeezed states (NSS) — which are squeezed in the number and spread in the phase — improve optical communications. It is worth noticing that the phase of the field actually does not correspond to a self-adjoint operator, and the evaluation of the pertinent statistics is addressed in the proper framework of quantum estimation theory.[7]

Originally the study of the squeezed states arose in the context of quantum communications and led to the investigation of two-photon coherent states[8,9] — the aforementioned QSS. Once the possible applications had been recognized, attention was focused on the problem of characterizing the optimum quantum measurements for various performance criteria and fixed quantum states:[10] this led to explore also the NSS.[11–13]

Both the QSS and NSS can lead to great improvements in optical communications, both enhancing the SNR at fixed power and attaining a better channel efficiency. In particular, nearly-number states make the channel noise-free in the ideal limit, and, at the same time, provide a suitable physical way of coding information. Originally it was emphasized that these states would also attain the ultimate channel capacity of the field (namely the channel capacity constrained only by power and bandwidth and not by any modulation restriction): however, this ultimate value does not differ significantly from that attainable through CS.[15]

One of the major limitations of squeezed states in optical communications is represented by the losses in the network, as they gradually destroy any kind of squeezing. One should distinguish between two kinds of environments, depending on the location of the relevant losses in the network: in the local area network (LAN) environment the relevant losses are located at the transceivers; in the long haul communications the main losses are due to the fibers. In the LAN environment number-states would make the method of state-duplication practicable for attaining virtually lossless transceivers (*optical taps*), without the need of amplifying the power down the line.[16] The choice of number-states is dictated by the fact that state-duplication is possible only for orthogonal states,[17] whereas neither the CS nor the QSS are orthogonal. Thus a NNS-operating LAN can be made more transparent for a larger number of users than a CS-operating one. In the long haul communications, on the other hand, the fibers' losses gradually destroy squeezing down the line, making the QSS and NSS less attractive. In this case one can choose between two alternative solutions: the first is to use soliton pulses which are continuously amplified by a pump light simultaneously transmitted through the fiber;[18] the second is to create special fibers with distributive amplification gain which matches the kind of squeezing of the states carrying information:[16] this notion of squeezing-matching amplifier will be reconsidered after in more detail.

The phase-squeezed states (PSS) complete the panorama of different types of squeezing. In recent years improvements of the optimized squeezed-state interferometry have been suggested[19] which utilize special kinds of PSS instead of the originally proposed QSS[20]. The possibility of further enhancing interferometric sensitivity is very attractive, in view of possible applications to gravitational-wave antennas[2] and laser gyroscopes;[22] however, no viable physical method of producing PSS has been proposed yet. In this paper a possible scheme for obtaining some particular PSS is illustrated which is based on number state-duplication.

In order to design a dynamical model attaining the squeezing transformation (1.2), the evolution of all the moments of the conjugated variables must be specified. The simplest moment transformation generalizing (1.2) is the homogeneous rescaling of the probability distributions

$$\langle \hat{O}_{1,2}^n \rangle \to e^{\mp n\rho} \langle \hat{O}_{1,2}^n \rangle \ . \tag{1.3}$$

Equation (1.3) represents an idealized case of squeezing which corresponds to the operator-scaling in the Heisenberg picture

$$\hat{O}_{1,2} \to e^{\mp\rho}\hat{O}_{1,2} \ . \tag{1.4}$$

In the form of Eq. (1.4) the squeezing transformation is viewed as a kind of ideal quantum amplification which preserves the SNR of both $\hat{O}_1$ and $\hat{O}_2$ and leaves the uncertainty product unchanged. One should notice that the transformation (1.4) also affects the signal $\langle\hat{O}_1\rangle$ itself: as a consequence, a squeezed state which carries a detectable signal is produced by either deamplifying a high-signal CS or deamplifying the zero-signal CS — namely squeezing the vacuum — and then coding the signal on the output state.

The above modeling strictly holds true when a pair of self-adjoint operators is concerned, the simplest situation being that of c-number commutator $[\hat{O}_1, \hat{O}_2] = ic$. In such case the evolutions (1.4) are unitary and are attained by the Hamiltonian

$$\hat{H} = k(\hat{O}_1\hat{O}_2 + \hat{O}_2\hat{O}_1) \ , \tag{1.5}$$

which, therefore, models the quantum amplifier which matches the squeezing of $\hat{O}_1$ and $\hat{O}_2$. The squeezing parameter is continuous and linearly increases with time. The case of quadrature-squeezing fits exactly into the present framework: the corresponding amplifier is the socalled *phase-sensitive amplifier* (PSA), which ideally rescales the quadratures $\hat{a}_\phi$ and $\hat{a}_{\phi+\pi/2}$.

The case of the number-phase pair, extensively analyzed in this paper, is more involved than the previous one, due to a variety of reasons. The first issue to emphasize is that the number operator does not have a conjugated selfadjoint operator, whereas classically it corresponds to the amplitude of the field and is conjugated to the phase. As already mentioned, the phase measurement can be analyzed in the framework of quantum estimation theory,[7] where the statistics are represented by positive-operator measures (POM) on the Hilbert space, extending the conventional description by selfadjoint operators: in this approach, the scaling transformation (1.4) is considered as acting on such POM. The second issue is related to the integer-valued nature of $\hat{n}$, which breaks the amplification/deamplification symmetry and allows exact amplification only for integer gains. The transformation

$$\hat{n} \to G\hat{n} \tag{1.6}$$

for integer G is not unitary, but only isometric: a unitary transformation can be constructed upon enlarging the Hilbert space and introducing an additional *idler* mode, similar to that involved in the conventional *phase-insensitive amplifiers* (PIA). The transformation (1.6) is thus recovered by tracing out the idler degrees of freedom, leading to a nonunitary dynamical map of the form of the completely positive maps (CP maps) of statistical mechanics.[23,24] The 'inverse' transformation of (1.6) turns out to be the approximated scaling

$$\hat{n} \to [G\hat{n}] \ . \tag{1.7}$$

Both (1.6) and (1.7) are CP maps of the same unitary evolution on the enlarged Hilbert space, and both attain the required amplification of the phase POM.

The ideal amplifier which matches the number-phase squeezing, attaining the transformations (1.6, 1.7), is the socalled *photon-number amplifier* (PNA), a novel device recently proposed by Yuen.[16,25–27] Although the PNA is well suited to produce NSS at the output, it is not the proper device to attain PSS. In fact, due to the 2π-periodicity the probability rescaling leaves the peak values unchanged, namely there is no improvement of phase sensitivity. A more effective scheme for achieving highly peaked phase distributions is proposed in Sec. 6.1 of this paper: it uses an ideal *photon-number duplicator* (PND) in series with a conventional PIA. The PND[16,25–27] is a device analogous to a gain-two PNA which, instead of amplifying the number of photons, provides two copies of the same input number-state, thus connecting two-mode with one-mode states. The PIA-PND series is effective in building PSS, because these states have very flat number distributions similar to those of the twin beams which are obtained at the output of a PIA with vacuum inputs.

Apart from the production of the different kinds of squeezed states, the squeezing-matching amplifier is a reference ideal device in many actual applications. For example, as already mentioned, the PSA and the PNA are key devices to obtain virtually lossless optical taps (in the homodyne and direct-detection modes respectively), whereas the PND itself can be used to attain taps superior to the PNA taps in avoiding the need for amplification down the line.

The intimate relationship between ideal amplifiers and squeezed states lies in their respective dynamical algebras, amplification and squeezing being essentially the Heisenberg and the Schrödinger picture of the same evolution. The former is the point of view of Refs. 28–31, where the dynamical symmetries of the PIA, PSA and beam splitter (BS) are analyzed in detail (the BS is also a useful schematization for linear losses); the dynamical groups are $SU(1,1)$ for the amplifier and $SU(2)$ for the loss. On the other hand, regarding the second point of view, several studies on the squeezing properties of group-theoretical states (GTS) have been performed in Refs. 32–37. The origin of this set of papers — which are partly reviewed in the present one — was the puzzling paper[38] by Fisher, Nieto and Sandberg. In it the authors, trying to generalize the customary two-photon squeezed states to multiphoton states by the simplest possible ansatz, run into unexpected difficulties connected with the non-analyticity of the vacuum. Even though such difficulties could be partly overcome from the computational point of view (Refs. 39, 40, the problem remains a deep one. A *non-naïve* way out of it was found in Refs. 32–37 on the basis of the observation that the conventional two-photon squeezed states are GTS of $SU(1,1)$, whereas naive multiphoton generalizations leads to infinite-dimensional algebras whose GTS cannot be defined in the usual sense.

The two main tools realizing the above program are the Brandt-Greenberg[41] multiphoton creators and annihilators, and the Holstein-Primakoff[42] realizations of Lie algebras. The new set of multiphoton squeezed states thus constructed has

several interesting features: besides naturally matching the dynamical algebras of the various amplifying devices, they achieve better number-phase sensitivity than the conventional squeezed states. Finally they lead to the notion, discussed in this paper with detail, of *photon fractioning*, which is the prototype CP map of the number deamplification (1.7).

The photon fractioning procedure was originally introduced in Ref. 43 in the form of inverse of the multiphoton transformation. In such a paper the fractional-photon modes were defined in terms of expectation values, claiming that, despite such modes do not really exist, they could describe physical experiments involving integral numbers of photons. In Ref. 44 physical mixed states were constructed which exhibit exactly the same probability distribution of the fractional modes. Once the number-phase squeezing features of these novel fractional-states had been recognized in Ref. 45, the fractioning CP map was derived in Refs. 46, 47. Finally in Refs. 48, 49 the multiboson and fractional boson transformations were related to the ideal photon number amplification.

In this paper the above concepts are reviewed in a new unifying framework based on a new class of nonlinear multimode realizations of Lie algebras and on the aforementioned CP-maps technique. The abstract algebraic transformations are revisited in terms of quantum amplification, showing the way of obtaining the GTS at the output of ideal amplifiers. New numerical results and analytical evaluations of the GTS phase-number statistics are presented in the context of quantum estimation theory. It is shown that the $SU(1,1)$ states are suited to describe phase-squeezing, leading to a novel scheme for enhancing the phase-sensitivity of the quantum states. On the other hand, it is shown how the multiphoton and photon-fractioning procedures constitute the natural idealizations of the number-amplification mechanisms, and how the latter could be approximated by a real device.

The paper is organized as follows. In Sec. 2, after a short review of the Dirac's[50,51] and Susskind-Glogower[52] customary approaches, the general lines of the quantum estimation theory[7,53] of the phase are recalled.

In Sec. 3 the CS and QSS are reviewed and the construction of the GTS is given. The novel Lie algebra realization is presented which leads to general multimode GTS. The one-mode and two-mode cases are analyzed in detail as regards their phase-number features. The multiboson and fractional-boson states are illustrated in the concluding subsections, with a general analysis of the properties of these states.

Section 4 is an overview on the customary quantum amplifiers and linear losses, with a brief illustration of the notion of squeezing-matching amplifier applied to the achievement of lossless optical taps. It is shown how the two-mode GTS can be obtained at the output of the quantum linear device.

Section 5 reviews the main results presented in Refs. 48, 49, studying the photon number-amplification mechanism in the ideal case. It is shown how the search for unitary evolutions leads to consider the idler mode, and how the multiphoton and fractional photon states of Secs. 3.6–3.7 can be recovered at the output of the

amplifier. In the last subsection the Hamiltonians of the ideal device is derived and compared with those of realistic systems.

In Sec. 6 the photon-number duplicator (PND) is analyzed, reviewing the main results of Ref. 49. The duplicating CP map is derived, along with its unitary extension and the corresponding Hamiltonian. In the last subsection I illustrate how the PND can be used in series with a PIA to obtain the PSS of Sec. 3.4.

The Appendices report some asymptotic evaluations involving nonstandard techniques.

2. The Optical Phase

In the classical theory of light waves the complex amplitude is usually written as a product of a real amplitude and a phase factor. The single-mode (single-polarized) electric field is written in the form

$$E(t) = E_0 \exp\left(-i\omega t + i\mathbf{h}\cdot\mathbf{r} + \mathbf{i}\phi_\mathbf{0}\right) , \tag{2.1}$$

$\mathbf{h}$ and ω being the wave vector and the angular frequency of the mode. The quantum-mechanical field corresponding to (2.1) is

$$\hat{E}(t) = i(\hbar\omega/2\varepsilon_0 V)^{1/2} a \exp(-i\omega t + i\mathbf{h}\cdot\mathbf{r}) , \tag{2.2}$$

where a is the annihilator of the mode. The operator analogue of the phase-amplitude factorization of Eq. (2.1) corresponds to rewrite the Bose operator a as the product of amplitude $\hat{A}$ and phase $e^{i\hat{\Phi}}$ operators

$$a = \hat{A} \exp(i\hat{\Phi}) , \tag{2.3}$$

Eq. (2.3) with $\hat{A} = (a^\dagger a + 1)^{1/2}$ was the original definition of the phase operator according to Dirac,[50] who presupposed the canonical commutation relations

$$[\hat{n}, \hat{\Phi}] = i \tag{2.4}$$

in agreement with the classical Poisson brackets. However, the von Neumann uniqueness theorem (of the irreducible representations of the canonical commutation relations) implies that the commutation (2.4) cannot be realized: more precisely, it can be proved that the polar decomposition (2.3) cannot be obtained with $\hat{A}$ and $\hat{\Phi}$ both self-adjoint operators.[11,52] The last assertions pose the problem for the quantum representation of the phase.

Recently, Pegg and Barnett[54,55] constructed a phase operator on a finite dimensional space and showed that it obeys a certain new commutation relation with the number operator. According to their approach the correct statistical prediction is given only after the limit process making the dimension infinity, although they failed to find the operator after the limit process. On the other hand, another approach has been established in quantum estimation theory,[7,53] a framework where

the most general optimization problems of quantum measurements can be analyzed. The statistics of measurements is represented by positive-operator-valued measures (POM) on a Hilbert space which extends the conventional description by self-adjoint operators. In this approach, the optimum POM for the estimation of the phase was found by Helstrom[56] and a mathematically rigorous development of this approach is given by Holevo.[53] Ozawa[57] has shown that the statistics of the phase obtained by Pegg and Barnett coincide with those represented by the optimum POM, whereas the limit of their exponential phase operator coincides with that of Susskind-Glogower.[52]

Here in the following, after a short review of the Dirac's and Susskind-Glogower's approaches (more often adopted in the literature), I recall the main lines of the quantum estimation theory of the phase, adopting the general framework of Ref. 7.

2.1. *Phase operators*

The Dirac phase operator $\hat{\Phi}_D$ is defined through the relation

$$\hat{e}^{\pm} = e^{\mp i\hat{\Phi}_D} , \tag{2.5}$$

where $\hat{e}^{\pm}$ are the shift operators

$$\hat{e}^{-} = (aa^{\dagger})^{-1/2}a , \quad \hat{e}^{+} = a^{\dagger}(aa^{\dagger})^{-1/2} . \tag{2.6}$$

The phase $\hat{\Phi}_D$ is not self-adjoint, because $\hat{e}^{\pm}$ are not unitary, as shown by

$$\hat{e}^{+}\hat{e}^{-} = 1 - |0\rangle\langle 0| , \tag{2.7}$$

even though

$$\hat{e}^{-}\hat{e}^{+} = 1 . \tag{2.8}$$

Instead of using $\hat{\Phi}_D$, a standard compromise in the literature is to work with the self-adjoint Susskind-Glogower[52] (SG) *sine* and *cosine* operators $\hat{s}$ and $\hat{c}$

$$\hat{s} = \frac{1}{2i}(\hat{e}^{-} - \hat{e}^{+}) , \qquad \hat{c} = \frac{1}{2}(\hat{e}^{-} + \hat{e}^{+}) . \tag{2.9}$$

Notice that, despite the defining relations (2.5) and (2.9), $\hat{s}$ and $\hat{c}$ cannot correspond to actual sine and cosine functions of $\hat{\Phi}_D$, because they neither commute nor provide correct n-linear functions (for example: $\hat{s}^n \neq \sin^n \hat{\Phi}_D$). However, as the commutator

$$[\hat{s}, \hat{c}] = -\frac{i}{2}|0\rangle\langle 0| \tag{2.10}$$

effectively vanishes for states with a negligible vacuum component, $\hat{s}$ and $\hat{c}$ give an approximate description of the optical phase in the high-energy limit. In this case $\hat{e}^{\pm}$ are approximately unitary and $\hat{\Phi}_D$ can be treated as self-adjoint. For states with small phase uncertainties $\langle \Delta\hat{\Phi}_D \rangle \ll 1$ and zero average $\langle \hat{\Phi}_D \rangle = 0$ the sine and cosine operators can be approximated as

$$\hat{s} \sim \hat{\Phi}_D , \quad \hat{c} \sim 1 . \tag{2.11}$$

Accordingly, one has the effective commutation relation

$$[\hat{n}, \hat{\Phi}_D] \sim [\hat{n}, \hat{s}] = i\hat{c} \sim i \ , \tag{2.12}$$

which corresponds to the Heisenberg relation

$$\langle \Delta\hat{n}^2 \rangle \langle \Delta\hat{\Phi}_D^2 \rangle \gtrsim \frac{1}{4} \ . \tag{2.13}$$

In conclusion, the Dirac approach can be usefully adopted in the high-energy limit, where the phase operator $\hat{\Phi}_D$ can be considered effectively self-adjoint and conjugated with the number operator.

The possibility to assign a 'phase' ϕ to a quantum state is related to the existence of simultaneous eigenstates of the phase operators (2.9). There are indeed certain special eigenstates of $\hat{e}^-$ which satisfy the above requirement. The following states

$$|\zeta\rangle = \sum_{n=0}^{\infty} \zeta^n |n\rangle \ , \quad |\zeta| < 1 \ , \tag{2.14}$$

are eigenstates of $\hat{e}^-$ and lead to the expectation values

$$\begin{aligned} \langle \hat{s} \rangle = |\zeta| \sin\phi \ , \quad \langle \hat{c} \rangle = |\zeta| \cos\phi \ , \quad \phi = \arg(\zeta) \ , \\ \langle \Delta\hat{s}^2 \rangle = \langle \Delta\hat{c}^2 \rangle = \frac{1}{2}(1 - |\zeta|^2) \ . \end{aligned} \tag{2.15}$$

From (2.14–2.15) it follows that, in the limit $|\zeta| \to 1$, the non-normalizable states[52]

$$|e^{i\phi}\rangle \doteq \sum_{n=0}^{\infty} e^{in\phi} |n\rangle \tag{2.16}$$

are simultaneous eigenstates of $\hat{s}$ and $\hat{c}$, with eigenvalues $\sin\phi$ and $\cos\phi$, respectively: in this sense they correspond to a definite 'phase' ϕ. In the next subsection we will see that the states (2.16) also provide the optimum POM for the quantum estimation of the phase.

2.2. *Quantum estimation of the phase*

A phase shift ϕ_0 of the form given in Eq. (2.1) is described by the Heisenberg free evolution of the field

$$\hat{U}^\dagger a \hat{U} = a e^{i\phi_0} \ , \tag{2.17}$$

where

$$\hat{U} = e^{i\phi_0 \hat{n}} \ . \tag{2.18}$$

Physically, ϕ_0 is related to a change in the optical path-length. The quantum state of the field undergoes the Schrödinger evolution

$$|\psi\rangle_{\rm out} = e^{i\phi_0 \hat{n}} |\psi\rangle_{\rm in} \ . \tag{2.19}$$

The problem of measuring ϕ_0 is now posed in the following abstract terms:[19]

> make an estimate of the value ϕ_0 of the phase shift ϕ by means of an appropriate quantum measurement on the a mode, and knowing the input state $|\psi\rangle_{\text{in}}$.

As the phase shift ϕ does not correspond to any self-adjoint operator, the problem is addressed in the more general framework of quantum estimation theory.[7]

Quantum estimation theory seeks the *best strategy* for estimating the value x_0 of a parameter x of the density operator $\hat{\rho}_x$ in a quantum-mechanical system. The observational strategies for estimating x_0 are expressed as *positive operator-valued measures* or *probability-operator measures* (POM) on the parameter space Ξ. A POM is a nonnegative-definite self-adjoint operator $d\hat{X}(x)$ associated with each point $x \in \Xi$, providing the resolution of the identity

$$\int_{\Xi} d\hat{X}(x) = 1 \ . \tag{2.20}$$

Whatever instrument is used (or calculation is performed) in a strategy, the resulting estimate x is a random variable. The conditional probability that x lies in a particular region $\Delta \subset \Xi$ when the true value is x_0, is written in the following way

$$P(x \in \Delta | x_0) = \text{Tr}\left[\hat{\rho}_{x_0} \int_{\Delta} d\hat{X}(x)\right] \ . \tag{2.21}$$

From Eq. (2.21) one sees that POM's generalize the customary projector-valued measures associated to the quantum observables. The POM's on the state space $\mathcal{H}$ include not only the observables on $\mathcal{H}$, but also measurements that are not observables on $\mathcal{H}$. On the other hand, there is no conflict with the assertion that only observables can be measured, as the Naimark theorem assures that every POM can be extended to a projection-valued measure on a larger Hilbert space[57] (which represents the original system interacting with an appropriate apparatus). For nonobservable POM's Eq.(2.21) provides the self-adjoint operators

$$\hat{X} = \int_{\Xi} x d\hat{X}(x) \ , \tag{2.22}$$

and, more generally,

$$\hat{f}_X = \int_{\Xi} f(x) d\hat{X}(x) \ , \tag{2.23}$$

where the notation $\hat{f}_X$ in Eq. (2.23) is used to account for the inequality

$$\hat{f}_X \neq f(\hat{X}) \ . \tag{2.24}$$

The expectation values are evaluated in the usual way

$$\langle \hat{f}_X \rangle = \text{Tr}\left[\hat{\rho}\hat{f}_X\right] \ , \tag{2.25}$$

$\hat{\rho}$ being the density matrix of the state.

Once the observational strategies are represented as POM's, the following step is to find the *optimum* POM corresponding to the best strategy for estimating the parameter x. This is done using the ***maximum-likelihood*** (ML) performance criterion. The ML estimate x_{ML} of x is the value which maximize the likelihood of getting the observed datum

$$x_{\mathrm{ML}}(x) = \arg \max_{y \in \Xi} p(x|y) \ . \tag{2.26}$$

The conditional probability density $p(x|y)$ is defined according to Eq. (2.21) as

$$p(x|y)dx = \mathrm{Tr}[\hat{\rho}_y d\hat{X}(x)] \ . \tag{2.27}$$

Restricting attention to POM's satisfying

$$x_{\mathrm{ML}} = x \ , \tag{2.28}$$

the estimate is optimized over the POM's by maximizing the peak likelihood $p(x|x)$, or, equivalently, by minimizing the reciprocal peak likelihood (RPL) δx

$$\delta x \doteq 1/p(x|x) \ . \tag{2.29}$$

For a uniform distribution δx is the width of the probability density, whereas for a Gaussian distribution it is proportional to the rms error.

In the case of the phase-shift estimation the parameter $x \equiv \phi$ can be confined to a 2π-interval, say, for example, $-\pi < \phi \leq \pi$. The class of POM's $d\hat{\Phi}(\phi)$ is provided by the self-adjoint resolutions of the identity

$$\int_{-\pi}^{\pi} d\hat{\Phi}(\phi) = 1 \tag{2.30}$$

on the Fock space of the single boson mode a. The conditional probability density for obtaining a phase value ϕ when the 'true value' is ϕ_0 reads

$$p(\phi|\phi_0)d\phi = {}_{\mathrm{out}}\langle\psi|d\hat{\Phi}(\phi)|\psi\rangle_{\mathrm{out}} \ , \tag{2.31}$$

where $|\psi\rangle_{\mathrm{out}}$ depends on ϕ_0 through the relation (2.19). For a general input state of the form

$$|\psi\rangle_{\mathrm{in}} = \sum_{n=0}^{\infty} |\psi_n| e^{i\chi_n} |n\rangle \ , \tag{2.32}$$

the optimum POM is[7,53,56]

$$d\hat{\Phi}(\phi) = |e^{i\phi}, \psi\rangle\langle e^{i\phi}, \psi| \frac{d\phi}{2\pi} \ , \tag{2.33}$$

where

$$|e^{i\phi}, \psi\rangle = \sum_{n=0}^{\infty} e^{in\phi + i\chi_n} |n\rangle \ . \tag{2.34}$$

As the probability density in (2.31) does not depend on the phases χ_n, one can assume that all the χ_n are zero, without loss of generality. The state (2.34) rewrites simply as follows

$$|e^{i\phi}, \psi\rangle \equiv |e^{i\phi}\rangle = \sum_{n=0}^{\infty} e^{in\phi}|n\rangle \,, \tag{2.35}$$

and coincides with the SG state in Eq. (2.16). The optimum POM

$$d\hat{\Phi}(\phi) = |e^{i\phi}\rangle\langle e^{i\phi}|\frac{d\phi}{2\pi} \tag{2.36}$$

provides operator functions of ϕ which agree with the following SG operators

$$\begin{aligned} &(\hat{e}^-)^r \equiv \int_{-\pi}^{\pi} e^{ir\phi} d\hat{\Phi}(\phi) \,, \quad r \geq 0 \,, \\ &\hat{s} \equiv \int_{-\pi}^{\pi} \sin(\phi) d\hat{\Phi}(\phi) \,, \quad \hat{c} \equiv \int_{-\pi}^{\pi} \cos(\phi) d\hat{\Phi}(\phi) \,. \end{aligned} \tag{2.37}$$

The RPL $\delta\phi$ corresponding to the POM (2.36) is given by

$$\delta\phi = 2\pi \left[\sum_{n=0}^{\infty} |\psi_n|\right]^{-2} \,, \tag{2.38}$$

and will be adopted as a pertinent definition of the phase uncertainty in the spirit of the quantum estimation theory.

3. Generalized Coherent States

In this section a large class of generalized coherent states is reviewed in a unified framework which generalizes both the customary CS[58] and QSS[9] in a fashion suited to describe the different kinds of quantum amplification. The construction uses a nonlinear multimode realization of Lie algebras and leads to a rich variety of coherent states, including, as particular cases, the two-mode states of Refs. 59–62 along with the one-mode states of Refs. 33, 35–37, 42.

Originally, the present group-theoretical construction was motivated by the difficulties which arise when one tries to generalize the two-photon squeezed states to multiphoton states.[38] Similarly in the case of the customary CS — which are obtained by displacing the vacuum with a unitary exponential of the annihilation and creation operators a and $a^\dagger$ — the QSS are obtained by 'squeezing' the vacuum with an exponential of a^2 and $(a^\dagger)^2$. However, the simplest possible generalizing ansatz — namely using k-degree polynomials of a and $a^\dagger$ instead of linear or quadratic forms — runs into the problem of the nonanalyticity of the vacuum vector.[63] On the other hand, k-photon group-theoretical constructions are suggested by the observation that the usual CS and QSS both are group-theoretical states (GTS), the former of the Weyl-Heisenberg (WH) group, whereas the latter of the two-photon realization of the $SU(1,1)$ group.

After shortly reviewing the CS and QSS and recalling the construction of the GTS, I present the multiboson realizations of Lie algebras, focusing attention on the simplest cases: wh, $su(2)$, $su(1,1)$. The one-mode and two-mode realizations are analyzed in detail: the former corresponds to the multiboson Holstein-Primakoff states introduced in Ref. 33, whereas the latter coincides, in the bilinear case, with the Schwinger-like states analyzed, for example, in Refs. 61. The main nonclassical features of these states are synthetically reviewed, with particular emphasis on the phase-number squeezing properties interesting for applications. Schemes for production of the states will be given in the successive sections. The notion of photon fractioning, which naturally arises from the multiboson construction as an inverse transformation, is given in the concluding subsection. Contrary to the previous ones, the fractional states are no longer pure states, and hence are written in terms of density matrices. In Sec. 5 it will be shown how these states can be obtained at the output of an ideal phase-number amplifier.

3.1. *Coherent and squeezed states*

Originally, coherent states (CS) of radiation were introduced in quantum optics by Glauber[58] in order to describe the high-order coherence of laser light. Full optical coherence corresponds to factorization of all normal-ordered Green functions of the electric field and is obtained when the radiation state is an eigenstate of the positive-frequency component of the field. For a single mode field corresponding to annihilation operator a, a CS $|\alpha\rangle$ satisfies the eigenvalue equation

$$a|\alpha\rangle = \alpha|\alpha\rangle \ , \tag{3.1}$$

where α is a complex number. A normalized solution $|\alpha\rangle$ of Eq. (3.1), corresponding to a fixed choice of the overall phase factor, can be obtained by 'displacing' the vacuum $|0\rangle$ as follows

$$|\alpha\rangle = \hat{D}(\alpha)|0\rangle \tag{3.2}$$

via the unitary displacement operator

$$\hat{D}(\alpha) = \exp(\alpha a^\dagger - \overline{\alpha} a) \ . \tag{3.3}$$

It is worth noticing that the operators $\hat{D}(\alpha)$ for varying α generate the WH group, with composition law $\hat{D}(\alpha)\hat{D}(\beta) = \exp(i\mathrm{Im}(\overline{\alpha}\beta))\hat{D}(\alpha+\beta)$. The corresponding Lie algebra is the usual one spanned by a, $a^\dagger$, and the identity 1, where $[a, a^\dagger] = 1$. In this fashion the set of coherent states can be regarded as the group orbit of the vacuum vector $|0\rangle$ under the action of the WH group: the natural generalization of this construction to different groups (and/or vacuum vectors) will lead to the definition of GTS.

The number representation of the state $|\alpha\rangle$ can be obtained after normal ordering the operator $\hat{D}(\alpha)$ through the BCH (Backer-Campbell-Hausdorff) formula given in Table 1.

Table 1. Defining commutations, UIR and BCH formulas for the relevant lowest dimensional Lie algebras.

	wh	$su(2)$	$su(1,1)$
Commutation relations	$[a, a^\dagger] = 1$	$[j^+, j^-] = 2j^3$ $[j^3, j^\pm] = \pm j^\pm$	$[\hat{K}^+, \hat{K}^-] = -2\hat{K}^3$ $[\hat{K}^3, \hat{K}^\pm] = \pm\hat{K}^\pm$
Casimir	1	$j(j+1) =$ $(j^3)^2 + \frac{1}{2}(j^+ j^- + j^- j^+)$	$\kappa(\kappa-1) =$ $(\hat{K}^3)^2 - \frac{1}{2}(\hat{K}^+\hat{K}^- + \hat{K}^-\hat{K}^+)$
Representation	$0 \le n$	$0 \le m \le 2j$	$0 \le m$
	—	$j^3\,\|m;j\rangle = (m-j)\|m;j\rangle$	$\hat{K}^3\,\|m;\kappa\rangle = (m+\kappa)\|m;\kappa\rangle$
	$\langle n+1\|a^\dagger\|n\rangle =$ $\sqrt{n+1}$	$\langle m+1, j\|j^+\|m;j\rangle =$ $\sqrt{(m+1)(2j-m)}$	$\langle m+1, \kappa\|\hat{K}^+\|m;\kappa\rangle =$ $\sqrt{(m+1)(m+2\kappa)}$
BCH	$\exp\left(\xi a^\dagger - \bar{\xi} a\right) =$ $e^{\zeta a^\dagger} e^{-\frac{1}{2}\|\zeta\|^2} e^{-\bar{\zeta} a}$	$\exp\left(\xi j^+ - \bar{\xi} j^-\right) =$ $e^{\zeta j^-} e^{\beta j^3} e^{-\bar{\zeta} j^-}$	$\exp\left(\xi \hat{K}^+ - \bar{\xi}\hat{K}^-\right) =$ $e^{\zeta \hat{K}^-} e^{\beta \hat{K}^3} e^{-\bar{\zeta}\hat{K}^-}$
	$\zeta = \xi$	$\zeta = \frac{\xi}{\|\xi\|}\tan\|\xi\|$ $\beta = \ln(1+\|\zeta\|^2)$	$\zeta = \frac{\xi}{\|\xi\|}\tanh\|\xi\|$ $\beta = \ln(1-\|\zeta\|^2)$

$$|\alpha\rangle = e^{-\frac{1}{2}|\alpha|^2} e^{\alpha a^\dagger}|0\rangle = e^{-\frac{1}{2}|\alpha|^2} \sum_{n=0}^{\infty} \frac{\alpha^n}{\sqrt{n!}}|n\rangle \ . \tag{3.4}$$

Equation (3.4) corresponds to a Poisson distribution of the number of photons, having the following average value and fluctuations

$$\langle \hat{n} \rangle = \langle \Delta \hat{n}^2 \rangle = |\alpha|^2 \ . \tag{3.5}$$

For the quadrature component a_ϕ of the radiation mode one has the averages

$$\alpha_\phi \doteq \langle a_\phi \rangle = \frac{1}{2}\left(\alpha e^{i\phi} + \bar{\alpha} e^{-i\phi}\right) \ , \qquad \langle \Delta a_\phi^2 \rangle = \frac{1}{4} \ . \tag{3.6}$$

Equation (3.6) shows that the quadrature fluctuations do not depend on the phase ϕ, and, as a consequence, $|\alpha\rangle$ is a minimum uncertainty state for any couple of quadratures a_ϕ and $a_{\phi+\pi/2}$. The construction (3.2) assures that coherent states have the same Gaussian probability distribution of the vacuum, but with mean value displaced to $\langle a_\phi \rangle = \alpha_\phi$.

The QSS (usually referred to as simply 'squeezed states') are minimum uncertainty states with ϕ-dependent quadrature fluctuations $\langle \Delta a_\phi^2 \rangle$. For a couple of quadratures one can have $\langle \Delta a_\phi^2 \rangle \ll 1/4$ and correspondingly $\langle \Delta a_\phi^2 \rangle \gg 1/4$, according to the Heisenberg uncertainty relation (1.1). In order to change the probability distribution of a_ϕ at fixed mean value α_ϕ one considers states of the form

$$|\alpha, \zeta\rangle = \hat{D}(\alpha)|\zeta\rangle \ , \qquad \langle \zeta | a | \zeta \rangle = 0 \ . \tag{3.7}$$

The customary squeezed states of Yuen[9] correspond to choosing

$$|\zeta\rangle = \hat{S}(\zeta)|0\rangle = \exp\left[\frac{1}{2}\left(\zeta a^{\dagger 2} - \bar{\zeta} a^2\right)\right]|0\rangle \ , \tag{3.8}$$

where the squeezing operator $\hat{S}(\zeta)$ provides the linear transformation of the field

$$\hat{S}^{\dagger}(\zeta)a\hat{S}(\zeta) = \mu a + \nu a^{\dagger} , \qquad \mu = \cosh\rho , \ \nu = e^{i\psi}\sinh\rho , \quad \zeta = \rho e^{i\psi} , \tag{3.9}$$

and therefore, leads again to Gaussian distribution for a_{ϕ}, but now with fluctuations

$$\langle \Delta a_{\phi}^{2} \rangle = \frac{1}{4}\left[\sinh 2\rho \cos(2\phi - \psi) + \cosh 2\rho\right] . \tag{3.10}$$

The maximum ratio between the two quadrature fluctuations is obtained for $\phi = \psi/2 + k\pi$: therefore, without loss of generality, one can choose $\psi = \phi = 0$. The quadrature fluctuations relative to their coherent value $\langle \Delta a_{\phi}^{2} \rangle_{\mathrm{coh}} = 1/4$ are measured by the squeezing factor S_{ϕ}

$$S_{\phi} = 4\langle \Delta a_{\phi}^{2} \rangle . \tag{3.11}$$

With the previous choice of phases one has

$$S_{0} = e^{2\rho} , \qquad S_{\pi/2} = e^{-2\rho} . \tag{3.12}$$

The number distribution of the squeezed state $|\alpha,\zeta\rangle = \hat{D}(\alpha)\hat{S}(\zeta)|0\rangle$ is not Poissonian in general. Here the relevant parameter measuring the 'squeezing' of the number distribution is the Fano factor

$$F = \frac{\langle \Delta\hat{n}^{2} \rangle}{\langle \hat{n} \rangle} , \tag{3.13}$$

which is a unit for the Poisson distribution. F is related to the second-order degree of coherence $g^{(2)}(0) = \langle : \hat{n}^{2} : \rangle / \langle \hat{n} \rangle^{2}$, namely the intensity autocorrelation function $g^{(2)}(t)$ for $t = 0$

$$g^{(2)}(0) = 1 + \langle \hat{n} \rangle^{-1}(F - 1) . \tag{3.14}$$

For subpoissonian distributions one has $F < 1$ and correspondingly $g^{(2)}(0) < 1$ (antibunching), whereas in the superpoissonian case ($F > 1$) one has $g^{(2)}(0) > 1$ (bunching). The squeezed states may be either sub or superpoissonian, depending on the squeezing parameter ζ

$$F = \frac{2|\mu\nu|^{2} + |\mu\alpha + \nu\overline{\alpha}|^{2}}{|\alpha|^{2} + |\nu|^{2}} . \tag{3.15}$$

The minimum achievable number-fluctuations are

$$\langle \Delta\hat{n}^{2} \rangle_{\mathrm{min}} \simeq 2^{-5/3}\langle \hat{n} \rangle^{2/3} , \tag{3.16}$$

which are obtained for real α at $\psi = \pi$, after minimizing with respect to α.[20]

3.2. *Group-theoretical states*

Fisher, Nieto and Sandberg[38] proposed generalizations of the squeezing operator $\hat{S}(\zeta)$ in the form

$$\hat{S}_k(\zeta) = \exp\left(\zeta a^{\dagger k} - \overline{\zeta} a^k + \hat{h}_k\right) , \tag{3.17}$$

for $k > 2$ and $\hat{h}_k$ denoting a polynomial in a and $a^\dagger$ with powers up to $k-1$. However, it turns out that the resulting squeezed vacuum $\hat{S}_k(\zeta)|0\rangle$ cannot be treated in general by analytic methods. For example, the Taylor expansion of the vacuum expectation value $\langle 0|\hat{S}_k(\zeta)|0\rangle$ has zero radius of convergence (see also Ref. 64), whereas numerical computations can be performed only resorting to Padé approximants.[39] Only very special cases of operators of the form (3.17) can be analytically handled, as, for example, when $\hat{S}_k$ is the exponential of a Hamiltonian which is a power of a bilinear function of a and $a^\dagger$.[40,65]

The appearance of the formal analytic divergencies induced by the operator (3.17) can be easily understood trying to compute its action on the vacuum. Doing that requires dealing with the BCH factorization of $\hat{S}_k(\zeta)$ in the form

$$\hat{S}_k(\zeta) = \exp\left[f(\zeta)a^{\dagger k}\right]\exp(\hat{o}) , \tag{3.18}$$

where $f(\zeta)$ is some suitable function of ζ and $\hat{o}$ is an operator which stabilizes the vacuum and produces only a normalization factor. Adopting this method one needs to compute iterated commutators of the form

$$\left[a^l, a^{\dagger m}\right] = p(a^\dagger a)a^{\dagger l-m} , \quad (\text{for} m \geq l) , \tag{3.19}$$

where $p(x)$ is a polynomial function. For $k > 2$ this procedure never ends, producing an infinite dimensional boson algebra, which accounts for the formal analytic divergencies. On the contrary, for $k = 2$ — as for the customary Yuen squeezed states — a finite dimensional Lie algebra is obtained, and the factorization (3.18) can be explicitly written. More precisely, the QSS are the generalized group-theoretical states (GTS) of $SU(1,1)$ according to the general definition for an arbitrary Lie group given by Perelomov[66] and Rasetti.[67] As already shown, the same considerations hold true for the customary CS themselves which are the GTS of the WH group. The last observation suggests that GTS are good candidates for *non-naïve* generalizations of squeezed states. In the following the general definition is briefly recalled.

The set of GTS for a Lie group G is obtained using a UIR (unitary irreducible representation) of the group and acting on the lowest weight vector (LWV) $|v\rangle$ of the representation space by the whole group: the manifold of GTS corresponds to the factor space G/H, H being the subgroup of G leaving $|v\rangle$ invariant (up to a phase factor). The GTS $|s\rangle$ are thus labelled by the points $s \in G/H$ which correspond to left cosets of G with respect to H.

According to the above definition I recall the construction of the GTS for the $SU(2)$ and $SU(1,1)$ *simple* groups, and the WH *solvable* group: according to the

Levi theorem these are essentially the simplest building blocks of every Lie group, and the main squeezing properties for higher rank GTS can be already recovered in these low-rank cases.[68,69]

In Table 1 the defining commutation relations and the pertaining UIR are reported. Resorting to the above definition, the GTS are written in the form

$$|\xi;\sigma\rangle_G = \exp\left(\xi\hat{R}^+ - \overline{\xi}\hat{R}^-\right)|0;\sigma\rangle \ , \tag{3.20}$$

where ξ is a complex number, σ labels the UIR (namely, it is related to the Casimir eigenvalue), $|0;\sigma\rangle$ is the LWV of the UIR and $\hat{R}^+$ represents the raising operator of the Lie algebra of G: $\hat{R}^+ = a^\dagger$ for $G = WH$, $\hat{R}^+ = \hat{J}^+$ for $G = SU(2)$ and $\hat{R}^+ = \hat{K}^+$ for $G = SU(1,1)$. Using the BCH formulas in Table 1 the states (3.20) are rewritten in the more convenient way

$$|\zeta;\sigma\rangle_G = \mathcal{N}_\sigma^{-1/2}(\zeta)\exp(\zeta\hat{R}^+)|0;\sigma\rangle = \mathcal{N}_\sigma^{-1/2}(\zeta)\sum_{n=0}^{\infty} c_n\zeta^n|n;\sigma\rangle \ . \tag{3.21}$$

Here $\mathcal{N}_\sigma(\zeta)$ is a normalization factor and the relation $\zeta = \zeta(\xi)$ between the labels in Eq.(3.20) and (3.21) is given in Table 1. Upon specializing the states (3.21) to the UIR in Table 1, one obtains

$$\begin{aligned}
|\zeta\rangle_{WH} &= \exp\left(-\frac{1}{2}|\zeta|^2\right)\sum_{n=0}^{\infty}\frac{\zeta^n}{\sqrt{n!}}|n\rangle \ , \\
|\zeta;j\rangle_{SU(2)} &= (1+|\zeta|^2)^{-j}\sum_{n=0}^{2j}\binom{2j}{n}^{1/2}\zeta^n|n;j\rangle \ , \\
|\zeta;\kappa\rangle_{SU(1,1)} &= (1-|\zeta|^2)^{\kappa}\sum_{n=0}^{\infty}\binom{2\kappa+n-1}{n}^{1/2}\zeta^n|n;\kappa\rangle \ .
\end{aligned} \tag{3.22}$$

In the following subsections the abstract states (3.22) will be translated into physical photon states, using multiboson realizations of the Lie algebras.

3.3. *Multiboson realizations of Lie algebras*

The following boson realization of Lie algebras generalizes to an arbitrary number of modes the one-mode construction of Refs. 33, 35–37 and the two-mode ones of Refs. 59–62. The method here is illustrated for the Lie algebras in Table 1, even though, as it will be evident, it could be straightforwardly extended to other higher-rank algebras as well.

The starting point is the construction of the raising operator $\hat{R}^+$ of the Lie algebra in terms of the boson shift operators $\hat{e}_l^{\pm}$ and the number operators $\hat{n}_l$ for each boson mode l

$$\begin{aligned}
&\hat{e}_l^{\pm}|n_1,\ldots,n_l,\ldots\rangle = |n_1,\ldots,n_l\pm 1,\ldots\rangle \ , \quad n_l \geq 1 \ , \\
&\hat{e}_l^{-}|n_1,\ldots,0,\ldots\rangle = 0 \ , \\
&\hat{n}_l|n_1,\ldots,n_l,\ldots\rangle = n_l|n_1,\ldots,n_l,\ldots\rangle \ .
\end{aligned} \tag{3.23}$$

Here $|n_1,\ldots,n_l,\ldots\rangle$ denotes the tensor product $|n_1\rangle\otimes\ldots\otimes|n_l\rangle\otimes\ldots$: as customary in quantum optics, the tensor product notation is implicit, writing for example $\hat{o}_1\hat{o}_2\ldots\hat{o}_l\ldots$, instead of $\hat{o}_1\otimes\hat{o}_2\otimes\ldots\otimes\hat{o}_l\otimes\ldots$. Also the following conventions will be adopted

$$\hat{e}^k=\begin{cases}(\hat{e}^+)^k & k>0\,,\\ \hat{1} & k=0\,,\\ (\hat{e}^-)^{|k|} & k<0\,,\end{cases}\qquad (a^\dagger)^k=\begin{cases}(a^\dagger)^k & k>0\,,\\ \hat{1} & k=0\,,\\ a^{|k|} & k<0\,.\end{cases}\tag{3.24}$$

With the above notation, the realization of the raising operator $\hat{R}^+$ is written in the form

$$\hat{R}^+_{\mathbf{k}\sigma}=\sqrt{F_{\mathbf{k}\sigma}(\hat{\mathbf{n}})}\prod_{l=1}^{\infty}e_l^{k_l}\,.\tag{3.25}$$

In Eq. (3.25) the raising operator depends on the vector $\mathbf{k}=(k_1,\ldots k_l,\ldots)$ and on the label σ of the representation. The prefactor $\sqrt{F_{\mathbf{k}\sigma}(\hat{\mathbf{n}})}$ (written under square root for later convenience) depends on the vector $\hat{\mathbf{n}}=(\hat{n}_1,\ldots\hat{n}_l,\ldots)$ of number operators, whereas the functional form of $F_{\mathbf{k}\sigma}(\hat{\mathbf{n}})$ is related to the particular Lie algebra pertaining $\hat{R}^+$. One should notice that the realization (3.25) is completely general once a diagonal representation on the number eigenstates is chosen for the commutators $[\hat{R}^+,\hat{R}^-]$. The monomial

$$\hat{e}^+_{\mathbf{k}}=\prod_{l=1}^{\infty}e_l^{k_l}\tag{3.26}$$

creates $k=\sum_{l=1}^{\infty}k_l<\infty$ photons and represents the shift operator on the representation space of the UIR

$$\hat{e}^+_{\mathbf{k}}|\mathbf{n}\rangle=|\mathbf{n}+\mathbf{k}\rangle\,.\tag{3.27}$$

In Eq. (3.27) the vector notation is extended to the Fock space, upon denoting $|\mathbf{n}\rangle=|n_1,\ldots,n_l,\ldots\rangle$.

A LWV $|\mathbf{v}\rangle$ for the UIR is annihilated by $\hat{e}^-_{\mathbf{k}}\equiv(\hat{e}^+_{\mathbf{k}})^\dagger$, namely

$$\hat{e}^-_{\mathbf{k}}|\mathbf{v}\rangle=0\,.\tag{3.28}$$

From Eq. (3.27) it follows that the components v_l of $\mathbf{v}$ are constrained by the inequalities

$$v_l\geq 0\,,\quad \min_{l\in L^+}\{v_l-k_l\}<0\,,\tag{3.29}$$

where $L^\pm$ denotes the sets of indices

$$L^+\doteq\{l|k_l>0\}\,,\quad L^-\doteq\{l|k_l<0\}\,.\tag{3.30}$$

Once the LWV $|\mathbf{v}\rangle$ has been fixed the basis of the UIR is obtained through iterated action of the raising operator $\hat{e}^+_{\mathbf{k}}$ on the vacuum

$$(\hat{e}^+_{\mathbf{k}})^n|\mathbf{v}\rangle=|\mathbf{v}+n\mathbf{k}\rangle\,.\tag{3.31}$$

Infinite-dimensional representations, as the UIR of the wh and $su(1,1)$ algebras, require k_l being nonnegative (the case of nonpositive k_l can be conveniently recovered using the involution corresponding to $\hat{R}^+ \to \hat{R}^-$). If some k_l is negative the representation has finite dimension d

$$d = 1 + \min_{l \in L^-} \{[v_l/k_l]\} \ , \tag{3.32}$$

where $[x]$ denotes the integer part of x. Also the vanishing of the prefactor $\sqrt{F_{\mathbf{k}\sigma}(\mathbf{n})}$ in Eq. (3.25) for some values of $\mathbf{n}$ may restrict the dimension d of the representation space, as it happens in some realizations of $su(2)$ which will be shown in the following.

The shift operators $\hat{e}^{\pm}_{\mathbf{k}}$ commute with the following operators

$$\hat{c}_{rs} = k_s \hat{n}_r - k_r \hat{n}_s \ , \tag{3.33}$$

$$\hat{\lambda}_s = k_s [\hat{n}_s/k_s] = \hat{n}_s - k_s \langle \hat{n}_s/k_s \rangle \ , \tag{3.34}$$

where $\langle x \rangle = x - [x]$ denotes the fractional part of x ($\hat{\lambda}_s = 0$ for $k_s = \pm 1$ and, by convention, also for $k_s = 0$). The constant operators $\hat{c}_{rs}$ and $\hat{\lambda}_s$ are not related to the Casimir of the UIR: on the other hand, fixing a functional dependence $\sigma = \sigma(\{\hat{c}_{rs}\}, \{\hat{\lambda}_s\})$ is equivalent to select a particular family of UIR's.

The function $F_{\mathbf{k}\sigma}(\mathbf{n})$ can be obtained using the UIR's in Table 1. For the wh algebra one can drop the label σ and write the equation

$$\langle \mathbf{v} + (n+1)\mathbf{k} | a^{\dagger}_{\mathbf{k}} | \mathbf{v} + n\mathbf{k} \rangle = \sqrt{F_{\mathbf{k}}(\mathbf{v} + (n+1)\mathbf{k})} = \sqrt{n+1} \ . \tag{3.35}$$

The solution of Eq. (3.35) is

$$F_{\mathbf{k}}(\mathbf{n}) = \min_{l \in L^+} \{[n_l/k_l]\} \ . \tag{3.36}$$

The function (3.36) can also be identified with the 'number' operator $a^{\dagger}_{\mathbf{k}} a_{\mathbf{k}}$

$$a^{\dagger}_{\mathbf{k}} a_{\mathbf{k}} = \min_{l \in L^+} \{[n_l/k_l]\} \ , \tag{3.37}$$

which satisfies the additional commutations

$$[a^{\dagger}_{\mathbf{k}} a_{\mathbf{k}}, a_{\mathbf{k}}] = -a_{\mathbf{k}} \ , \quad [a^{\dagger}_{\mathbf{k}} a_{\mathbf{k}}, a^{\dagger}_{\mathbf{k}}] = a^{\dagger}_{\mathbf{k}} \ , \tag{3.38}$$

and is represented as follows

$$a^{\dagger}_{\mathbf{k}} a_{\mathbf{k}} | \mathbf{v} + n\mathbf{k} \rangle = n | \mathbf{v} + n\mathbf{k} \rangle \ . \tag{3.39}$$

Notice that the present realization provides a faithful representation of wh only when k_l are nonnegative: otherwise one has a 'truncated' representation on a space

with finite dimension d given by Eq. (3.32). In such case $a_{\mathbf{k}}$ and $a_{\mathbf{k}}^{\dagger}$ are no longer genuine boson operators. In fact, one has

$$a_{\mathbf{k}}^{\dagger}|\mathbf{v}+(d-1)\mathbf{k}\rangle = 0 \ , \tag{3.40}$$

and, as a consequence,

$$[a_{\mathbf{k}}, a_{\mathbf{k}}^{\dagger}]|\mathbf{v}+(d-1)\mathbf{k}\rangle = (d-1)|\mathbf{v}+(d-1)\mathbf{k}\rangle \neq |\mathbf{v}+(d-1)\mathbf{k}\rangle \ . \tag{3.41}$$

However, the truncated bosons are conveniently used in the finite-dimensional representations of $SU(2)$. Using the following identity written in the notation (3.24)

$$(a^{\dagger})^k = \left[\frac{\hat{n}!}{(\hat{n}-k)!}\right]^{\mathrm{sign(k)}} e^k \ , \tag{3.42}$$

the operator $a_{\mathbf{k}}^{\dagger}$ is rewritten in terms of the creators $a_l^{\dagger}$

$$a_{\mathbf{k}}^{\dagger} = \left\{ \min_{l\in L^+}\{[n_l/k_l]\} \left[\prod_{s=1}^{\infty} \frac{(\hat{n}_s-k_s)!}{\hat{n}_s!}\right]^{\mathrm{sign(k_s)}} \right\}^{1/2} \prod_{l=1}^{\infty} (a_l^{\dagger})^{k_l} \ . \tag{3.43}$$

In the case of the $su(1,1)$ algebra the UIR in Table 1 provides the equation

$$F_{\mathbf{k}\kappa}(\mathbf{v}+(n+1)\mathbf{k}) = (n+1)(n+2\kappa) \ , \tag{3.44}$$

which has the solution

$$F_{\mathbf{k}\kappa}(\mathbf{n}) = a_{\mathbf{k}}^{\dagger} a_{\mathbf{k}} [a_{\mathbf{k}}^{\dagger} a_{\mathbf{k}} + 2\kappa - 1] \ . \tag{3.45}$$

Equations (3.25) and (3.43) allow to rewrite the raising operator in terms of the particle operators $a_{\mathbf{k}}$ and $a_{\mathbf{k}}^{\dagger}$, namely

$$\hat{K}_{\mathbf{k}\kappa}^{+} = (a_{\mathbf{k}}^{\dagger} a_{\mathbf{k}} + 2\kappa - 1)^{1/2} a_{\mathbf{k}}^{\dagger} \ . \tag{3.46}$$

The diagonal element $\hat{K}_{\mathbf{k}\kappa}^{3}$ is generated under commutations. One obtains

$$\hat{K}_{\mathbf{k}\kappa}^{3} = a_{\mathbf{k}}^{\dagger} a_{\mathbf{k}} + \kappa \ . \tag{3.47}$$

Notice that, similarly to the case of wh, all the k_l must be non-negative in order to get a faithful representation of $su(1,1)$.

The $su(2)$ realizations are obtained in a way completely analogous to those of $su(1,1)$. In this case one has

$$\begin{aligned} \hat{J}_{\mathbf{k}j}^{+} &= (2j+1-a_{\mathbf{k}}^{\dagger} a_{\mathbf{k}})^{1/2} a_{\mathbf{k}}^{\dagger} \ . \\ \hat{J}_{\mathbf{k}j}^{3} &= a_{\mathbf{k}}^{\dagger} a_{\mathbf{k}} - j \ . \end{aligned} \tag{3.48}$$

Here k_l are no longer restricted to non-negative values, the only requirement being the following compatibility condition between $\mathbf{k}$ and the dimension $d = 2j + 1$ of the UIR

$$2j \leq \min_{l \in L^-} \{[v_l/k_l]\} \ . \tag{3.49}$$

In Table 2 the above Lie algebra constructions are summarized. One can see that the cases of $Su(2)$ and $Su(1,1)$ algebras generalize the Holstein-Primakoff[42] procedure. In addition, the present realization contains as particular cases all the boson realizations which appeared in the literature: these are reported in Table 3.

Table 2. Summary of the general of multiboson-multimode realizations.

Algebra	Realization	$\mathbf{k}$	$\|\mathbf{v}\rangle$
wh	$a^\dagger_{\mathbf{k}} = \left(a^\dagger_{\mathbf{k}} a_{\mathbf{k}} \left[\prod_{s=1}^{\infty} \frac{(\hat{n}_s - k_s)!}{\hat{n}_s!}\right]^{\mathrm{sign}(k_s)}\right)^{1/2} \prod_{l=1}^{\infty} (a^\dagger_l)^{k_l}$ $a^\dagger_{\mathbf{k}} a_{\mathbf{k}} = \min_{l \in L^+} \{[n_l/k_l]\}$	$k_l \geq 0$	$v_l \geq 0$, $\min_{l \in L^+} \{v_l - k_l\} < 0$
$su(1,1)$	$\hat{K}^+_{\mathbf{k}\kappa} = \left(a^\dagger_{\mathbf{k}} a_{\mathbf{k}} + 2\kappa - 1\right)^{1/2} a^\dagger_{\mathbf{k}}$ $\hat{K}^3_{\mathbf{k}\kappa} = a^\dagger_{\mathbf{k}} a_{\mathbf{k}} + \kappa$	$k_l \geq 0$	$v_l \geq 0$, $\min_{l \in L^+} \{v_l - k_l\} < 0$
$su(2)$	$\hat{J}^+_{\mathbf{k}j} = \left(2j + 1 - a^\dagger_{\mathbf{k}} a_{\mathbf{k}}\right)^{1/2} a^\dagger_{\mathbf{k}}$ $\hat{J}^3_{\mathbf{k}j} = a^\dagger_{\mathbf{k}} a_{\mathbf{k}} - j$	$k_l \in Z$	$v_l \geq 0$, $\min_{l \in L^+} \{v_l - k_l\} < 0$, $2j \leq \min_{l \in L^-} \{[v_l/k_l]\}$

3.4. *One-mode states*

The one-mode states are obtained by substituting in Eq. (3.21) the raising operators $\hat{R}^+ \ (\equiv a^\dagger_{(k)}, \hat{J}^+_{(k)j}, \hat{K}^+_{(k)\kappa})$ and the corresponding LWV given in Table 3 for $\mathbf{k} = (k, 0, 0, \ldots)$. Such states have been extensively analyzed in Refs. 33–37, where the squeezing properties of the $k = 1, 2$ cases are studied. Here I focus attention only on the one-boson $(k = 1)$ case: the transformation to multiboson $(k > 1)$ states will be analyzed later in Sec. 3.6.

For $k = 1$ the LWV of the representation coincides with the vacuum for all Lie algebras. Therefore, one has the states

$$\begin{aligned}
|\zeta\rangle_{WH} &= \exp\left(-\frac{1}{2}|\zeta|^2\right) \sum_{n=0}^{\infty} \frac{\zeta^n}{\sqrt{n!}} |n\rangle \ , \\
|\zeta; j\rangle_{SU(2)} &= (1 + |\zeta|^2)^{-j} \sum_{n=0}^{2j} \binom{2j}{n}^{1/2} \zeta^n |n\rangle \ , \\
|\zeta; \kappa\rangle_{SU(1,1)} &= (1 - |\zeta|^2)^{\kappa} \sum_{n=0}^{\infty} \binom{2\kappa + n - 1}{n}^{1/2} \zeta^n |n\rangle \ ,
\end{aligned} \tag{3.50}$$

Table 3. Multiboson-multimode realizations in the literature.

Reference	Realization	k	$\|v\rangle$
Holstein-Primakoff $su(2)$ Refs. 33,35–37,42	$\hat{J}_j^+ = (2j+1-\hat{n})^{1/2}\,a^\dagger$ $\hat{J}_j^3 = \hat{n} - j$	$(1,0,0,\ldots)$	$\|0\rangle$
Holstein-Primakoff $su(1,1)$ Refs. 33,35–37,42	$\hat{K}_\kappa^+ = (2\kappa-1+\hat{n})^{1/2}\,a^\dagger$ $\hat{K}_\kappa^3 = \hat{n} + \kappa$	$(1,0,0,\ldots)$	$\|0\rangle$
Katriel-Hummer wh Refs. 48,49,60	$a^\dagger_{(1,1)} = \frac{a^\dagger b^\dagger}{\sqrt{\max\{a^\dagger a, b^\dagger b\}}}$ $a^\dagger_{(1,1)} a_{(1,1)} = \min\{a^\dagger a, b^\dagger b\}$	$(1,1,0,\ldots)$	$\|N,M\rangle$ $NM = 0$
Schwinger $su(2)$ Refs. 59,61,62	$\hat{J}^+_{(1,-1)j} = a^\dagger b$ $\hat{J}^3_{(1,-1)j} = \frac{1}{2}(a^\dagger a - b^\dagger b)$ $2j = a^\dagger a + b^\dagger b$	$(1,-1,0,\ldots)$	$\|0,N\rangle$ $2j = N$
Schwinger $su(1,1)$ Refs. 59,61,62	$\hat{K}^+_{(1,1)\kappa} = a^\dagger b^\dagger$ $\hat{K}^3_{(1,1)\kappa} = \frac{1}{2}(a^\dagger a + b^\dagger b + 1)$ $2\kappa = \|a^\dagger a - b^\dagger b\| + 1$	$(1,1,0,\ldots)$	$\|N,M\rangle$ $2k = \|N-M\|+1$
Brandt-Greenberg multiboson wh Refs. 33–37,41	$a^\dagger_{(k)} = \left\{\frac{[\hat{n}/k](\hat{n}-k)!}{\hat{n}!}\right\}^{1/2}(a^\dagger)^k$ $a^\dagger_{(k)} a_{(k)} = [\hat{n}/k]$	$(k,0,0,\ldots)$	$\|\lambda\rangle$ $0 \le \lambda \le k-1$
Holstein-Primakoff multiboson $su(2)$ Refs. 33–37,41	$\hat{J}^+_{(k)j} = (2j+1-a^\dagger_{(k)}a_{(k)})^{1/2} a^\dagger_{(k)}$ $\hat{J}^3_{(k)j} = a^\dagger_{(k)}a_{(k)} - j$	$(k,0,0,\ldots)$	$\|\lambda\rangle$ $0 \le \lambda \le k-1$
Holstein-Primakoff multiboson $su(1,1)$ Refs. 33–37,41	$\hat{K}^+_{(k)\kappa} = (2\kappa-1+a^\dagger_{(k)}a_{(k)})^{1/2} a^\dagger_{(k)}$ $\hat{K}^3_{(k)\kappa} = a^\dagger_{(k)}a_{(k)} + \kappa$	$(k,0,0,\ldots)$	$\|\lambda\rangle$ $0 \le \lambda \le k-1$
two-boson $su(1,1)$ Refs. 9,34	$\hat{K}^+_{(2)\kappa} = \frac{1}{2}(a^\dagger)^2$ $\hat{K}^3_{(2)\kappa} = \frac{1}{2}(a^\dagger a + 1/2)$	$(2,0,0,\ldots)$	$\|\lambda\rangle$ $\lambda = 0,1$ $4\kappa = 1+\lambda$

where $0 \leq |\zeta| \leq \infty$ for WH and $SU(2)$, whereas $0 \leq |\zeta| \leq 1$ for $SU(1,1)$. In Table 4 the average number $\langle \hat{n} \rangle$ and the Fano factor F of the states (3.50) are reported. One can see that they are related to the parameters $|\zeta|$, j, and κ by simple algebraic relations. It follows that the three set of states can be related through a suitable analytical continuation: the $SU(1,1)$ states correspond to the $SU(2)$ states for $j = -\kappa < 0$ and $|\zeta| \to -|\zeta|$, whereas the WH states are obtained in the limit $j \to \pm\infty$ for constant $2|j||\zeta|^2_{SU(2),SU(1,1)} \equiv |\zeta|^2_{WH}$, namely for constant average number of photons $\langle \hat{n} \rangle = n_0$. When allowed to have negative values j can be rewritten in terms of the physical variables n_0 and F as follows

$$2j = \frac{n_0}{1-F} \,. \tag{3.51}$$

The $SU(2)$ states ($j > 0$) corresponds to $F < 1$, $SU(1,1)$ ($j < 0$) to $F < 1$, and the WH limiting case ($j \to \infty$) to $F \to 1$. Using the analytic continuations for the binomial coefficients

$$\binom{-\alpha}{n} = (-)^n \binom{\alpha + n - 1}{n} \,, \tag{3.52}$$

and the asymptotic expansion

$$\lim_{\alpha \to +\infty} \binom{\alpha}{n} = \frac{\alpha^n}{n!} + \mathcal{O}(\alpha^{n-1}) \,, \tag{3.53}$$

the three sets of states in Eqs. (3.50) can be rewritten as a function of the three parameters n_0, F and $\psi = \arg(\zeta)$ in the following unified way

$$|n_0; F; \psi\rangle = F^{\frac{n_0}{2(1-F)}} \sum_{n=0}^{\infty} \sqrt{\binom{\frac{n_0}{1-F}}{n}} (F^{-1} - 1)^n e^{in\psi} |n\rangle \,, \tag{3.54}$$

where the sum is over a finite range of n values for vanishing binomial coefficients, namely for integer $n_0/(1-F) = 2j > 0$.

Table 4. Parameters of the number distributions of the one-mode states.

	WH	$SU(2)$	$SU(1,1)$
c_n	$1/\sqrt{n!}$	$\binom{2j}{n}^{1/2}$	$\binom{2\kappa + n - 1}{n}^{1/2}$
$\mathcal{N}^{-1/2}(\zeta)$	$\exp\left(-\frac{1}{2}|\zeta|^2\right)$	$\left(1 + |\zeta|^2\right)^{-j}$	$\left(1 - |\zeta|^2\right)^{\kappa}$
$\langle \hat{n} \rangle$	$|\zeta|^2$	$2j|\zeta|^2 / \left(1 + |\zeta|^2\right)$	$2\kappa|\zeta|^2 / \left(1 - |\zeta|^2\right)$
F	1	$\left(1 + |\zeta|^2\right)^{-1}$	$\left(1 - |\zeta|^2\right)^{-1}$
Range of $|\zeta|$	0-∞	0-∞	0-1

The analytic form of the states (3.54) is particularly suited to analyze various probability distributions for different observables as a function of the parameters of the number distribution $n_0 = \langle \hat{n} \rangle$ and $F = \langle \Delta \hat{n}^2 \rangle / \langle \hat{n} \rangle$. The number distribution of the set of states (3.54) ranges from the binomial distributions in the subpoissonian case to negative-binomial distributions in the opposite superpoissonian case. Examples of such distributions are depicted in Fig. 1.

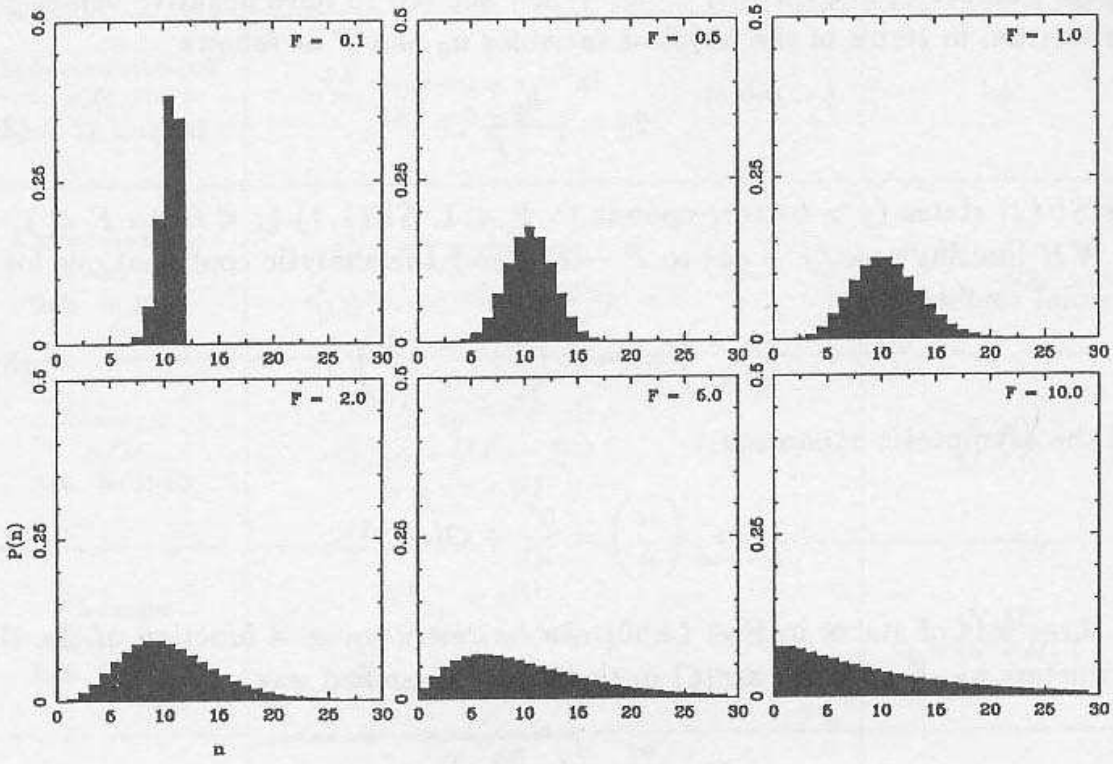

Fig. 1. Number distributions for $\langle \hat{n} \rangle = 10$ and various Fano factors.

Corresponding to the increasing number fluctuations one has a phase narrowing, namely the states (3.54) behave like phase-number minimum-uncertainty states. This is qualitatively evident from the Q-function representations in Fig. 2, where the quasiprobability

$$Q(z) = \frac{1}{2\pi} \langle z | \hat{\rho} | z \rangle \tag{3.55}$$

is given as a function of z for various values of F and for fixed n_0. For small $F < 1$ one can see that the quasiprobability expands in the phase (tangential) direction and is squeezed in the number (radial) direction. The opposite behaviour results for increasing $F > 1$, where the Q-function expands in the radial direction and is squeezed in the tangential one. (The squeezing of the Q-function actually is not apparent in Fig. 2: this is an artifact of the particular two-dimensional representation, where the level curves linearly range from the minimum to the maximum value of the function, instead of enclosing linearly increasing probability areas.)

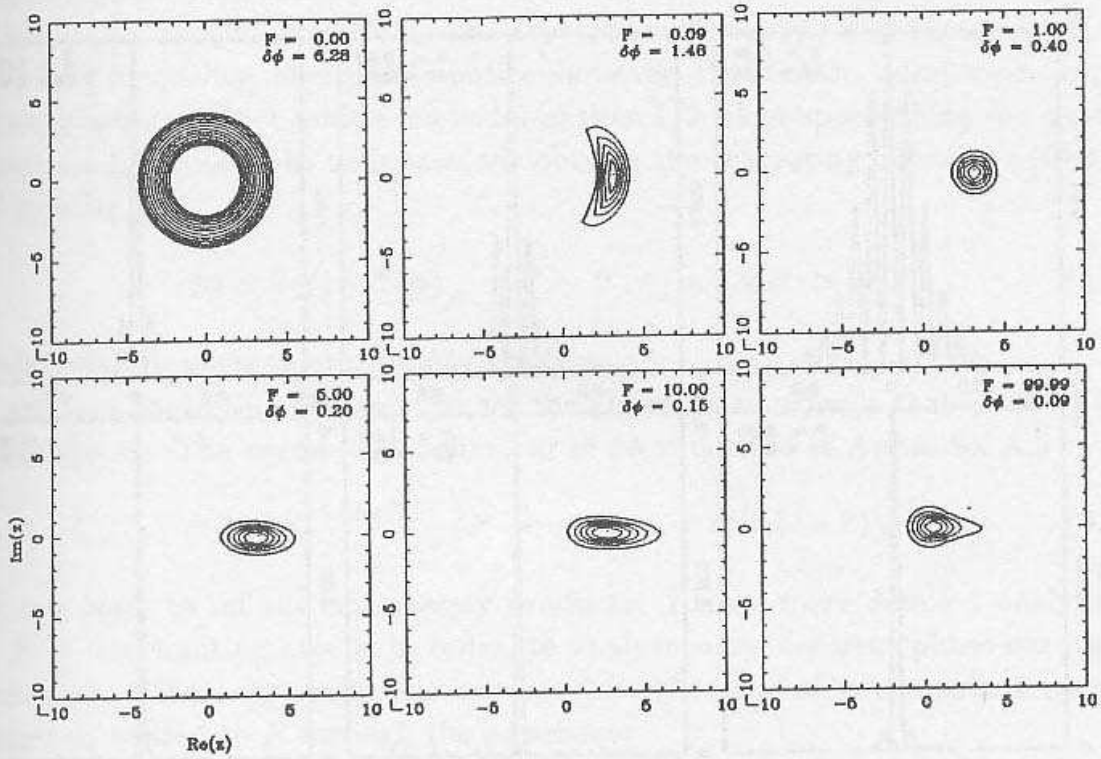

Fig. 2. Q-functions of the states for $\langle \hat{n} \rangle = 10$ and various Fano factors.

A quantitative analysis of the phase squeezing of the states (3.54) can be performed by plotting the phase probability distribution

$$P(\phi)d\phi = \mathrm{Tr}\left[\hat{\rho} d\hat{\Phi}(\phi)\right] \ , \tag{3.56}$$

using the optimum POM $d\hat{\Phi}(\phi)$ in Eq. (2.36). In Fig. 3 the probability $P(\phi)$ is plotted as a function of ϕ for various values of F and fixed n_0. The narrowing of the distribution is evident for increasing F. The oscillatory behaviour as a function of ϕ (which could not be inferred from the plots of the Q-function in Fig. 2) shows that a decreasing F in the states (3.54) does not correspond to exact squeezing of the phase distribution: the latter can only be obtained through the photon-fractioning procedure, as it will be shown in Sec. 3.6. In Fig. 4 the RPL $\delta\phi$ of Eq. (2.29) is plotted versus the number fluctuations δn for fixed n_0. On varying n_0 one obtains points which lie very near to the same curve. The log-log plot shows that $\delta\phi$ is almost inversely proportional to δn, the largest deviations from this functional dependence being in the region of very small δn, where $\delta\phi$ saturates to its highest value 2π. The asymptotic behaviours of $\delta\phi$ as a function of δn for some limiting F values are evaluated in Appendix A.2. The product of uncertainties in the neighbour of $F = 1$ is

$$\delta n \delta\phi \simeq \sqrt{\frac{\pi}{2}} \ , \quad (F \to 1 \ , n_0 = \text{const.} > 0) \ , \tag{3.57}$$

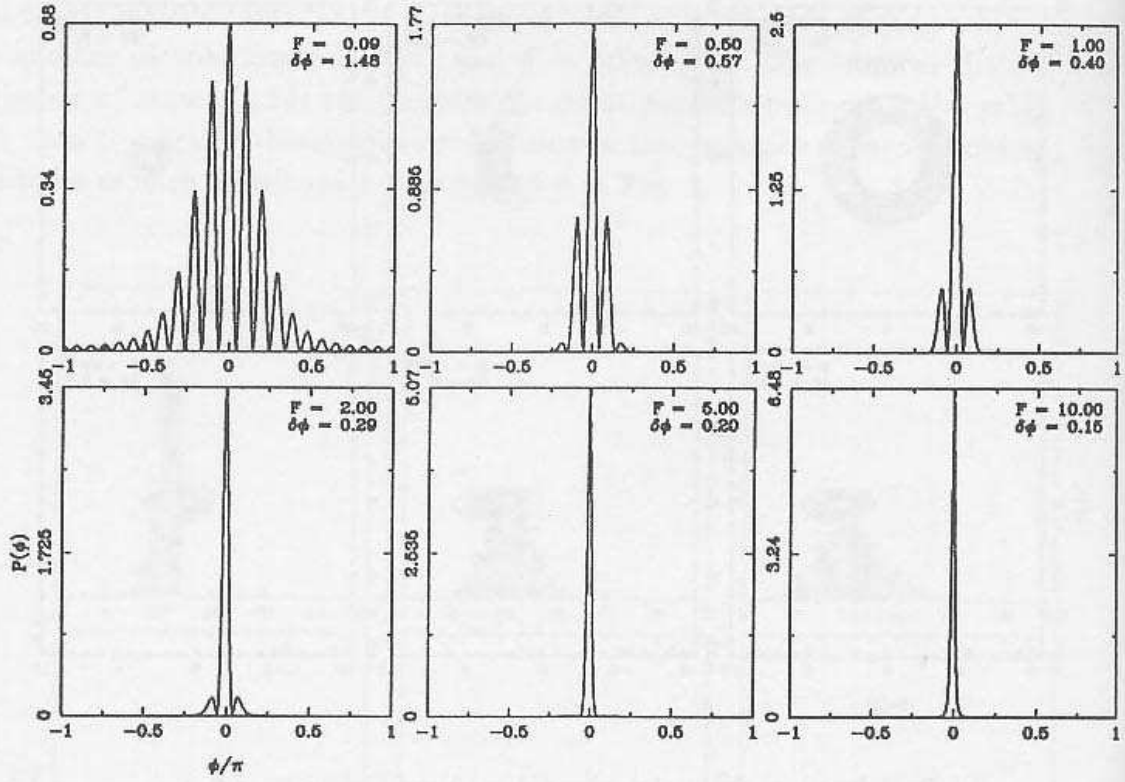

Fig. 3. Phase probability distributions of the states for $\langle \hat{n} \rangle = 10$ and various Fano factors.

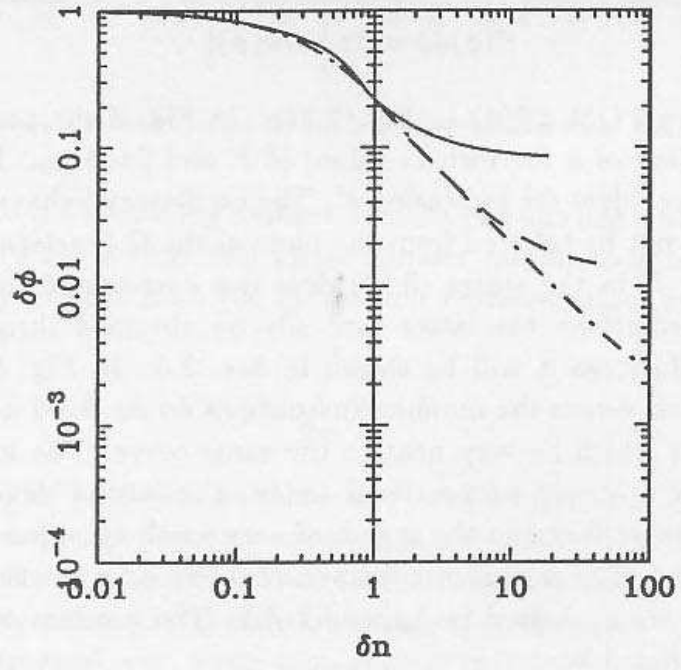

Fig. 4. Reciprocal peak likelihood $\delta\phi$ vs. the number fluctuations δn for $\langle \hat{n} \rangle = n_0 = 1$ (full line), $n_0 = 10$ (dashed line), $n_0 = 100$ (dot-dash line).

in agreement with the value obtained in Ref. 19. The value of the uncertainty product in Eq. (3.57) is almost twice the one expected in agreement with the conventional Heisenberg inequality. One should notice, however, that for the number-phase pair the uncertainty product could even be lower than 1/2 when approaching the number eigenstates for $F \to 0$. In such case one obtains the saturating behaviour (derived in Appendix A.2)

$$\delta\phi \simeq 2\pi(1 - 2\delta n) \ , \quad (F \to 0 \ , n_0 = \text{const.} > 0) \ , \tag{3.58}$$

which leads to vanishing uncertainty products.

An other interesting limiting case for the phase distribution is that for $F \to +\infty$ at constant n_0. The asymptotic behaviour of $\delta\phi$ is derived in Appendix A.2

$$\delta\phi \simeq n_0^{-1+n_0/F} \quad (F \to +\infty \ , n_0 = \text{const.} > 0) \ , \tag{3.59}$$

and now leads to infinite uncertainty products. Here a more detailed analysis of the $F \to +\infty$ limiting case is in order, to analyze some different phase-narrowing mechanisms. More generally one can consider the case of non-constant average number n_0 related to F through the power-law

$$n_0 = cF^{\nu} \ . \tag{3.60}$$

Different families of limiting states are obtained from Eq. (3.54), depending on the values of ν. For $\nu > 1$ one obtains highly excited states which are very similar to coherent states, but slightly distorted in a way corresponding to superpoissonian distributions. In this case the effect due to large average numbers n_0 dominates that due to increasing F. For $\nu = 1$ highly excited $SU(1,1)$ states are obtained corresponding to Bargmann index $\kappa = c/2$. In particular for $c = 1$ the following states are obtained

$$|F; F; \psi\rangle \simeq_{F\to+\infty} F^{-1/2} \sum_{n=0}^{\infty} \left(1 - F^{-1}\right)^{n/2} e^{in\psi} |n\rangle \ , \tag{3.61}$$

which for infinite F give exactly the SG states (2.16). For the states (3.61) the phase probability distribution can be analytically evaluated. One obtains

$$\begin{aligned} P(\phi) &= \frac{F^{-1}}{2\pi} \left(1 - 2\sqrt{1 - F^{-1}} \cos(\phi - \psi) + 1 - F^{-1}\right)^{-1} \\ &\simeq \frac{F^{-1}}{2\pi} \frac{2}{8 \sin^2\left[\frac{1}{2}(\phi - \psi)\right] + F^{-2}} \ , \end{aligned} \tag{3.62}$$

which approaches a delta-like distribution in the limit of infinite F. Equation (3.62) leads to the following RPL

$$\delta\phi \simeq \pi F^{-1} \equiv \pi n_0^{-1} \quad (F = n_0 \to +\infty) \ , \tag{3.63}$$

and to the uncertainty product

$$\delta\phi\delta n \simeq \pi \ . \tag{3.64}$$

In the present limiting case a perfectly sharp probability distribution is obtained at the cost of infinite average number n_0. This leads us to consider in more detail the case of constant n_0 ($\nu = 0$), which gives the RPL in Eq. (3.59). The corresponding asymptotic states are evaluated in Appendix A.2

$$|n_0; F; \psi\rangle \simeq_{F\to+\infty} F^{-\frac{n_0}{2F}} \left[|0\rangle + \sqrt{\frac{n_0}{F}} \sum_{n=1}^{\infty} \frac{(1-F^{-1})^{n/2}}{\sqrt{n}} e^{in\psi}|n\rangle\right] \ . \tag{3.65}$$

In Table 5 the phase performances of the various asymptotic states are summarized. For comparison the truncated phase states and the optimum states of Ref. 19 are reported. The truncated phase states read as follows

$$|\psi\rangle = (2n_0+1)^{-1/2} \sum_{n=0}^{2n_0} e^{in\psi}|n\rangle \ , \tag{3.66}$$

whereas the optimum states, which minimize $\delta\phi$ at fixed n_0,[19] have the form

$$|\psi\rangle = \frac{\sqrt{6}}{\pi} \sum_{n=0}^{M} (1+n)^{-1} e^{in\psi}|n\rangle \ , \quad M \sim \frac{6}{\pi^2} e^{\frac{\pi^2}{6}n_0} \ . \tag{3.67}$$

The states (3.61) and (3.66) have the same limiting phase-distribution for infinite F and, therefore, they exhibit the same asymptotic $\delta\phi$ for large n_0. The states (3.61, 3.66) have a peak likelihood which is π times that of the states (3.65); however, there is no improvement in the power-law dependence of $\delta\phi$ versus the average number $\delta\phi \sim n_0^{-1}$, which should be compared with the optimal behaviour $(12/\pi)n_0^{-2}$ of the states (3.67). The similar 'long-range' number distributions $P(n) \sim n^{-\alpha}$ of the states (3.65, 3.67) lead to analogous phase probability distributions. The latter are compared in Fig. 5 for the same values of n_0 and F. One can see that the two distributions are both heavy-tailed and exhibit a sharp peak around the average value. Near the average value the tails decrease faster for the states (3.65), but are higher near the boundaries $\phi = \pm\pi$. For small average numbers n_0 the states (3.65) show a RPL slightly improved with respect to that of (3.67): this should not be surprising, as the states (3.67) actually are optimal states only for large n_0. Further considerations of these particular probability distributions can be found in Refs. 19, 70.

I end this subsection with some numerical results regarding the squeezing properties of the one-mode states. In Ref. 33 the behaviour of the squeezing parameter for the states (3.50) versus j, κ is reported: here the relationship between squeezing and phase-number distribution is considered in more detail.

Table 5. Reciprocal peak likelihood $\delta\phi$ and uncertainly product a high average photon number n_0 for the various asymptotic states considered in the text (GTS: group theoretical states).

States		$\delta\phi$	$\delta\phi\delta n$	See Eq.
Coherent states		$(\pi/2n_0)^{1/2}$	$(\pi/2)^{1/2}$	(3.57)
GTS	$F \to 0$, n_0 =const.	2π	0	(3.58)
	$F \to \infty$, $n_0 = F$	πn_0^{-1}	π	(3.61) (3.62) (3.63) (3.64)
	$F \to \infty$, n_0 =const.	n_0^{-1}	∞	(3.59) (3.65)
Truncated phase states		πn_0^{-1}	$\pi/\sqrt{3}$	(3.66) (Ref. 19)
Optimum states		$(12/\pi)n_0^{-2}$	∞	(3.67) (Ref. 19)

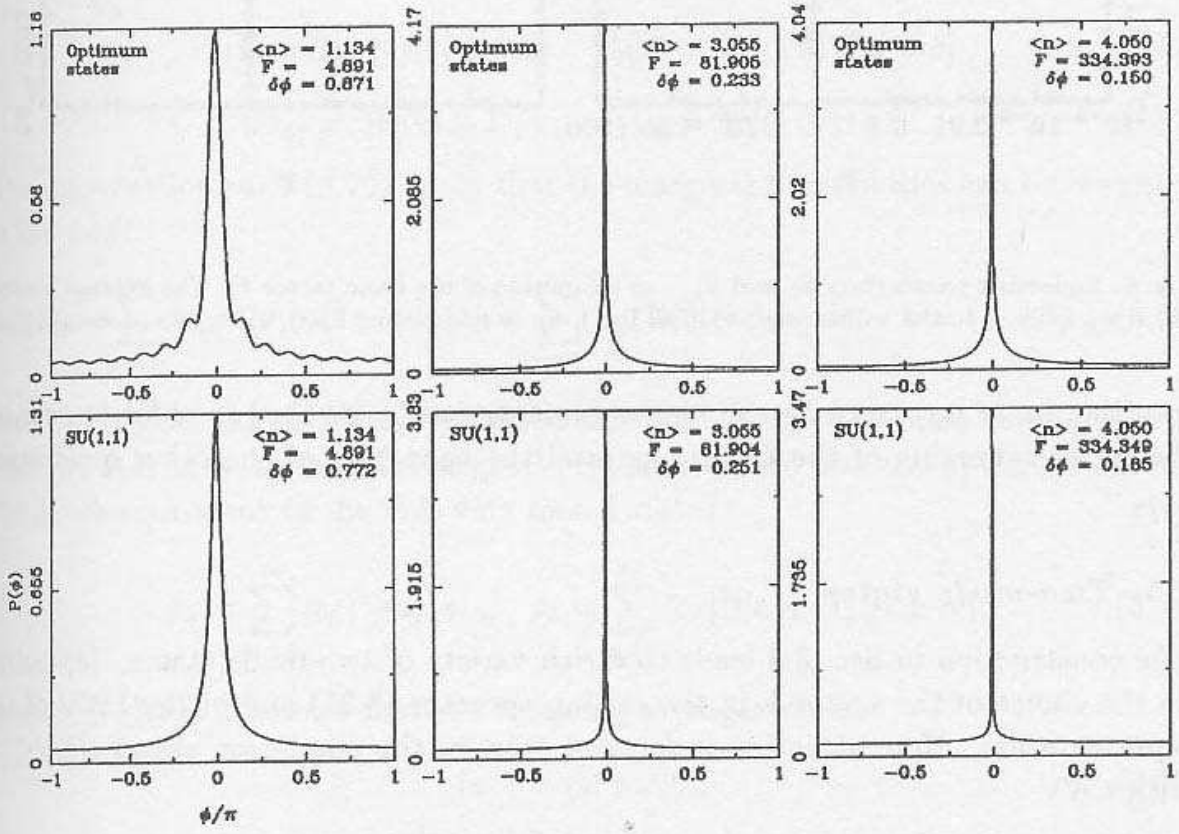

Fig. 5. Comparison between the phase distributions of the optimum states and $SU(1,1)$ states.

In Fig. 6 the squeezing parameters S_0 and $S_{\pi/2}$ are plotted as a function of F for fixed $\langle\hat{n}\rangle = n_0$. The curves representing $S_{\pi/2}$ show a minimum for $F < 1$ which becomes lower and moves towards higher F for increasing n_0. $S_{\pi/2}$ increases monotonically for increasing $F > 1$. The behaviour of S_0 is complementary to that of $S_{\pi/2}$, the quadrature $\hat{a}_{\pi/2}$ being squeezed in the superpoissonian range and unsqueezed for $F < 1$. The main features of the above plots can be qualitatively understood looking at the behaviour of the Q-function (3.55) on the complex plane z, where the real axis corresponds to $\langle a_0\rangle$ and the imaginary one to $\langle a_{\pi/2}\rangle$. A moderate number-squeezing also corresponds to a_0-squeezing, whereas for higher number-squeezing the Q-function begins to spread in the horizontal direction,

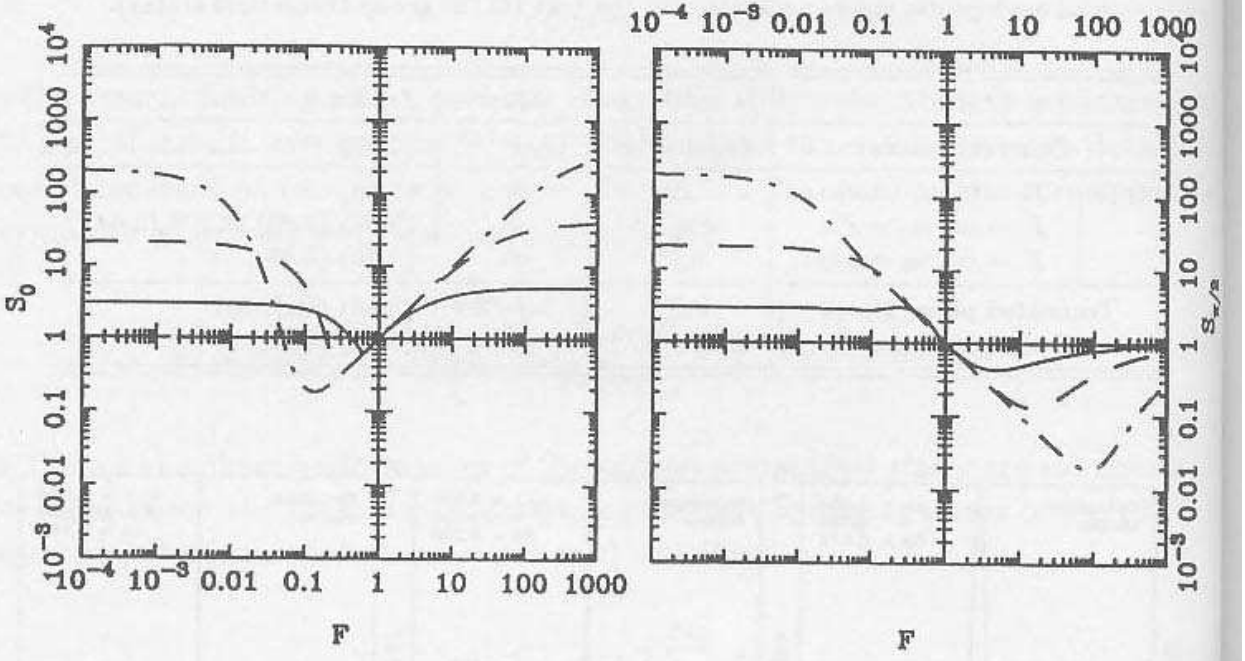

Fig. 6. Squeezing parameters S_0 and $S_{\pi/2}$ as a function of the Fano factor F. The average numbe $\langle\hat{n}\rangle = n_0$ is fixed to the values: $n_0 = 1$ (full line), $n_0 = 10$ (dashed line), $n_0 = 100$ (dot-dash line)

resulting in an increased S_0. Similar arguments can be invoked in order to connec the phase-squeezing of the Q-function and the squeezing of the other quadratur $\hat{a}_{\pi/2}$.

3.5. *Two-mode states*

The construction in Sec. 3.3 leads to a rich variety of two-mode states, dependin on the choice of the vector $\mathbf{k}$ in the raising operator (3.25) and of the LWV of th representation. Here attention is focused only on the one-boson states ($|k_l| \leq 1$ with LWV

$$|\mathbf{v}\rangle = |0, N\rangle \ . \tag{3.68}$$

The effect of multiboson ($|k_l| > 1$) transformation will be considered in Sec. 3.6.

The Schwinger-like realizations correspond to angular momentum $j = N/2$ fo $SU(2)$ and to Bargmann index $\kappa = (N+1)/2$ for $SU(1,1)$; the WH case is recovere as a limit for infinite j or κ. Using Eq. (3.21) and the realizations in Table 2, th two-mode states can be written as follows

$$|\zeta; N\rangle_{WH} = \exp\left(-\frac{1}{2}|\zeta|^2\right) \sum_{n=0}^{\infty} \frac{\zeta^n}{\sqrt{n!}} |n, N+n\rangle \ ,$$

$$|\zeta; j; N; \pm\rangle_{SU(2)} = (1+|\zeta|^2)^{-j} \sum_{n=0}^{2j} \binom{2j}{n}^{1/2} \zeta^n |n, N \pm n\rangle \ , \tag{3.69}$$

$$|\zeta;\kappa;N\rangle_{SU(1,1)} = (1-|\zeta|^2)^{\kappa}\sum_{n=0}^{\infty}\binom{2\kappa+n-1}{n}^{1/2}\zeta^n|n,N+n\rangle\ .$$

Notice that there are two possible set of states for $SU(2)$ (here denoted by $|\zeta;j;N;\pm\rangle_{SU(2)}$), depending on the choice of the possible vectors $\mathbf{k}=(1,\pm1)$. Depending on $\mathbf{k}$ the surpositions (3.69) satisfy the conservation rules

$$b^\dagger b \mp a^\dagger a = N\ , \qquad \mathbf{k}=(1,\pm1)\ . \tag{3.70}$$

For the two-mode states the quantum statistics are described by the joint-probability distributions of two observables. On the other hand, whenever only one mode is considered one uses the marginal distributions and averages

$$P_a(\theta) = \mathrm{Tr}[(|\theta\rangle\langle\theta|\otimes\hat{1})\hat{\rho}] \quad P_b(\theta) = \mathrm{Tr}[(\hat{1}\otimes|\theta\rangle\langle\theta|)\hat{\rho}]\ , \tag{3.71}$$

$$\langle\hat{\Theta}_a\rangle = \mathrm{Tr}[(\hat{\Theta}\otimes\hat{1})\hat{\rho}]\ , \quad \langle\hat{\Theta}_b\rangle = \mathrm{Tr}[(\hat{1}\otimes\hat{\Theta})\hat{\rho}]\ . \tag{3.72}$$

The conservation rules (3.70) imply that the marginal probabilities can be rewritten in the form

$$P_a(\theta) = \sum_{n=0}^{\infty}|c_n|^2|\langle\theta|n\rangle|^2\ , \quad P_b(\theta) = \sum_{n=0}^{\infty}|c_n|^2|\langle\theta|N\pm n\rangle|^2\ , \quad \mathbf{k}=(1,\pm1)\ , \tag{3.73}$$

where c_n denote the expansion coefficients in Eqs. (3.69). The main consequence of Eqs. (3.73) is that, as long as marginal probabilities are concerned, the pure states (3.69) are equivalent to the following mixed states

$$\hat{\rho}_a = \sum_{n=0}^{\infty}|c_n|^2||n\rangle\langle n|\ , \quad \hat{\rho}_b = \sum_{n=0}^{\infty}|c_n|^2||n\pm N\rangle\langle n\pm N|\ . \tag{3.74}$$

From Eq. (3.74) it follows that the following averages vanish

$$\langle a^n\rangle = \langle b^n\rangle = 0\ , \tag{3.75}$$

and, therefore, one has

$$S_{a_\phi} = 1+2\langle a^\dagger a\rangle\ , \qquad S_{b_\phi} = 1+2\langle b^\dagger b\rangle\ , \tag{3.76}$$

namely there is no squeezing and the squeezing parameter is isotropic. Also from Eq. (3.74) if follows that the marginal number distributions are identical to those of the corresponding one-mode states.

Regarding the phase of the field Eq. (3.74) lead to constant marginal probability distributions. The conservation laws (3.70) imply the following algebraic rules for the phase joint-probability distributions $P^{(2)}$

$$P^{(2)}(\phi_a,\phi_b) = P(\phi_a\pm\phi_b)\ , \quad \mathbf{k}=(1,\pm1)\ , \tag{3.77}$$

where $P(x)\equiv P^{(1)}(x)$ denotes the corresponding one-mode distribution.

I now turn attention to the cross-correlation properties of the present two-mode GTS. They are given by the (normalized) correlation functions[62] $G^{(2)}$

$$G^{(2)} = \frac{\langle a^\dagger b^\dagger b a\rangle}{\langle a^\dagger a\rangle\langle b^\dagger b\rangle} \,. \tag{3.78}$$

Using the expansions (3.69) one obtains

$$G^{(2)} = \begin{cases} \dfrac{N+1+|\zeta|^2}{N+|\zeta|^2} \,, & (WH) \,, \\ \dfrac{N+1+(2\kappa-N)|\zeta|^2}{N+(2\kappa-N)|\zeta|^2} \,, & (SU(1,1)) \,, \\ \dfrac{N\pm1+(N\pm2j)|\zeta|^2}{N+(N\pm2j)|\zeta|^2} \,, & (SU(2)) \,. \end{cases} \tag{3.79}$$

For $\mathbf{k} = (1,1)$ one has $G^{(2)} \geq 1$ for any value of N and ζ, reflecting the tendency for the two modes to be created or annihilated simultaneously. The opposite behaviour happens for the $SU(2)$ states at $\mathbf{k} = (1,-1)$, which turns out to be never cross-correlated. High correlation functions can be obtained for $N = 0$ and small ζ for $\mathbf{k} = (1,1)$. The 'classical' limits $N \to \infty$ or $\zeta \to \infty$ lead to $G^{(2)} = 1$, corresponding to the fact that the photons in the different modes are created or annihilated independently.

3.6. *Multiboson states*

In the previous subsections I considered only one-boson states, namely states generated from the vacuum through the action of a raising operator $\hat{R}^+_{\mathbf{k}\sigma}$ which creates no more than one boson for each mode ($|k_l| \leq 1$). In this subsection I analyze the effects on the quantum statistics due to the simultaneous creation of $k_l > 1$ bosons for the same field mode l. For simplicity I restrict attention only to the one-mode states. In Sec. 4 I will show how these states can be generated using an ideal photon-number amplifier.

The transformation $\mathcal{M}^{(k)}$ from the one-boson to the k-boson states is the following ($k > 1$)

$$\mathcal{M}^{(k)}(|\psi\rangle) = |\psi\rangle_{(k)} \,, \quad |\psi\rangle = \sum_{n=0}^{\infty} c_n |n\rangle \,, \quad |\psi\rangle_{(k)} = \sum_{n=0}^{\infty} c_n |kn\rangle \,. \tag{3.80}$$

It is equivalent to rewriting the boson realization of the Lie algebra of the state by substituting a and $a^\dagger$ with the corresponding k-boson operators $a_{(k)}$ and $a^\dagger_{(k)}$ given in Table 3. This can be readily shown upon writing the transformation $\mathcal{S}^{(k)}$ of a general operator $\hat{O}$ in the number representation

$$\hat{O} = \sum_{nm=0}^{\infty} O_{nm} |n\rangle\langle m| \longrightarrow \mathcal{S}^{(k)}(\hat{O}) = \sum_{\lambda=0}^{k-1} \sum_{nm=0}^{\infty} O_{nm} |nk+\lambda\rangle\langle mk+\lambda| \,. \tag{3.81}$$

One can check the following transformations

$$\mathcal{S}^{(k)}\left(a^{\dagger}\right)=a_{(k)}^{\dagger}=\left\{\frac{[\hat{n}/k](\hat{n}-k)!}{\hat{n}!}\right\}^{1/2}(a^{\dagger})^{k}\ ,\quad \mathcal{S}^{(k)}(a)=a_{(k)}\equiv\left[\mathcal{S}^{(k)}\left(a^{\dagger}\right)\right]^{\dagger}\ ,$$
$$\mathcal{S}^{(k)}\left(\hat{O}(a,a^{\dagger})\right)=\hat{O}\left(a_{(k)},a_{(k)}^{\dagger}\right)\ , \tag{3.82}$$

where $\hat{O}(a,a^{\dagger})$ represents the functional dependence of $\hat{O}$ on the particle operators a and $a^{\dagger}$. Two examples of multiboson realizations are given in Table 3 — the k-boson Holstein-Primakoff $su(2)$ and $su(1,1)$: the corresponding states are analyzed in Ref. 33.

The effect of the transformation $\mathcal{M}^{(k)}$ on the number distribution is the rescaling

$$p_{(k)}(n)\doteq|_{(k)}\langle\psi|n\rangle|^{2}=\begin{cases}p_{(1)}(n/k) & \langle n/k\rangle=0\ ,\\ 0 & \text{otherwise}\ .\end{cases} \tag{3.83}$$

Correspondingly the mth moment is multiplied by the factor k^{m}, namely

$$\langle\hat{n}^{m}\rangle_{(k)}=k^{m}\langle\hat{n}^{m}\rangle\ . \tag{3.84}$$

Both the average number and the Fano factor are amplified by k.

The effect of the multiboson transformation (3.90) on the phase distribution is the inverse of that on the number distribution. Using the POM in Eq. (2.36) one obtains

$$p_{(k)}(\phi)d\phi\doteq|_{(k)}\langle\psi|e^{i\phi}\rangle|^{2}\frac{d\phi}{2\pi}\equiv p_{(1)}(k\phi)d\phi\ . \tag{3.85}$$

For functions $f(\phi)$ which are periodic of $2\pi/k$, Eq. (3.85) yields the relations between averages

$$\langle\hat{f}_{\Phi}\rangle_{(k)}=\langle\hat{g}_{\Phi}\rangle_{(1)}\ ,\quad g(\phi)=f(\phi/k)\ . \tag{3.86}$$

Notice that Eq. (3.85) leads to a RPL $\delta\phi$ which is constant as a function of k.

From Eqs. (3.85–3.86) one concludes that the multib3.oson transformation $\mathcal{M}^{(k)}$ simultaneously amplifies the number and deamplifies the phase by the same factor k. This is shown in Fig. 7, where the distributions of a coherent state are compared with those of the $k=4$ transformed state. The combined effect on the number-phase distributions is qualitatively recovered in the Q-function representation: in the phase space the multiboson transformation corresponds to a symmetrical splitting of the quantum distribution into k identical replicas, with enhanced number-fluctuations and reduced phase-uncertainties (the quantum distribution becomes longer in the radial direction and narrower in the tangential one). The origin of the symmetrical splitting of the Q-function becomes evident upon rewriting the k-photon state as a superposition of one-photon states

$$|\psi\rangle_{(k)}=k^{-1}\sum_{\lambda=0}^{k-1}|\psi_{\lambda}^{(k)}\rangle\ ,\quad |\psi_{\lambda}^{(k)}\rangle=\sum_{n=0}^{\infty}c_{[n/k]}e^{i2\pi\lambda\langle n/k\rangle}|n\rangle\ . \tag{3.87}$$

The phase factors in Eq. (3.87) are responsible for the splitting in the phase space, whereas the fractional labels of the coefficients $c_{[n/k]}$ produce the spreading in the radial direction.

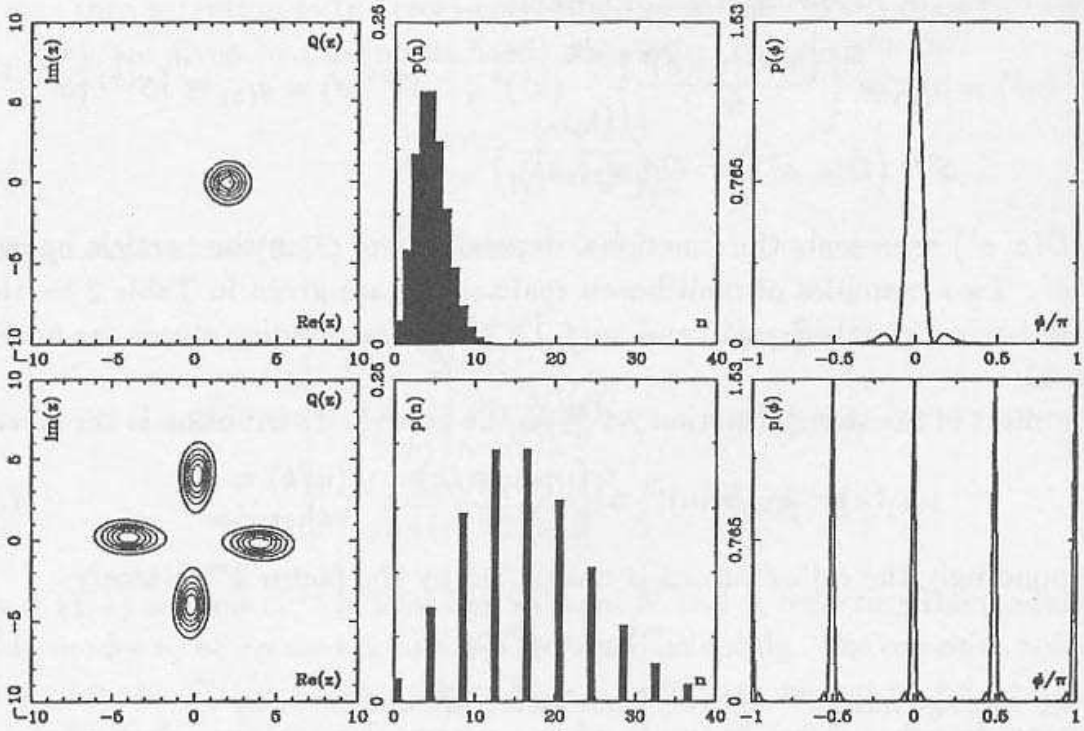

Fig. 7. The effect of the multiboson transformation (3.80) on the coherent state $|\alpha\rangle$, for $k = 4$ and $\alpha = 2$. The one-oson and multiboson distributions $Q(z)$, $p(n)$ and $p(\phi)$ are compared.

As regards the squeezing properties of the multiphoton states, a simple check shows that squeezing is possible only for $k \leq 2$. More generally, one can define $2m$-th order squeezing S_ϕ^{2m} as the ratios of the $2m$-th moments of a_ϕ over the corresponding value for the vacuum : then, $2m$-th order squeezing is possible only for $k \leq 2m$.[34] Numerical results for the probability distribution of a_ϕ and the squeezing S_ϕ^{2m} as a function of the average number are reported in Ref. 34 for the two-photon WH GTS, in Ref. 33 for the two-photon Holstein-Primakoff GTS, whereas in Ref. 35 the behaviour of the minimum squeezing S_ϕ^{2m} is analyzed for various k-photon GTS as a function of $\langle \Delta n^2 \rangle$. The numerical evaluations lead to universal scaling laws of the form

$$S_\phi^{2m} \sim \langle \Delta n^2 \rangle^{-\gamma_k(m)} , \tag{3.88}$$

where the exponent $\gamma_k(m)$ ranges between 0 and 1.

3.7. *Fractional states*

In Sec. 3.6 the transformation $\mathcal{S}_{(k)}$ in Eq. (3.82) was defined for positive integer k only. One can notice that $\mathcal{S}_{(1)}(a^\dagger) = a^\dagger$, and, with a little algebra,

$$\mathcal{S}_{(k)} \circ \mathcal{S}_{(h)} \left(a^\dagger\right) = \mathcal{S}_{(kh)} \left(a^\dagger\right) . \tag{3.89}$$

From Eq. (3.89) it follows that one may, at least formally, extend the semigroup of nonlinear transformations (3.82) to the Abelian group $\{\mathcal{S}_{(k)}$ rational $k > 0\}$, by

defining the inverse transformation $\mathcal{S}_{(k)}^{-1}$ as follows

$$\mathcal{S}_{(k)}^{-1} \circ \mathcal{S}_{(k)} \left(a^\dagger\right) = a^\dagger = \mathcal{S}_{(1)} \left(a^\dagger\right) \ . \tag{3.90}$$

One can therefore equate $\mathcal{S}_{(k)}^{-1} = \mathcal{S}_{(1/k)}$, whence

$$\mathcal{S}_{(k)}^{-1} \circ \mathcal{S}_{(h)} = \mathcal{S}_{(h/k)} = \mathcal{S}_{(r)} \ , \tag{3.91}$$

where $r \equiv h/k$ is a positive rational number. It is this extension of the multiboson transformation which leads to the notion of *fractional photons* introduced in Ref. 43.

The above formal structure is equivalent to considering the action of h-boson operators on k-photon states, producing matrix elements of the form

$$\langle km| \left(a_{(h)}^\dagger\right)^u (a_{(h)})^v |kn\rangle = \left(\frac{[tm]![tn]!}{[tm-u]![tn-v]!}\right)^{\frac{1}{2}} \delta_{u,v+t(m-n)} \ , \quad t^{-1} = r = h/k \ . \tag{3.92}$$

When $u = v$ the expectation (3.92) always has nonzero values for $m = n$. When $u \neq v$, the expression (3.92) vanishes unless $(h/k)(u-v)$ is an integer.

Note that expression (3.92) depends on h and k only through their ratio: $t^{-1} = r = h/k$. Here r is the positive rational fraction of the fractional transformation $\mathcal{S}_{(r)}$. One may equate expression (3.92) *formally* to an expectation involving fractional photons

$$\langle km| \left(a_{(h)}^\dagger\right)^u (a_{(h)})^v |kn\rangle = \langle m| \left(a_{(r)}^\dagger\right)^u (a_{(r)})^v |n\rangle \ . \tag{3.93}$$

Thus the claim of Ref. 43 is not that such fractional photon modes really exist, but that physical experiments involving integral numbers of photons can be interpreted as behaving in such fractional mode.

In Ref. 44 physical quantum states are constructed which exhibit the probability distributions of fractional photon states. More precisely, the physical states have probability distributions for the usual one-photon observables $\hat{O} = \hat{O}_{(1)}$ which are identical to the fractional probabilities $p_{(t)}(O)$ for any observable $\hat{O}_{(h)} = \hat{O}(a_{(h)}, a_{(h)}^\dagger)$ of the form (3.82). The definition of the probability distribution for fractional photon states is based on the construction of a complete set of simultaneous eigenvectors of $\hat{O}_{(h)}$ and the 'Casimir' operator

$$\hat{D}_{(h)} = a^\dagger a - h a_{(h)}^\dagger a_{(h)} \ , \tag{3.94}$$

which commutes with all the h-boson operators. The eigenkets of $\hat{O}_{(h)}$ are written in terms of the eigenkets $|O\rangle$ of the operator $\hat{O} = \hat{O}_{(1)}$ as follows

$$\hat{O}_{(h)}|O,\lambda\rangle_{(h)} = O|O,\lambda\rangle_{(h)} \ , \qquad \hat{D}_{(h)}|O,\lambda\rangle_{(h)} = \lambda|O,\lambda\rangle_{(h)} \ ,$$
$$|O,\lambda\rangle_{(h)} = \sum_{l=0}^{\infty} |lh+\lambda\rangle\langle l|O\rangle \ . \tag{3.95}$$

Then, the probability distribution for $\hat{O}_{(h)}$ in the k boson state $|\psi\rangle_{(k)}$ reads

$$p_{(t)}(O) = \sum_{\lambda=0}^{h-1} |_{(h)}\langle O, \lambda|\psi\rangle_{(k)}|^2 \ . \tag{3.96}$$

For example, the 'number operator' $\hat{N}_{(h)} = a^\dagger_{(h)} a_{(h)}$ has the probability distribution[44]

$$p_{(t)}(N) = \sum_{\lambda=0}^{h-1} |_{(h)}\langle N, \lambda|\psi\rangle_{(k)}|^2 = \sum_{l,m=0}^{\infty} \overline{c}_m c_l \delta_{[tm],N} \delta_{[tl],N} \delta_{\langle tm\rangle,\langle tl\rangle} \ . \tag{3.97}$$

Now I require that the observables $\hat{O}$ describing the physical system are functions of the usual particle operators a and $a^\dagger$ — instead of $a_{(h)}$ and $a^\dagger_{(h)}$ — looking for a quantum state $\hat{\rho}^{(t)}_\psi$ with probability distributions

$$p_{(t)}(O) = \mathrm{Tr}\left[|O\rangle\langle O|\hat{\rho}^{(t)}_\psi\right] \tag{3.98}$$

identical to the fractional probabilities (3.97) for all observables $\hat{O}$.[44,45] The attempt to construct such a state leads to reconsider the distribution $p_{(t)}(O)$ in the form

$$\begin{aligned} p_{(t)}(O) &= \sum_{\lambda=0}^{h-1} \sum_{l,m=0}^{\infty} {}_{(k)}\langle\psi|lh+\lambda\rangle\langle l|O\rangle\langle O|m\rangle\langle mh+\lambda|\psi\rangle_{(k)} \\ &= \sum_{l,m=0}^{\infty} \langle l|O\rangle\langle O| \left[\sum_{\lambda=0}^{h-1} |m\rangle\langle mh+\lambda|\psi\rangle_{(k)} \cdot {}_{(k)}\langle\psi|lh+\lambda\rangle\langle l|\right] |l\rangle \ . \end{aligned} \tag{3.99}$$

Equation (3.99) shows clearly that $p_{(t)}(O)$ is reproduced by the $\hat{O}$-probability distribution of the following mixed state

$$\hat{\rho}^{(t)}_\psi = \sum_{\lambda=0}^{h-1} |\psi^{(t)}_\lambda\rangle\langle\psi^{(t)}_\lambda| \ , \tag{3.100}$$

where

$$|\psi^{(t)}_\lambda\rangle = \sum_{m=0}^{\infty} \psi^{(t)}_{\lambda,m} |m\rangle \ , \quad \psi^{(t)}_{\lambda,m} = e^{i\phi_\lambda} \langle mh+\lambda|\psi\rangle_{(k)} \tag{3.101}$$

and ϕ_λ are arbitrary phases. One can easily check that the density matrix $\hat{\rho}^{(t)}_\psi$ is correctly normalized

$$\mathrm{Tr}\hat{\rho}^{(t)}_\psi = \sum_{m=0}^{\infty} \sum_{\lambda=0}^{r-1} |\psi^{(t)}_{\lambda,m}|^2 = |\psi|^2 = 1 \ . \tag{3.102}$$

In the above framework, the 'inverse' of the multiboson transformation $\mathcal{M}^{(k)}$ is given by

$$\mathcal{M}^{(1/k)}(|\psi\rangle\langle\psi|) = \hat{\rho}^{(1/k)}_\psi = \sum_{\lambda=0}^{k-1} |\psi^{(1/k)}_\lambda\rangle\langle\psi^{(1/k)}_\lambda| \ . \tag{3.103}$$

One should notice, however, that $\mathcal{M}^{(1/k)} \circ \mathcal{M}^{(k)} = 1$, whereas $\mathcal{M}^{(k)} \circ \mathcal{M}^{(1/k)} \neq 1$: in Sec. 5.4 I will show that invertible transformations can be defined upon enlarging the underlying Hilbert space $\mathcal{H}$ and introducing an auxiliary boson mode.

The transformation $\mathcal{M}^{(1/k)}$ in Eq. (3.103) is referred to as *fractional-photon transformation* or simply *photon fractioning*, as opposed to the multiphoton transformation of Eq. (3.80). The effects of the photon fractioning on the quantum statistics of the state are essentially the inverse of those of the multiboson transformation, as one would expect. In particular, the number distribution is transformed as follows

$$p_{(1/k)}(n) \doteq \mathrm{Tr}\left[\hat{\rho}_{\psi}^{(1/k)}|n\rangle\langle n|\right] = \sum_{\lambda=0}^{k-1} p_{(1)}(nk+\lambda) \;, \tag{3.104}$$

and produces the moments

$$\langle \hat{n}^m \rangle_{(1/k)} = \langle [\hat{n}/k]^m \rangle \;. \tag{3.105}$$

For highly excited states Eq. (3.105) approximates the inverse of the multiboson scaling (3.84), namely

$$\langle \hat{n}^m \rangle_{(1/k)} \simeq k^{-m} \langle \hat{n}^m \rangle \;, \quad (\langle \hat{n} \rangle \gg k) \;. \tag{3.106}$$

The transformed phase-distribution is evaluated through the following steps

$$p_{(1/k)}(\phi)d\phi \doteq \mathrm{Tr}[\hat{\rho}_{\psi}^{(1/k)} d\hat{\Phi}(\phi)] = \frac{d\phi}{2\pi} \sum_{\lambda\mu=0}^{k-1} \sum_{nm=0}^{\infty} \delta_{\lambda\mu} \bar{c}_{nk+\lambda} c_{mk+\mu} e^{i(nk+\lambda-mk-\mu)k^{-1}\phi}$$

$$= \frac{d\phi}{2k\pi} \sum_{\nu=0}^{k-1} \sum_{nm=0}^{\infty} \bar{c}_n c_m e^{i(n-m)k^{-1}(\phi+2\pi\nu)} \;, \tag{3.107}$$

which lead to the relation

$$p_{(1/k)}(\phi)d\phi = \sum_{\lambda=0}^{k-1} p_{(1)}(k^{-1}\phi + 2\pi k^{-1}\lambda) d(k^{-1}\phi) \;, \tag{3.108}$$

and give the following averages for any 2π-periodic function $f(\phi)$

$$\langle \hat{f}_{\Phi} \rangle_{(1/k)} = \langle \hat{g}_{\Phi} \rangle \;, \quad g(\phi) = f(k\phi) \;, \tag{3.109}$$

where the definition (2.23) has been used. In Ref. 71 the above phase properties of the photon fractioning are revisited in the Pegg-Barnett formalism.[54]

In Fig. 8 the distribution of a coherent state are compared with those of the corresponding fractional state for $k = 10$. The simultaneous number-narrowing and phase-broadening are apparent also in the Q-representation, which exhibits reduced radial fluctuations and is spread out in the tangential direction (for numerical and asymptotical evaluations of $Q(z)$ for large k and $\langle \hat{n} \rangle$ see Ref. 45). On the other hand, as regards the customary quadrature squeezing, the photon fractioning attains

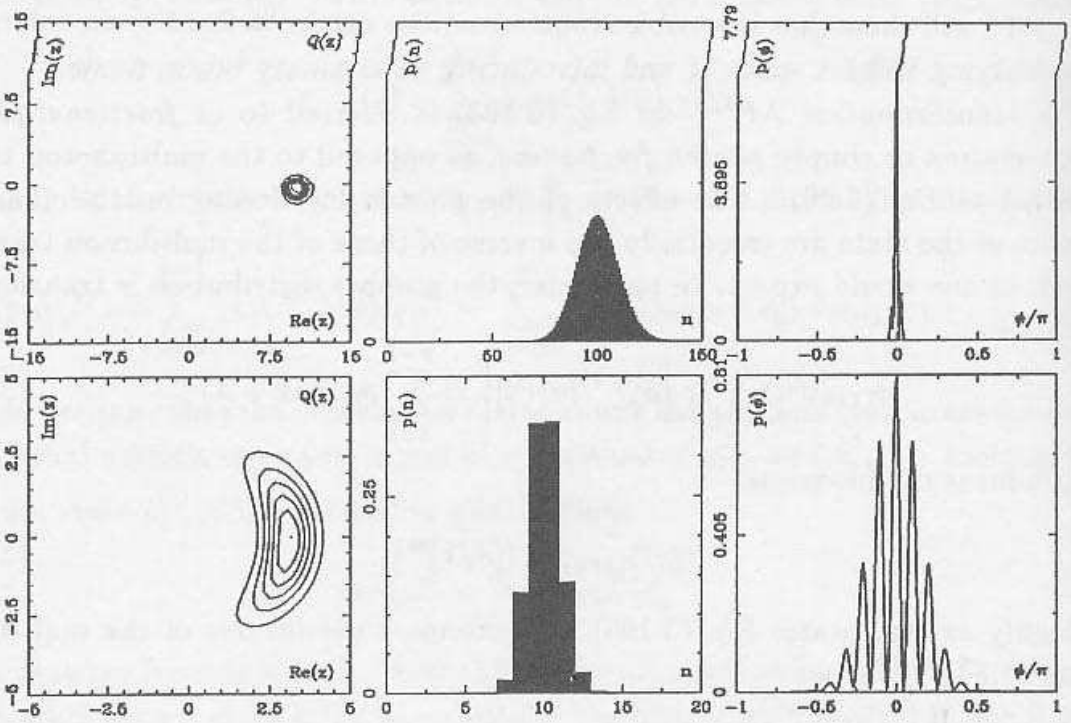

Fig. 8. The effect of photon fractioning (3.103) on the statistics of a coherent state $|\alpha\rangle$. Here $k = 10$ and $\alpha = 10$. The $Q(z)$, $p(n)$ and $p(\phi)$ distributions are compared.

squeezing for all $k > 1$, the squeezing going asymptotically to zero as $S_\phi \sim k^{-1}$ for large k and $\langle \hat{n} \rangle$.[44]

The multiphoton and photon-fractioning transformations, which in the present section have been derived only in an algebraic framework, will be reconsidered in Sec. 5, showing that they describe the ideal photon-number amplification of radiation.

4. Linear Amplification and Loss: An Overview

In this section I briefly recall the quantum description of linear amplifiers and losses. I show that the two-mode $SU(1,1)$ states of Sec. 3.5 can be generated using a phase-insensitive amplifier (PIA), whereas the two-mode $SU(2)$ states are obtained at the output of a beam splitter (BS). In this schematic approach a number eigenstate is needed at an input of the devices, and actually — apart from the case of the vacuum — nearly-number states are very difficult to produce experimentally. Hence, to be complete, the present scheme needs also a device which can produces nearly-number states: as we will see in Sec. 5 this could be provided by an ideal photon-number amplifier (PNA) operating as a high-gain deamplifier on a highly-excited coherent input. On the other hand, an interesting case where only vacuum inputs are needed is that of a particular set of $SU(1,1)$ states attained at the output of a PIA. Such states (sometimes referred to as *twin beams*) will be used in Sec. 6.2

at the input of a photon-number duplicator (PND) in order to produce Susskind-Glogower states. In an analogous way the two-mode states attained through a PIA could be converted into the corresponding one-mode states by means of an ideal PND.

In Sec. 4.4, after recollecting the noise-figures of the linear devices — which depend in general on the input noise of the measured observable — I recall the Yuen's proposal[16,25–27] of improving the noise-figures of the optical taps by means of quantum ideal amplifiers. In the homodyne-detection mode one needs an ideal phase-sensitive amplifier (PSA), essentially a PIA where the two modes — the amplified mode and the *idler* — degenerate on the same mode. For a vacuum input the PSA produces a two-photon GTS of $SU(1,1)$, namely the customary 'squeezed vacuum'. In the direct-detection mode one needs an ideal PNA: the optical taps improved through ideal amplification can be made essentially lossless, making the ideal amplifiers key-devices for applications to local area networks (LAN).

4.1. *Phase insensitive amplification: two-mode* $SU(1,1)$ *states*

Classically, an ideal linear amplifier is represented by the relation between averages

$$\langle A \rangle = G^{1/2} \langle a \rangle \ , \tag{4.1}$$

where a and A are the input and output field modes, and $G > 1$ is the amplification gain. Relation (4.1) is independent of any other feature of the amplifier (apart from G) and contains no randomness in principle. Quantum mechanics introduces unavoidable added noise intrinsic in the amplification mechanism. In fact, relation (4.1) cannot be quantized in the form

$$A = G^{1/2} a \ , \tag{4.2}$$

since that would violate the boson commutations

$$[A, A^\dagger] = [a, a^\dagger] = 1 \ . \tag{4.3}$$

To preserve linearity and commutations one must add a *noise* operator b with $\langle b \rangle = 0$ and satisfying the commutations $[b, b^\dagger] = 1$ and $[a, b] = [a, b^\dagger] = 0$ (the corresponding field mode is usually referred to as *idler mode*). In this fashion the quantum version of the transformation (4.1) can be written in either one of the alternative ways

$$A = ma + nb \ , \tag{4.4}$$

$$A = \mu a + \nu b^\dagger \ , \tag{4.5}$$

where preservation of the commutation relation (4.3) implies the constraints

$$|m|^2 + |n|^2 = 1 \ , \tag{4.6}$$

$$|\mu|^2 - |\nu|^2 = 1 \ . \tag{4.7}$$

Here the quantities corresponding to the gain G in Eq. (4.1) are $|m|^2 < 1$ and $|\mu|^2 > 1$. Therefore, only the transformation (4.5) strictly describes a linear amplification by a gain $G \equiv |\mu|^2 > 1$, whereas the transformation (4.4) is more appropriate for a linear *loss* $\eta = |m|^2 < 1$. In the following I analyze the case of the linear amplifier, and I postpone to the next subsection the study of the linear loss.

The coefficients μ, ν are complex number, accounting also for a phase change in the field evolution. The present amplifier is also called *phase insensitive amplifier* (PIA) because the gain G does not depend on the phase of the homodyne detected electric field, namely $|\langle A_\phi \rangle|^2 = G|\langle a_\phi \rangle|^2$. Corresponding to the second input mode b another output mode B must be considered. Upon a suitable choice of the B phase the commutations $[A, B] = [A, B^\dagger] = 0$ lead to the input-output linear transformations

$$\begin{pmatrix} A \\ B^\dagger \end{pmatrix} = \mathbf{N} \begin{pmatrix} a \\ b^\dagger \end{pmatrix} , \qquad \mathbf{N} = \begin{pmatrix} \mu & \nu \\ \overline{\nu} & \overline{\mu} \end{pmatrix} , \quad |\mu|^2 - |\nu|^2 = 1 . \tag{4.8}$$

The introduction of the idler mode b implies a representation of the quantum amplifier as a four-port device (Fig. 9), in contrast with the classical two-port representation (4.1). If the port b is unused, then its mode is considered in the vacuum state and, therefore, it becomes responsible of added noise.

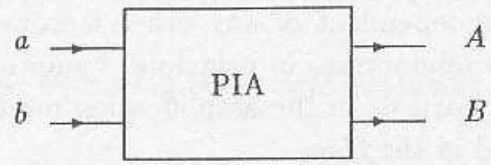

Fig. 9. Scheme of phase insensitive amplifier as a four-port device.

From the algebraic point of view, Eq. (4.8) corresponds to a $SU(1,1)$ transformation. It can be written in the form of unitary evolution of the field as follows

$$\mathbf{N} \begin{pmatrix} a \\ b^\dagger \end{pmatrix} = \hat{N}^\dagger \begin{pmatrix} a \\ b^\dagger \end{pmatrix} \hat{N} . \tag{4.9}$$

Fixing for simplicity the phase of the output A in order to have a real coefficient μ, the unitary operator $\hat{N}$ simply reads

$$\hat{N} = \exp\left(\xi a^\dagger b^\dagger - \overline{\xi} b a\right) , \qquad \xi = \frac{\nu}{|\nu|} \operatorname{atanh} \left| \frac{\nu}{\mu} \right| . \tag{4.10}$$

The operator (4.10) is a two-mode realization of a $SU(1,1)$ group element (see Table 3). As a consequence, the PIA realizes the two-mode $SU(1,1)$ states in Eq. (3.69). More precisely, for an input state of the form

$$|\psi\rangle_{\text{in}} = |0, N\rangle , \tag{4.11}$$

one obtains the output state

$$|\psi\rangle_{\rm out} = |\zeta;\kappa;N\rangle_{SU(1,1)} = (1-|\zeta|^2)^{\kappa}\sum_{n=0}^{\infty}\binom{2\kappa+n-1}{n}^{1/2}\zeta^n|n,N+n\rangle\,,\quad \zeta=\frac{\nu}{|\mu|}\,. \tag{4.12}$$

In practice the state (4.12) can be actually realized at least for $N=0$, namely when the two input states are both vacuum. The states with $N>0$ require a number eigenstate at one input port, which, as already mentioned, could be provided by strongly deamplifying a highly excited coherent state through a PNA. The states (4.12) for $N=0$ are the so-called 'twin beams' which will be used in Sec. 6.2 to produce Susskind-Glogower states.

As regards the Hamiltonian of the PIA, one should notice that the argument of the exponential in Eq. (4.10) is proportional to the interaction Hamiltonian of the device in the Dirac picture. It follows that the interaction Hamiltonian in the Schrödinger picture should depend parametrically on time in the form

$$\hat{H}_I = k\left(a^\dagger b^\dagger e^{-i\Omega t+\phi} + bae^{i\Omega t-\phi}\right)\,, \tag{4.13}$$

where $\Omega=\omega_a+\omega_b$, $kt=|\xi|$ and $\phi=\arg(\xi)$. The parametric dependence on t can be attained using a third *pumping* mode c at frequency Ω, which can be considered classical as long as it is in a highly excited coherent state. Such approximation is usually referred to as *parametric approximation* (equivalently, one says that 'the pump is classical and undepleted').

From the above considerations one concludes that in the parametric approximation a PIA can be attained through a three-wave mixing medium, with Hamiltonian

$$\hat{H}_I = \chi^2\left(a^\dagger b^\dagger c + c^\dagger ba\right)\,,\qquad \omega_c=\omega_a+\omega_b\,, \tag{4.14}$$

or, equivalently, through a degenerate four-wave mixing, namely

$$\hat{H}_I = \chi^3\left(a^\dagger b^\dagger c^2 + (c^\dagger)^2 ba\right)\,,\qquad 2\omega_c=\omega_a+\omega_b\,. \tag{4.15}$$

We will see that the above description of the PIA — where *idler* and *pump* modes are introduced to account for unitarity and energy conservation — is general for all kinds of quantum amplifiers, including the ideal PNA and PND, the only exception being the PSA, where the idler and the amplified modes are degenerate.

4.2. *Beam splitter/frequency converter: two-mode $SU(2)$ states*

The transformation (4.4) corresponding to a linear loss can be treated in a way completely analogous to the PIA. Upon introducing a second output mode B, one obtains the linear transformation

$$\begin{pmatrix}A\\B\end{pmatrix} = \mathrm{M}\begin{pmatrix}a\\b\end{pmatrix}\,,\qquad \mathrm{M}=\begin{pmatrix}m & n\\ -\overline{n} & \overline{m}\end{pmatrix}\,,\quad |m|^2+|n|^2=1\,, \tag{4.16}$$

Eqs. (4.16) describe the Heisenberg evolution of the e.m. field at a beam splitter (BS) with transmission coefficient $\eta = |m|^2$. Eq. (4.16) is a $SU(2)$ transformation. The corresponding unitary evolution reads

$$\mathrm{M}\begin{pmatrix} a \\ b \end{pmatrix} = \hat{M}^\dagger \begin{pmatrix} a \\ b \end{pmatrix} \hat{M} \ , \tag{4.17}$$

and for real m the unitary operator $\hat{M}$ has the form

$$\hat{M} = \exp\left(\xi a^\dagger b - \bar{\xi} b^\dagger a\right) \ , \qquad \xi = \frac{n}{|n|} \arctan\left|\frac{n}{m}\right| \ . \tag{4.18}$$

The operator (4.10) belongs to the two-mode Schwinger realization of the $SU(2)$ group given in Table 3; as a consequence, the BS realizes the two-mode $SU(2)$ states in Eq. (3.69). For an input of the form (4.11) one obtains the output

$$|\psi\rangle_{\mathrm{out}} = |\zeta; j; N; -\rangle_{SU(2)} = (1+|\zeta|^2)^{-j} \sum_{p=0}^{2j} \binom{2j}{p}^{1/2} \zeta^p |p, N-p\rangle \ , \tag{4.19}$$

where

$$\zeta = \frac{n}{|m|} \ . \tag{4.20}$$

Regarding the possibility to realize the input state (4.11), the same arguments discussed for the case of the PIA hold.

As in a BS the frequencies of the two input modes are the same, no pump mode is needed. For different frequencies $\omega_a \neq \omega_b$ the above framework is suited to describe a *frequency converter* (FC). In this case the same three- or four-wave-mixing media used for the PIA can be adopted. It follows that also the FC — as a particular kind of amplifier — needs a pump for energy conservation, whereas the idler mode is that at the converted frequency. Finally, regarding the production of two-mode $SU(2)$ states, the FC works exactly as a BS, the only difference being that in the latter case the two modes have the same frequency (but different wavevectors or polarization).

4.3. *Phase sensitive amplification: SU(1,1) two-photon states*

The phase-sensitive amplifier is a device which ideally would affect the following transformations for a couple of quadratures

$$A_\phi = G^{1/2} a_\phi \ , \quad A_{\phi+\pi/2} = G^{-1/2} a_{\phi+\pi/2} \ , \tag{4.21}$$

namely the gain is 'sensitive' to the phase of the selected quadrature. It is readily seen that Eq. (4.21) corresponds to the following transformation of the field

$$A = \mu a + \nu a^\dagger \ , \tag{4.22}$$

where

$$\mu = \frac{1}{2}\left(G^{1/2} + G^{-1/2}\right) \ , \quad \nu = \frac{e^{2i\phi}}{2}\left(G^{1/2} - G^{-1/2}\right) \ . \tag{4.23}$$

The transformation (4.22) has the same form of (3.9). As opposite to the defining Heisenberg evolutions of the PIA and BS/FC which are not unitary, Eq. (4.22) can be unitarily attained without the need for an auxiliary idler mode. One has

$$A = \hat{U}^\dagger a \hat{U} \ , \qquad \hat{U} = \exp\left\{ -\frac{1}{4} \ln G \left[\left(a^\dagger\right)^2 e^{-i\phi} - a^2 e^{i\phi} \right] \right\} \ . \tag{4.24}$$

From Eq. (4.24) it follows that (in the parametric approximation) the ideal PSA can be attained through degenerate three- or four-wave mixing, tuning the frequency of the pump mode at $\Omega = 2\omega_a$ or $\Omega = \omega_a$ respectively.

Regarding the output states, Eq. (4.22) implies that the PSA transforms an input CS into an output QSS (3.7) as follows

$$|\alpha\rangle \longrightarrow |\alpha', \zeta\rangle \ , \quad \alpha' = \alpha\mu + \overline{\alpha}\nu \ , \quad \zeta = e^{i \arg(\nu)} a\tanh \left| \frac{\nu}{\mu} \right| \ . \tag{4.25}$$

In particular, using a vacuum input one obtains an output 'squeezed vacuum' (3.8), namely a $SU(1,1)$ state corresponding to the two-photon $\lambda = 0$ realization in Table 3.

4.4. *Noise figures: the preamplified optical tap*

The noise operator b in the quantum description of both the PIA and the BS/FC degrades the SNR from the input a to the output A. Qualitatively the SNR degradation is described by the *noise figure* of the device

$$\mathcal{N}(\hat{O}) = \frac{SNR(\hat{O})_{\text{in}}}{SNR(\hat{O})_{\text{out}}} \ , \tag{4.26}$$

where the SNR depends on the observable $\hat{O}$ which is actually detected

$$SNR(\hat{O}) = \frac{\langle \hat{O} \rangle^2}{\langle \Delta \hat{O}^2 \rangle} \ . \tag{4.27}$$

The cases of interest are $\hat{O} = \hat{n}$ (direct detection) and $\hat{O} = \hat{a}_\phi$ (homodyne detection), with b in the vacuum state. (Actually the heterodyne detection, which corresponds to the measurement of both the quadratures of the field, has an intrinsic added noise of 3dB due to the joint measurement of two noncommuting observables.[1,72,73]) Using the transformation (4.5) one obtains the following noise figures for the PIA

$$\mathcal{N}(\hat{a}_\phi) = 1 + \frac{G-1}{GS_\phi} \ , \quad \mathcal{N}(\hat{n}) \simeq 1 + \frac{G-1}{GF} \ , \quad \langle \hat{n} \rangle_{\text{in}} \gg 1 \ . \tag{4.28}$$

Both the squeezing S_ϕ and the Fano factor F are evaluated at the input (the simple form for the direct detection noise figure is obtained in the limit of large input powers). For the BS/FC the noise figures are

$$\mathcal{N}(\hat{a}_\phi) = 1 + \frac{1-\eta}{\eta S_\phi} \ , \quad \mathcal{N}(\hat{n}) = 1 + \frac{1-\eta}{\eta F} \ . \tag{4.29}$$

For coherent input states (corresponding to $S_\phi = F = 1$) 3dB noise-figures are obtained for both a high-gain PIA and a 50-50 BS. As suggested by Yuen,[16,25–27] the noise figures (4.28-4.29) can be improved by means of a suitable pre-amplification. The method is simply to enhance the input squeezing S_ϕ or the Fano factor F in Eqs. (4.28–4.29) without adding substantial preamplification noise. This would be achieved using a high-gain preamplifier with unit noise figure $\mathcal{N}(\hat{O})$ for the observable of interest. For example, in the homodyne detection mode the ideal preamplifier would be a high-gain $\hat{a}_\phi$-amplifier having unit noise figure $\mathcal{N}(\hat{a}_\phi)$: this amplifier coincides with the PSA analyzed in Sec. 4.3. In the same fashion, in the direct-detection mode the ideal amplifier would be a high-gain photon-number amplifier (PNA), which, by definition, has a unit noise figure $\mathcal{N}(\hat{n})$.

The above method for improving the noise figures can be used to reduce losses in optical taps, enabling a very large number of users to obtain the same performance as the first one.[27] The idea is simply to use quasi-ideal (namely nearly-unit noise-figure) amplifiers as tap preamplifiers. The tap can be actually schematized as a BS (see Fig. 10) where the input information is coded on the a mode, the user taps from the B mode, and the A mode carries the information for the other users (the b mode is unused and is responsible for the loss of the tap). Thus, using phase-sensitive preamplification would improve the tap in the homodyne detection mode, whereas photon-number preamplification would be suited to the direct-detection mode. In LAN environments, where nearly-number states and direct-detection optimize the network transparency, the PNA would provide the required low-loss tap. However, the present scheme requires to amplify the signal at every user-node down the line: this problem can be overcome only using PND taps, as it will be shown in Sec. 6.

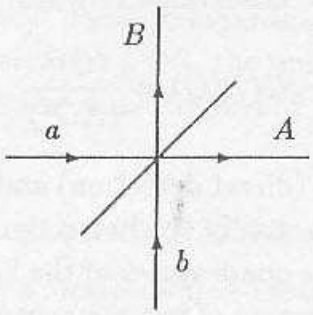

Fig. 10. Scheme of beam splitter.

5. Phase-Number Amplification

In this section the photon number-amplification mechanism is analyzed in the ideal case, reviewing some main results in Refs. 48, 49. It is shown that the search for unitary evolutions leads to consider also a number-deamplification mechanism, and the symmetry between amplification and deamplification is broken by the integer-

valued nature of the number operator. As for the case of the PIA the construction of a unitary evolution leads to consider an auxiliary idler mode of the field, which turns out here to be amplified in the inverse way. We will also see that the two outputs of the ideal photon-number amplifier reproduce the multiphoton and fractional photon states of Secs. 3.6 and 3.7. Moreover, ignoring one of the two field modes is equivalent to consider the amplifier as an open system, and this will lead to entropy production.

In the last subsection I give the Hamiltonians of the ideal device, comparing it with those of realistic systems. I will show that the amplification is driven by a peculiar dependence of the polarizability on the phase of the field in the frequency range of the amplified mode.

5.1. *The ideal amplifier*

In order to attain the ideal noise-figure $\mathcal{N}(\hat{n}) = 1$, the photon number-amplifier should effect the state transformation

$$|n\rangle \rightarrow |Gn\rangle \ , \tag{5.1}$$

for an integer $G > 1$, thus preserving the direct detection signal-to-noise ratio: the evolution (5.1) is noting but the G-boson transformation $\mathcal{M}^{(G)}$ in Eq. (3.80).

In a way analogous to the phase-sensitive amplification — where two conjugated quadrature components of the electric field are inversely amplified — an ideal PNA should inversely amplify the number and the phase. In this fashion the state transformation (5.1), involving only number eigenstates, becomes too restrictive. Therefore, as a definition of the number amplification, I adopt the Heisenberg evolution

$$\hat{n} \rightarrow G\hat{n} \ , \tag{5.2}$$

whereas the state of the field is described in general by a density matrix $\hat{\rho}$. Another point which I consider is the possibility of deamplifying $\hat{n}$, namely of amplifying $\hat{n}$ by a noninteger gain $G < 1$. The integer-valued nature of $\hat{n}$ breaks the symmetry between amplification and deamplification, as it forbids exact deamplification. The transformation (5.2) can be generalized to the following one

$$\hat{n} \rightarrow [G\hat{n}] \ , \tag{5.3}$$

which is defined for real gains G. The transformation (5.3) coincides with (5.2) for integer G. In Sec. 5.3 I will show that only the cases $G \equiv$ *integer* and $G \equiv$ *inverse of integer* lead to unitary evolutions, the second case corresponding to using the amplifier in the output-input reversed direction.

As regards the phase amplification one should write an Heisenberg evolution for a suitable phase operator. An exact phase amplification — inverse of the amplification (5.2) — can be defined using the SG operators $\hat{e}^{\pm}$ as follows

$$\hat{e}^{\pm} \rightarrow (\hat{e}^{\pm})^{G^{-1}} \ . \tag{5.4}$$

In the high-energy limit Eq. (5.4) corresponds to the amplification of the Dirac operator

$$\hat{\Phi}_D \to G^{-1}\hat{\Phi}_D \ . \tag{5.5}$$

Equation (5.4) shows how the integer-valued nature of $\hat{n}$ reflects on the phase operators $\hat{e}^{\pm}$: the amplification (5.4) can simply be attained for $G^{-1} = r$ integer, raising the shift operators to the integer power r, whereas, for the number operator, preservation of its integer-valued nature requires G itself to be an integer. Despite this fact, we will see that the phase amplification (5.4) leads to the correct amplification of the optimum POM (2.36) for both cases $G \equiv$ *integer* and $G^{-1} = r \equiv$ *integer*. The second case can be readily proven after recognizing that the transformation (5.4) for $G^{-1} = r$ integer corresponds to the algebra transformation $\mathcal{S}^{(r)}$ in Eq. (3.82), namely

$$(\hat{e}^{\pm})^r = \mathcal{S}^{(r)}(\hat{e}^{\pm}) \ . \tag{5.6}$$

Evaluations similar to those in Eq. (3.107) yield

$$\mathcal{S}^{(r)}(d\hat{\Phi}(\phi)) = \sum_{\lambda=0}^{r-1} d\hat{\Phi}(r^{-1}\phi + 2\pi r^{-1}\lambda) \ , \tag{5.7}$$

which leads to the exact scaling for 2π-periodic functions

$$\mathcal{S}_H^{(r)}(\hat{f}_\Phi) = \hat{g}_\Phi \ , \quad g(\phi) = f(r\phi) \ . \tag{5.8}$$

On the other hand, in Sec. 5.5 I will define a map $\mathcal{S}_H^{(1/r)}$ which attains the deamplification of the phase

$$\mathcal{S}_H^{(1/r)}(d\hat{\Phi}(\phi)) = d\hat{\Phi}(r\phi) \ , \tag{5.9}$$

leading to the scaling of the $2\pi/r$-periodic functions

$$\mathcal{S}_H^{(1/r)}(\hat{f}_\Phi) = \hat{g}_\Phi \ , \quad g(\phi) = f(\phi/r) \ . \tag{5.10}$$

Both the maps $\mathcal{S}_H^{(r)}$ and $\mathcal{S}_H^{(1/r)}$ will be obtained by means of a unitary transformation on an enlarged two-mode system.

5.2. *CP maps*

One of the major difficulties encountered in the quantum mechanical treatment of the number amplification is related to the nonunitarity of the transformations (5.1-5.3). This can be simply understood by considering that $\{|Gn\rangle\}$ span only a proper subspace of the Fock space $\mathcal{H}$ (which is spanned by $\{|n\rangle\}$). As suggested in Ref. 26 and as already seen in the case of the PIA, a way to overcome this problem is to consider an auxiliary degree of freedom — the analogous of the idler mode for the PIA — and construct a unitary operator on an enlarged Hilbert space $\mathcal{H} \otimes \mathcal{H}'$, $\mathcal{H}'$ being infinite dimensional. Here I recall the construction of the unitary operator presented is in Refs. 48, 49.

The first step is to recognize that the transformations (5.2) and (5.3) are unit-preserving *normal completely positive maps* (shortly CP maps).[23,24] CP maps are used to describe the subdynamics of the open quantum systems. A normal unit-preserving CP map has the general form

$$\mathcal{T}(\hat{O}) = \sum_{\alpha} \hat{V}_{\alpha}^{\dagger} \hat{O} \hat{V}_{\alpha} \ , \tag{5.11}$$

where

$$\sum_{\alpha} \hat{V}_{\alpha}^{\dagger} \hat{V}_{\alpha} = 1 \ . \tag{5.12}$$

The space of the CP maps is closed under: i) convex combination $\sum_i p_i \mathcal{T}_i$; ii) composition $\mathcal{T}_1 \mathcal{T}_2$; iii) tensor product $\mathcal{T}_1 \otimes \mathcal{T}_2$; iv) partial trace: namely, if $\mathcal{T}$ is CP on $\mathcal{H}_1 \otimes \mathcal{H}_2$ and $\hat{\rho}_2$ is a density operator on $\mathcal{H}_2$, then

$$\mathcal{T}_1(\hat{O}) = \mathrm{Tr}_2[\hat{\rho}_2 \mathcal{T}(\hat{O} \otimes \hat{1})] \tag{5.13}$$

is CP on $\mathcal{H}_1$. The last point means that if one has a unitary evolution in a closed system and if subdynamics on a (open) subsystem can be defined — i.e. partial trace on the subsystem degrees of freedom — then these subdynamics are normal unit-preserving CP maps. The Stinespring theorem[74,75] assures that every normal unit-preserving CP map has a unitary extension, namely there exists a quantum state and a unitary evolution such that the CP map is the partial trace on the subsystem degrees of freedom. In some cases it is also possible to reconstruct unitary evolutions on enlarged systems independently of the quantum state. This is the case, for example, when $\hat{V}_{\alpha}$ satisfy the orthogonality relations

$$\hat{V}_{\alpha} \hat{V}_{\beta}^{\dagger} = \delta_{\alpha\beta} \ . \tag{5.14}$$

Then, the following operator is unitary on $\mathcal{H}_1 \otimes \mathcal{H}_2$, $(\mathcal{H}_1 \equiv \mathcal{H}_2)$

$$\hat{U} = \sum_{\alpha} \hat{V}_{\alpha} \otimes \hat{W}_{\alpha}^{\dagger} \ , \quad \hat{W}_{\alpha} = \hat{A} \hat{V}_{\alpha} \hat{B} \ , \tag{5.15}$$

$\hat{A}$ and $\hat{B}$ being unitary operators on $\mathcal{H}_2$. The CP map in Eq. (5.11) corresponds to the partial trace (5.13) where $\mathcal{T}$ is the unitary evolution given by the operator (5.15). In the next subsection I show that this is exactly the case of the phase-number amplification given by Eqs. (5.3) and (5.4) for $G^{-1} = r$ integer: on the other hand, the transformations for integer G will be obtained later from the unitary transformation.

5.3. *The amplifying map*

Hereafter I will distinguish between the Heisenberg and the Shrödinger-picture versions of a map $\mathcal{S}$ using the symbols $\mathcal{S}_H$ and $\mathcal{S}_S$: the two are related through the identity

$$\mathrm{Tr}(\hat{\rho} \mathcal{S}_H(\hat{O})) = \mathrm{Tr}(\mathcal{S}_S(\hat{\rho}) \hat{O}) \ , \tag{5.16}$$

which states invariance of averages under the picture.

In the previous subsection we have recognized that the map in Eq. (5.6) attaining integer gain-r phase-amplification is equivalent to the r-photon transformation of the algebra, hereafter denoted by $\mathcal{S}_H^{(r)}$. From Eq. (3.81) it turns out that the $\mathcal{S}_H^{(r)}$ acting on a generic operator $\hat{O}$ has the general form

$$\mathcal{S}_H^{(r)}(\hat{O}) = \sum_{\lambda=0}^{r-1} (\hat{S}_\lambda^{(r)})^\dagger \hat{O} \hat{S}_\lambda^{(r)} \ , \quad \hat{S}_\lambda^{(r)} = e^{i\phi_\lambda} \sum_{n=0}^{\infty} |n\rangle\langle nr+\lambda| \ , \tag{5.17}$$

and the phase factors, being totally ineffective in the action (5.17), will be dropped in the following. The operators $\hat{S}_\lambda^{(r)}$ in the definition of the map (5.17) satisfy the following relations

$$\sum_{\lambda=0}^{r-1} \left(\hat{S}_\lambda^{(r)}\right)^\dagger \hat{S}_\lambda^{(r)} = 1 \ , \tag{5.18}$$

$$\hat{S}_\lambda^{(r)} \left(\hat{S}_\mu^{(r)}\right)^\dagger = \delta_{\lambda\mu} \ , \tag{5.19}$$

$$\hat{S}_\lambda^{(r)} \hat{S}_\mu^{(s)} = \hat{S}_{\lambda s+\mu}^{(rs)} \ . \tag{5.20}$$

Equation (5.18) is analogous to the completeness relation (5.12) and assures that $\mathcal{S}_H^{(r)}$ is a normal unit-preserving CP map. Equation (5.19) corresponds to the orthogonality relation (5.14) and thus allows one to recover a unitary evolution on an enlarged quantum system. I postpone to the following subsections the construction of the corresponding unitary evolution and the related Hamiltonians, to continue the discussion on the properties of the map.

Equation (5.20) leads to semigroup composition of the maps $\mathcal{S}_H^{(r)}$

$$\mathcal{S}_H^{(r)} \circ \mathcal{S}_H^{(s)} = \mathcal{S}_H^{(rs)} \ , \tag{5.21}$$

which has already been given in Eq. (3.89). On the other hand, as a consequence of the completeness and orthogonality relations (5.18) and (5.19), $\mathcal{S}_H^{(r)}$ preserves the operator products and the adjoint operation, thus transforming consistently the whole operator algebra. The preservation of the operator product implies that the transformation $\mathcal{S}_H^{(r)}$ applied to a generic operator $\hat{O} = \hat{O}(a, a^\dagger)$ (self-adjoint analytic function of a and $a^\dagger$) can simply be obtained substituting a and $a^\dagger$ with $a_{(r)}$ and $a_{(r)}^\dagger$, i.e. $\mathcal{S}_H^{(r)}(\hat{O}) = \hat{O}(a_{(r)}, a_{(r)}^\dagger)$.

The completeness and orthogonality relations (5.18) and (5.19) are preserved by similarity transformations

$$\hat{S}_\lambda'^{(r)} = \hat{V} \hat{S}_\lambda^{(r)} \hat{W} \ , \tag{5.22}$$

$\hat{V}$ and $\hat{W}$ being unitary operators. However, the only similarity transformations which preserve the Heisenberg evolutions (5.3) and (5.4) are the permutations of the λ's

$$\hat{S}_\lambda'^{(r)} = \hat{P} \hat{S}_\lambda^{(r)} = \hat{S}_{P(\lambda)}^{(r)} \ , \tag{5.23}$$

where $\hat{P}$ denotes the operator representing a permutation of the λ's, namely $\hat{P}|nr+\lambda\rangle = |nr + P(\lambda)\rangle$.

5.4. *The unitary transformation*

The unitary evolution corresponding to $\mathcal{S}_H^{(r)}$ can be constructed as indicated in Eq. (5.15) by using two different photon modes in the amplification process. The unitary operator is the following one acting on the Fock space of the composite system $\mathcal{H} \otimes \mathcal{H}$

$$\hat{U}_{(r)} = \sum_{\lambda=0}^{r-1} \hat{S}_\lambda^{(r)} \otimes (\hat{R}_\lambda^{(r)})^\dagger \ . \tag{5.24}$$

Here $\hat{R}_\lambda^{(r)}$ are similar to $\hat{S}_\lambda^{(r)}$ in the sense of Eq. (5.23). The semigroup property (5.20) reflects on the composition law for the operators $\hat{U}_{(r)}$

$$\hat{U}_{(r)}\hat{U}_{(s)} \simeq_P \hat{U}_{(rs)} \ , \tag{5.25}$$

the symbol $\simeq_P$ denoting similarity under permutations (5.23).

Among all operators $\hat{U}_{(r)}$ the case of $\hat{R}_\lambda^{(r)} = \hat{S}_\lambda^{(r)}$, namely

$$\hat{U}_{(r)} = \sum_{\lambda=0}^{r-1} \hat{S}_\lambda^{(r)} \otimes \left(\hat{S}_\lambda^{(r)}\right)^\dagger \ , \tag{5.26}$$

is particularly interesting, because the second field mode undergoes the transposed transformation of $\mathcal{S}_H^{(r)}$. One should notice, however, that the action on the second mode generally depends on the first input state $\hat{\rho}_1$. As a matter of fact, fact, the action of $\hat{U}_{(r)}$ on number eigenstates is not symmetric with respect to the two modes, as a consequence of the broken symmetry between the amplification and deamplification. One has

$$\hat{U}_{(r)}|n,m\rangle = |[n/r], mr + \langle n/r \rangle\rangle \ , \tag{5.27}$$

and the second mode undergoes an exact number-amplification only if the first field is in a r-photon state — namely it contains only number of photons multiple of r — in particular if it is in the vacuum state. Equation (5.27) may be rewritten in the following more symmetrical form

$$\hat{U}_{(G^{-1})}|n,m\rangle = |[Gn] + G\langle G^{-1}m\rangle,\ [G^{-1}m] + G^{-1}\langle Gn\rangle\rangle \ , \tag{5.28}$$

which coincides with Eq. (5.27) for $G^{-1} = r$ integer, whereas, for G integer, corresponds to the same equation, but with the roles of the two modes interchanged: this is a consequence of the identity

$$\hat{U}_{(G)}^\dagger = \hat{U}_{(G)}^{-1} = \hat{U}_{(G^{-1})} \ . \tag{5.29}$$

Notice that Eq. (5.28) leads to integer-valued number of photons only if either G or G^{-1} is an integer.

The subdynamics of the two modes are obtained as marginal dynamics, namely upon evaluating the expectation of one-mode operators through partial tracing. The subdynamics of the first photon mode correspond to $\mathcal{S}_H^{(r)}$

$$\left\langle \hat{U}_{(r)}^{\dagger}\hat{O}_1\hat{U}_{(r)}\right\rangle = \mathrm{Tr}\left[(\hat{\rho}_1\otimes\hat{\rho}_2)\hat{U}_{(r)}^{\dagger}(\hat{O}_1\otimes\hat{1})\hat{U}_{(r)}\right] = \mathrm{Tr}_1\left[\hat{\rho}_1\mathcal{S}_H^{(r)}(\hat{O}_1)\right] , \qquad (5.30)$$

where the uncorrelated pair of states $(\hat{\rho}_1\otimes\hat{\rho}_2)$ represents the input of the amplifier. As regards the subdynamics of the second photon mode, one has

$$\langle \hat{U}_{(r)}^{\dagger}\hat{O}_2\hat{U}_{(r)}\rangle = \mathrm{Tr}\left[(\hat{\rho}_1\otimes\hat{\rho}_2)\hat{U}_{(r)}^{\dagger}(\hat{1}\otimes\hat{O}_2)\hat{U}_{(r)}\right] = \mathrm{Tr}_2\left(\hat{\rho}_2\sum_{\lambda=0}^{r-1}(\hat{V}_{\lambda}^{(r)})^{\dagger}\hat{O}_2\hat{V}_{\lambda}^{(r)}\right) , \qquad (5.31)$$

where

$$\hat{V}_{\lambda}^{(r)} = c_{\lambda}\left(\hat{S}_{\lambda}^{(r)}\right)^{\dagger} , \quad c_{\lambda} = \left\{\mathrm{Tr}_1\left[\hat{\rho}_1(\hat{S}_{\lambda}^{(r)})^{\dagger}\hat{S}_{\lambda}^{(r)}\right]\right\}^{1/2} . \qquad (5.32)$$

Therefore, the number-amplified mode undergoes the CP map

$$\mathcal{S}_H^{(1/r)}(\hat{O}) = \sum_{\lambda=0}^{r-1}\left(\hat{V}_{\lambda}^{(r)}\right)^{\dagger}\hat{O}\hat{V}_{\lambda}^{(r)} , \qquad (5.33)$$

which, due to the form of operators $\hat{V}_{\lambda}^{(r)}$ in Eq. (5.32), depends on the state $\hat{\rho}_1$ of the other field (this is a consequence of the amplifying-deamplifying broken symmetry). The case of $\hat{\rho}_1$ equal to the vacuum state is particularly simple

$$\mathcal{S}_H^{(1/r)}(\hat{O}) = (\hat{V}_0^{(r)})^{\dagger}\hat{O}\hat{V}_0^{(r)} , \quad \hat{V}_0^{(r)} \equiv (\hat{S}_0^{(r)})^{\dagger} = \sum_{n=0}^{\infty}|rn\rangle\langle n| , \qquad (5.34)$$

and corresponds to the exact number-amplification

$$\mathcal{S}_H^{(1/r)}(f(\hat{n})) = f(r\hat{n}) . \qquad (5.35)$$

On the other hand, as already announced, the map (5.33) for a general $\hat{\rho}_1$ produces the desired phase-deamplification. In fact, the optimum POM transforms as follows

$$\begin{aligned}\mathcal{S}_H^{(1/r)}(d\hat{\Phi}(\phi)) &= \frac{d\theta}{2\pi}\sum_{n,m,p,q=0}^{\infty}\sum_{\lambda=0}^{r-1}|c_{\lambda}|^2 e^{i(n-m)\theta}|p\rangle\langle pr+\lambda|n\rangle\langle m|qr+\lambda\rangle\langle q| \\ &= \sum_{\lambda=0}^{r-1}|c_{\lambda}|^2\frac{d\theta}{2\pi}\sum_{p,q=0}^{\infty}e^{i(p-q)r\theta}|p\rangle\langle q| = d\hat{\Phi}(r\phi) , \end{aligned} \qquad (5.36)$$

and leads to the exact scaling (5.8) for $2\pi/r$-periodic functions.

The subdynamics of the two modes in the Schrödinger picture can be evaluated through the identity (5.16). For the first mode one obtains

$$\mathcal{S}_S^{(r)}(\hat{\rho}) = \sum_{\lambda=0}^{r-1}\hat{S}_{\lambda}^{(r)}\hat{\rho}\left(\hat{S}_{\lambda}^{(r)}\right)^{\dagger} , \qquad (5.37)$$

whereas, for the second mode, in the exact number-amplification case one has

$$\mathcal{S}_S^{(1/r)}(\hat{\rho}) = \hat{V}_0^{(r)} \hat{\rho} \left(\hat{V}_0^{(r)}\right)^\dagger \ . \tag{5.38}$$

Comparing Eq. (5.37) with Eq. (3.103) one can see that $\mathcal{S}_S^{(r)} \equiv \mathcal{M}^{(1/r)}$, namely the Schrödinger evolution of the first mode is the photon-fractioning transformation. Analogously, by comparing Eq. (5.38) with Eq. (3.80) one finds that $\mathcal{S}_S^{(1/r)} = \mathcal{M}^{(r)}$, i.e. the Schrödinger evolution of the second mode is the r-photon transformation. Therefore, the two modes undergoes inverse number-amplification: the exact number-amplification is equivalent to the multiphoton transformation, whereas the number deamplification corresponds to the photon fractioning. It follows that both multiboson and fractional states can be produced at the output of the PNA.

Apart from the pump mode, the ideal PNA in the present framework is a four-port nonlinear device, as schematically sketched in Fig. 11. In practical applications, however, it is useful to consider the PNA as a two-port device, focusing attention only on the subdynamics of one field mode and actually ignoring the other one. This description is equivalent to considering the PNA as an open quantum system, which no longer preserves both the energy and the entropy of the input field. However, the amplification and the deamplification cases now become quite different, due to the the broken-symmetry between the two. Despite that the exact amplification (5.38) is not unitary (it is only an isometry), it preserves the Newmann-Shannon entropy

$$S(\hat{\rho}) = -\mathrm{Tr}\hat{\rho} \log \hat{\rho} \ . \tag{5.39}$$

The entropy conservation follows from the orthogonality conditions (5.19) which imply that $\left(\hat{V}_0^{(r)}\right)^\dagger \hat{V}_0^{(r)} = 1$ (but $\hat{V}_0^{(r)}(\hat{V}_0^{(r)})^\dagger \neq 1$). Thus, the physical picture of the abstract number-amplification $|n\rangle \rightarrow |rn\rangle$ corresponds to an ideal PNA operating with the auxiliary field in the vacuum (namely a PNA at zero temperature). As long as the number-amplification is attained exactly, no entropy change of the field occurs.

On the other hand, the number-deamplification (5.37) corresponds to an isometric evolution which no longer preserves the entropy (5.39). Here, the entropy change depends only on the gain $G^{-1} = r$ and on the input state of the deamplified field (and not on the other field). It is worth noticing that the entropy during deamplification can either increase or decrease as a function of r. As the photon number-deamplification leads to the vacuum state for $r = G^{-1} \rightarrow \infty$, the entropy is asymptotically a decreasing function of r for large r. On the other hand, the evolution (5.37) would in general transform a pure state into a mixed one (the only state which are left pure being the number eigenstates and the r-photon states), and thus leads to an increase of entropy in this case. Therefore, when a pure state is number-deamplified, the entropy exhibits at least one maximum as a function of the inverse gain r. In Fig. 12 the Newmann-Shannon entropy (5.39) is plotted as

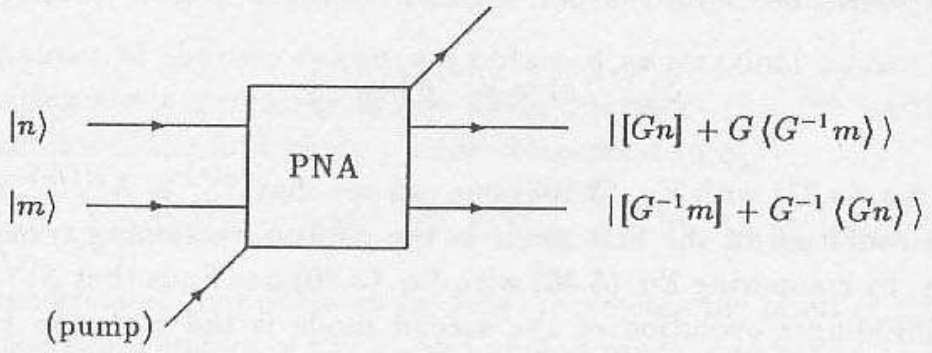

Fig. 11. Scheme of the ideal PNA.

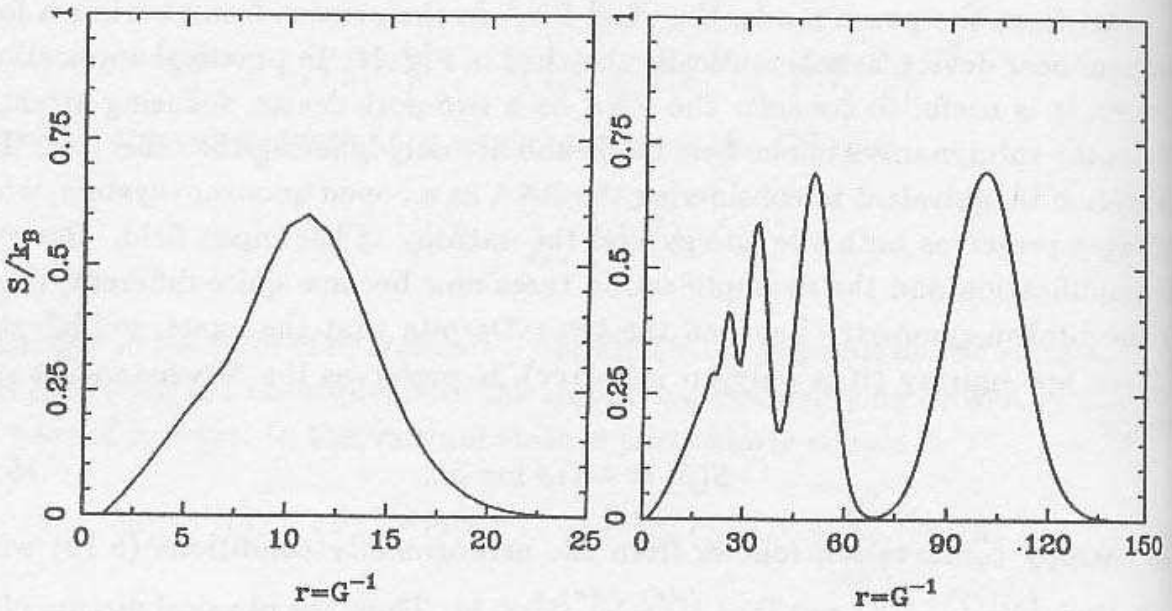

Fig. 12. Deamplification Newmann-Shannon entropy versus the inverse gain $r = G^{-1}$ for a coherent state with $\langle \hat{n} \rangle = 10$ photons (figures on the left) and $\langle \hat{n} \rangle = 100$ photons.

a function of r, for two different input coherent states. One can see that for small average number of input photons the entropy has only one maximum, whereas for intense input fields several maxima appear and local very low minima can occur (corresponding to almost pure states). As a rule, for coherent inputs the maxima are located approximately at $r \simeq |\alpha|^2/l$, $|\alpha|^2$ being the average number of input photons and $l = 1, 2, \ldots$: the maxima decrease for increasing l and the entropy S is always smaller than $\log 2$, which is the entropy of two pure states mixing.

5.6. *The Hamiltonian*

I consider the operator $\hat{U}_{(G^{-1})}$ in Eq. (5.27) only for the case $G^{-1} = r$ integer, as the integer-G case $\hat{U}_{(G)}$ corresponds to the inverse operator $\hat{U}^{\dagger}_{(G^{-1})}$. I denote by $a^{\dagger}$ and $b^{\dagger}$ the particle operators of the two modes, namely

$$|n,m\rangle = \frac{(a^\dagger)^n}{\sqrt{n!}}\frac{(b^\dagger)^m}{\sqrt{m!}}|0,0\rangle \ . \tag{5.40}$$

Comparing the transformation (5.28) with the action of the multiboson operator $a^\dagger_{(r)}$

$$a^\dagger_{(r)}|n\rangle = \sqrt{[n/r]+1}|n+r\rangle \ , \tag{5.41}$$

one can see that the ideal amplification (5.27) can be attained by interchanging $a^\dagger$ with $b^\dagger_{(r)}$ and then permuting $a^\dagger$ with $b^\dagger$. The operator permuting the a and b modes has the form (apart from a sign)

$$\hat{V} = \exp\left[\frac{\pi}{2}\left(a^\dagger b - b^\dagger a\right)\right] \ . \tag{5.42}$$

As a consequence, the operator $\hat{U}_{(r)}$ is given by

$$\hat{U}_{(r)} = \exp\left[\frac{\pi}{2}\left(a^\dagger b - b^\dagger a\right)\right]\exp\left[-\frac{\pi}{2}\left(a^\dagger_{(r)} b - b^\dagger a_{(r)}\right)\right] \ . \tag{5.43}$$

The representation (5.27) of the operator $\hat{U}_{(r)}$ in Eq. (5.43) can be checked directly using Eqs. (5.40) and (5.41). The product of exponentials in Eq. (5.43) corresponds to the series of two four-port devices. The first exponential describes a parametric FC from ω_a to ω_b, with classical pump at frequency $\Omega' = \omega_a - \omega_b$. The second device corresponds to a phase-number amplifier which simultaneously converts frequencies, having a classical pump at frequency $\Omega = r\omega_a - \omega_b$. The corresponding interaction Hamiltonian has the form

$$\hat{H}_I = -ik\left(a^\dagger_{(r)} b e^{-i\Omega t} - b^\dagger a_{(r)} e^{i\Omega t}\right) \tag{5.44}$$

and the interaction length L is given by

$$kL = \pi/2 \ , \tag{5.45}$$

k being the gain coefficient per unit length.

The Hamiltonian (5.44) is complicated by the presence of the multiboson operators $a_{(r)}$. However, for high average number of photons $\langle a^\dagger a\rangle \gg r$ the multiboson operators behave asymptotically as follows

$$\begin{aligned} a^\dagger_{(r)} &= \left\{\frac{[a^\dagger a/r]\,(a^\dagger a - r)!}{a^\dagger a!}\right\}^{1/2}(a^\dagger)^r \\ &= [a^\dagger a/r]^{1/2}\,(a^\dagger a - r + 1)^{-1/2}\, r^{\frac{1}{2}}\hat{\kappa}^{(r)}_\Phi a^\dagger \sim \hat{\kappa}^{(r)}_\Phi a^\dagger \ , \end{aligned} \tag{5.46}$$

where

$$\kappa^{(r)}(\phi) = r^{-\frac{1}{2}} e^{-i(r-1)\phi} \ , \tag{5.47}$$

and the notation of Eq. (2.23) is used. Taking into account also the pumping field mode, the phase-number amplifier would require a medium with a $\chi^{(2)}$ susceptibility and an interaction Hamiltonian of the form

$$\hat{H}_I \sim \lambda\hat{\kappa}^{(r)}_\Phi a^\dagger b c + \text{h.c.} \ , \tag{5.48}$$

c denoting the annihilator of the pump mode. From Eq. (5.48) it follows that i order to attain phase-number amplification one should use a $\chi^{(2)}$ medium havin polarizability which depends on the phase of the field according to (5.47) in limited frequency range containing ω_a. The amplifier gain r is involved only in th phase factor (5.47), whereas the interaction length has to be tuned at the complet conversion value $L = \pi/[2\lambda I_c^{1/2}]$, I_c being the average power flux of the (classica undepleted) pump and $\lambda \propto \chi^{(2)}$. For $r = 1$ the usual parametric frequency converte is obtained, and the two exponentials in (5.43) cancel each other, leading to th identity operator. For $r > 1$ the phase dependent coupling in Eq. (5.48) may al be regarded in terms of an intensity dependent coupling for a $\chi^{(r+1)}$ medium (a one can simply check using the polar decomposition of the particle operators). I practice, for a constant coupling one can tune the interaction length as a functio of the intensity, thus obtaining approximate number-amplification in the avera values. For example, for $r = 2$ one has $\hat{\kappa}_\Phi^{(2)} = 2^{-\frac{1}{2}}\hat{e}^+ = (2a^\dagger a)^{-\frac{1}{2}}a^\dagger$. In this way, the usual degenerate four-wave mixing Hamiltonian (5.48) is considered

$$\hat{H}_I = \kappa \left(a^\dagger\right)^2 bc + \text{h.c.} \qquad (5.4$$

($\kappa \propto \chi^{(3)}$), an approximate gain-2 number-amplification can be attained upo choosing an interaction length $L = \pi/[2\kappa\sqrt{I_a I_c}]$.[76] Similar arguments hold for ana ogous $\chi^{(r+1)}$ amplifying media for $r > 2$, as in the resonance fluorescence schem proposed in Ref. 25. On the other hand, the analytic form of Hamiltonian (5.4 also may suggest that improvements in the ideal behaviour of the amplifier could b attained through modulation of the nonlinear susceptibility at wavelengths submu tiple of that carrying the amplified mode (see Eq. (5.47). Very intense, localized an highly nonlinear susceptibilities could be obtained using quantum wells: this ma prefigure a quasi-ideal amplifier in the form of a heterostructure-designed devic Work is in progress along these lines.

6. Number Duplication

As already mentioned, the photon-number duplicator (PND) is a device analogou to a gain-two PNA which, instead of amplifying the number of photons, produc two copies of the same input state for eigenstates of the number operator. Suc a device would be extremely useful in LAN applications, because it provides convenient realization of the quantum nondemolition measurement of the photo number, beside itself realizing lossless optical taps superior to the amplifier tap.[1

The PND is the only state-duplicating device which can be realized in principl In fact, a general 'cloning' device producing multiple copies of a (generally no orthogonal) input set of states would violate unitarity[26,17] (thus, for example, it not possible to duplicate coherent states, as they are not orthogonal).

In the first subsection I give the duplicating CP map and construct a unitar evolution and the corresponding PND Hamiltonian. Arguments related to unitarit — similar to those used for the ideal PNA — lead to the need of a third auxiliar

field mode, thus representing the PND as a six-port device. Input-output energy conservation are taken into account either by means of a classical pump or through frequency-conversion, in a way completely analogous to the case of the PNA.

In the last subsection I will show how a PND can be used in the reverse output-input direction to obtain the one-mode states of Sec. 3.4. In particular this would allow the production of the SG states starting from the $SU(1,1)$ two-mode states (or *twin beams*): the latter, in turn, are produced using a PIA with two vacuum inputs, as already seen in Sec. 4.1.

6.1. *The duplicating map and the Hamiltonian*

For the ideal PNA the unitary transformation was obtained starting from the amplifying CP map defined by the relation

$$\mathcal{S}_H^{(r)}(\hat{e}^{\pm}) = (\hat{e}^{\pm})^r \ . \tag{6.1}$$

The case of the ideal PND can be obtained in strict analogy with Eq. (6.1) by means of the duplicating CP map

$$\mathcal{S}_H(\hat{e}^{\pm}) = \hat{e}^{\pm} \otimes \hat{e}^{\pm} \ . \tag{6.2}$$

The general transformation attaining the duplication of the shift operators (6.2) has the form

$$\mathcal{S}_H(\hat{O}) = \sum_{\lambda=-\infty}^{\infty} \hat{S}_\lambda^\dagger \hat{O} \hat{S}_\lambda \ , \tag{6.3}$$

where the nonunitary operators $\hat{S}_\lambda$ ($\hat{S}_\lambda : \mathcal{H} \otimes \mathcal{H} \to \mathcal{H}$) are given by

$$\hat{S}_\lambda = \sum_{n,m=0}^{\infty} \delta_{m,n+\lambda} |\min\{n,m\}\rangle\langle m,n| \ , \tag{6.4}$$

and satisfy the orthogonality and completeness relations

$$\hat{S}_\lambda \hat{S}_\mu^\dagger = \delta_{\lambda\mu} \hat{1} \ , \tag{6.5}$$

$$\sum_{\lambda=-\infty}^{\infty} \hat{S}_\lambda^\dagger \hat{S}_\lambda = \hat{1} \otimes \hat{1} \ . \tag{6.6}$$

By adding a third photon mode we can write a unitary operator $\hat{U}$ ($\hat{U} : \mathcal{H}\otimes\mathcal{H}\otimes\mathcal{H} \to \mathcal{H}\otimes\mathcal{H}\otimes\mathcal{H}$) as follows

$$\begin{aligned} \hat{U} &= \sum_{\lambda=-\infty}^{\infty} \hat{S}_\lambda \otimes \hat{S}_\lambda^\dagger \\ &= \sum_{\lambda=-\infty}^{\infty} \sum_{n_1,n_2,m_1,m_2=0}^{\infty} \\ &\quad \delta_{\{m_l\},\{n_l+\lambda\}} |\min\{n_1,m_1\}\rangle\langle\min\{n_2,m_2\}| \otimes |n_2\rangle\langle n_1| \otimes |m_2\rangle\langle m_1| \ . \end{aligned} \tag{6.7}$$

The operator $\hat{U}$ is involutive (i.e. $\hat{U}^2 = 1$) and produces the intertwinning

$$\hat{U}(\hat{e}^{\pm} \otimes \hat{1} \otimes \hat{1})\hat{U} = \hat{1} \otimes \hat{e}^{\pm} \otimes \hat{e}^{\pm} ,$$
$$\hat{U}(\hat{1} \otimes \hat{e}^{\pm} \otimes \hat{e}^{\pm})\hat{U} = \hat{e}^{\pm} \otimes \hat{1} \otimes \hat{1} , \tag{6.8}$$

which corresponds to the Fock representation

$$\hat{U}|l,m,n\rangle = \begin{cases} |m,l,l+n-m\rangle & n \geq m , \\ |m,l-n+m,l\rangle & n \leq m . \end{cases} \tag{6.9}$$

In particular, one has $\hat{U}|l,n,n\rangle = |n,l,l\rangle$, and for the actually interesting case of the second and

$$\hat{U}|n,0,0\rangle = |0,n,n\rangle , \tag{6.10}$$

which is the required duplication. The scheme of the ideal PND is depicted in Fig. 13. In a way analogous to the PNA, which intertwines the one-particle operator $a^\dagger$ with the r-particle operator $b^\dagger_{(r)}$, the PND performs a change between the one-mode operator $a^\dagger$ and the two-mode operator $b^\dagger_{(1,1)}$ given in Table 3, namely

$$b^\dagger_{(1,1)} = b^\dagger c^\dagger \left(\max\{b^\dagger b, c^\dagger c\} + 1\right)^{-1/2} . \tag{6.11}$$

It follows that the Hamiltonian in the Dirac picture is

$$\hat{H}^D_I = -ik\left(a^\dagger b_{(1,1)} - b^\dagger_{(1,1)} a\right) , \tag{6.12}$$

with the same interaction length (5.45). Conservation of energy now requires a classical pump at frequency $\Omega = \omega_a - \omega_b - \omega_c$ — apart from the case of frequency matching $\omega_a = \omega_b + \omega_c$, which preserves the input energy $E = \omega_a l + \omega_b m + \omega_c n$. The device described in the present context is more precisely a PND followed by a FC: in order to keep the frequency constant during the duplication one can choose $\omega_b = \omega_c$ and put a parametric FC on the input mode a.

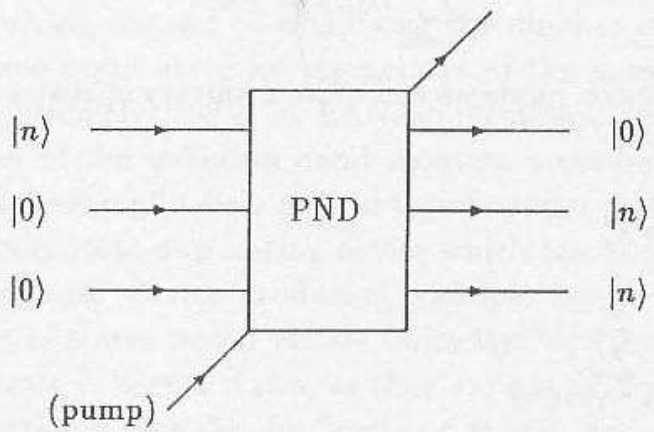

Fig. 13. Scheme of the ideal PND.

6.2. *Phase-squeezed states*

The PND can be used to transform two-mode into one-mode states. In fact, a particular case of the transformations (6.9) is the following

$$\hat{U}|0, n, N+n\rangle = |n, 0, N\rangle \ . \tag{6.13}$$

Equation (6.13) implies that the PNA can transform the states for $\mathbf{k} = (1,1)$ in Eq. (3.69) into those given in Eq. (3.50). In practice, the only interesting case is that of the $SU(1,1)$ states for $N = 0$, as these can be realized (in the parametric approximation) using three- or four-wave mixing from input vacuum states. In this way one obtains the $|\zeta; 1/2\rangle_{SU(1,1)}$ states in Eq. (3.50) ($\kappa = (N+1)/2 = 1/2$) which approximate the SG states (2.16) asymptotically for $\zeta \to 1$. Thus, schematically, the SG states can be obtained using a series made of a high-gain PIA and an ideal PND. The former converts two input vacuum into a pair of twin beams (the $N = 0$ two-mode $SU(1,1)$ states), whereas the latter converts the twin beams into a one-mode SG state. This scheme is depicted in Fig. 14.

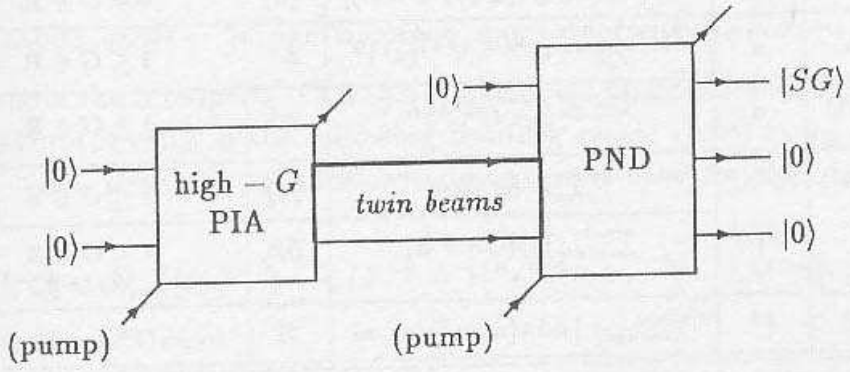

Fig. 14. Ideal scheme of generation of SG states.

The previous scheme is ideal, in that it requires a PND. However, one can get an approximate duplicating device using a conventional four-wave mixer. In such case it turns out that a small downconversion of the twin beams is more effective than a larger one in obtaining an improved-phase state. In fact, a large downconversion would produce undesirable multiple peaks in the phase probability distribution.[76] In practice, to obtain a state having a higher RPL than the customary squeezed state (at the same average energy $\langle \hat{n} \rangle$) one could use a high-gain PIA in series with a low-gain four-wave mixer.

7. Concluding Remarks

In this review article some number-phase squeezing mechanisms have been considered which can be partially handled by analytic methods. It has been shown that the multiphoton and photon fractioning procedures are prototype maps representing ideal photon amplification. All the amplifying maps analyzed in this paper are

unit preserving normal CP maps (see Table 6). This kind of nonunitary evolutions is probably the most general class of amplifying maps and leads to a general description of the quantum amplifier in terms of a three-mode (or six-port) device: one mode is the amplified one, a second mode — the idler — restores unitarity of the map, and the third mode — the pump — accounts for energy conservation. The above description follows from the fact that every CP map has a unitary extension on a larger Hilbert space, where a unitary evolution provides the correct marginal probabilities upon suited choice of the idler-mode state.[77] The photon fractioning and the multiphoton maps have additional interesting properties: the former has unitary extension which is independent of the state of the idler mode, whereas the latter preserves the Newmann-Shannon entropy.

Table 6. Summary of the amplifying maps: $\alpha_G(\hat{O}) = Sum_{\alpha\in I}\hat{V}_\alpha^\dagger \hat{O}\hat{V}_\alpha$. $\hat{O}$ represents the amplified observable/POM.

Device	$\hat{O}$	$\hat{V}_\alpha$	I	Comments
PSA	$\hat{a}_\phi$	$\exp[i \ln G(a_\phi a_{\phi+\pi/2} + \text{h.c.})]$	$\{0\}$	$0 \neq G \in \mathbf{R}$
PIA	a	$\frac{(G^2-1)^{\alpha/2}}{\sqrt{\alpha!}} G^{-(a^\dagger a+1)}(a^\dagger)^\alpha$	$\mathbf{Z}^+$	$1 \leq G \in \mathbf{R}$
BS/FC	a	$\frac{(1-G^2)^{\alpha/2}}{\sqrt{\alpha!}} G^{a^\dagger a} a^\alpha$	$\mathbf{Z}^+$	$1 \geq G \in \mathbf{R}$
PNA	$a^\dagger a$,	$\sum_{n=0}^\infty \lvert Gn\rangle\langle n\rvert$	$\{0\}$	$1 \leq G \in \mathbf{Z}$
	$\Phi(\cdot)$	$\sum_{n=0}^\infty \lvert n\rangle\langle Gn+\alpha\rvert$	$\mathbf{Z}_G$	$1 \leq G \in \mathbf{Z}$ $\alpha_{G^{-1}}(\hat{n}) = [G^{-1}\hat{n}]$
PND	$\hat{e}^\pm$	$\sum_{nm=0}^\infty \lvert \min\{n,m\}\rangle\langle m,n\rvert$	$\mathbf{Z}$	$\alpha_{\text{PND}}(\hat{e}^\pm) = \hat{e}^\pm \otimes \hat{e}^\pm$

The CP-map description naturally connects the quantum amplification process to the quantum measurement process,[78] where the unitary extension represents the measured system interacting with an appropriate apparatus. At present a general theory of the quantum amplification is still lacking, and the above observations seem to give new insight and suggest guidelines for future studies.

Acknowledgment

This work has been supported by the Ministero dell'Università e della Ricerca Scientifica e Tecnologica.

Appendices

A.1. *Abbreviations*

BCH Backer-Campbell-Hausdorff (formula)
CP Completely positive (map)

FC	Frequency converter
GTS	Group theoretical states
LAN	Local area network
LWV	Lowest weight vector
ML	Maximum likelihood
NSS	Number-squeezed states
PIA	Phase-insensitive amplifier
PNA	Photon-number amplifier
PND	Photon-number duplicator
POM	Probability operator-valued measure
PSA	Phase-sensitive amplifier
PSS	Phase-squeezed states
QSS	Quadrature-squeezed states
RPL	Reciprocal peak likelihood
SG	Susskind-Glogower
SNR	Signal-to-noise ratio
UIR	Unitary irreducible representation
WH	Weyl-Heisenberg (group)

A.2. *One-mode states: phase-number asymptotic behaviours*

In this appendix the one-mode GTS (3.54) and their phase-number fluctuations are evaluated asymptotically in the following limiting cases: i) $\langle\hat{n}\rangle = n_0$, $F \to 0, 1, \infty$; ii) $\langle\hat{n}\rangle = F \to \infty$. Hereafter, the following notation is used for the quantum state

$$|n_0; F; \psi\rangle = \mathcal{N}^{-1/2}(F) \sum_{n=0}^{\infty} c_n (F^{-1} - 1)^n e^{in\psi} |n\rangle = \sum_{n=0}^{\infty} d_n e^{in\psi} |n\rangle \ . \tag{A.1}$$

Furthermore, the case of zero ψ is considered, as it affects only the average phase.

• $\langle\hat{n}\rangle = n_0$, $F \to 0$

To the order $\mathcal{O}(F)$, the asymptotic behaviour of the normalization factor of the states (3.54) is

$$\mathcal{N}^{-1/2}(F) \sim F^{n_0/2} \ , \tag{A.2}$$

whereas the coefficients c_n behave as follows

$$c_n \sim \binom{n_0}{n}^{1/2} F^{-n/2} \ . \tag{A.3}$$

From Eqs. (A.2, A.3) the asymptotic state is obtained (n_0 integer)

$$|n_0; F; 0\rangle = |n_0\rangle + (n_0 F)^{1/2} |n_0 - 1\rangle + \mathcal{O}(F) \ , \tag{A.4}$$

having a sum of the coefficients d_n

$$\sum_{n=0}^{\infty} |d_n| \sim 1 + (n_0 F)^{1/2} = 1 + \delta n \ , \tag{A.5}$$

and corresponding to the peak likelihood $\delta\phi$

$$\delta\phi = 2\pi \left[\sum_{n=0}^{\infty} |d_n|\right]^{-2} \sim 2\pi(1 - 2\delta n) \,. \tag{A.6}$$

• $\langle \hat{n} \rangle = n_0, \; F \to 1$
The asymptotic normalization factor is (to the order $\mathcal{O}((1-F)^2)$)

$$\mathcal{N}^{-1/2}(F) \sim e^{-n_0/2} \left[1 - \frac{n_0}{4}(1-F)\right] \,. \tag{A.7}$$

Using the following expansion for the binomial coefficients ($x \gg 1$)

$$\binom{x}{n} = \frac{x^n}{n!} \left\{1 - x^{-1}\binom{n}{2} + x^{-2}\left[3\binom{n}{4} + 2\binom{n}{3}\right] + \mathcal{O}(x^{-3})\right\} \tag{A.8}$$

one obtains the asymptotic behaviour

$$c_n \sim \frac{n_0^{n/2}}{\sqrt{n!}} \left[1 - \frac{1}{2}\left(\frac{n(n-1)}{2n_0} - n\right)(1-F)\right] \,. \tag{A.9}$$

After multiplying by the normalization factor one has

$$d_n \sim e^{-\frac{n_0}{2}} \frac{n_0^{n/2}}{\sqrt{n!}} \left[1 - \frac{1}{2}\left(\frac{n_0}{2} + \frac{n(n-1)}{2n_0} - n\right)(1-F)\right] \,. \tag{A.10}$$

The sum of the coefficients d_n is

$$\sum_{n=0}^{\infty} |d_n| \sim \Delta(n_0) \left[1 - \frac{1}{4}(1-F)\right] \,, \tag{A.11}$$

where the function $\Delta(x)$ is defined as

$$\Delta(x) = e^{-x/2} \sum_{n=0}^{\infty} \frac{x^{n/2}}{\sqrt{n!}} \,. \tag{A.12}$$

Using the Gaussian approximation for the Poisson distribution one has

$$\Delta(x) \sim (2\pi x)^{-1/4} \int_{-\infty}^{+\infty} dy e^{-\frac{(y-x)}{4x}} = \sqrt{2}(2\pi x)^{1/4} \,, \tag{A.13}$$

which allows to rewrite (A.11) for large n_0 as

$$\sum_{n=0}^{\infty} |d_n| \sim \sqrt{2}(2\pi n_0)^{1/4} \left[1 - \frac{1}{4}(1-F)\right] \,. \tag{A.14}$$

The peak likelihood $\delta\phi$ reads

$$\delta\phi \sim \sqrt{\frac{\pi}{2}} n_0^{-1/2} \left[1 + \frac{1}{2}(1-F)\right] \,. \tag{A.15}$$

The number fluctuations δn are approximated to the same order in $(1-F)$ in the following way

$$\delta n = F^{1/2} n_0^{1/2} \sim n_0^{1/2} \left[1 - \frac{1}{2}(1-F)\right] , \tag{A.16}$$

leading to the uncertainty product

$$\delta n \delta\phi \sim \sqrt{\frac{\pi}{2}} . \tag{A.17}$$

• $\langle \hat{n} \rangle = n_0, \ F \to \infty$

In this case, the asymptotic states are obtained using the following approximation for the binomial coefficients ($x \ll 1$)

$$\binom{x+n-1}{n} \begin{cases} \frac{x}{n} + \mathcal{O}(x^2) & n \geq 1 , \\ 1 & n = 0 . \end{cases} \tag{A.18}$$

Equation (A.18) leads to the asymptotic state

$$|n_0; F; 0\rangle \sim F^{-\frac{n_0}{2F}} \left[|0\rangle + \sqrt{\frac{n_0}{F}} \sum_{n=1}^{\infty} \frac{\left(1 - F^{-1}\right)^{n/2}}{\sqrt{n}} |n\rangle\right] , \tag{A.19}$$

which has the following sum of coefficients

$$\sum_{n=0}^{\infty} |d_n| \sim F^{-\frac{n_0}{2F}} \left[1 + \sqrt{\frac{n_0}{F}}(1 - F^{-1}) \phi((1-F^{-1})^{1/2}, 1/2, 1)\right] , \tag{A.20}$$

where the function $\phi(z, s, v)$ is defined as follows[79]

$$\phi(z, s, v) = \sum_{n=0}^{\infty} (v+n)^{-s} z^n , \qquad |z| < 1 , v \neq 0, -1, \ldots . \tag{A.21}$$

Using the limit

$$\lim_{z \to 1} (1-z)^{1-s} \phi(z, s, v) = \Gamma(1-s) , \tag{A.22}$$

$\Gamma(x)$ being the usual gamma-function, one has

$$\sum_{n=0}^{\infty} |d_n| \sim F^{-\frac{n_0}{2F}} \left[1 + \sqrt{2\pi n_0}(1 - F^{-1})\right] \sim \begin{cases} F^{-\frac{n_0}{2F}} & n_0 \ll 1 , \\ \sqrt{2\pi n_0} F^{-\frac{n_0}{2F}} & n_0 \gg 1 . \end{cases} \tag{A.23}$$

Equation (A.23) leads to the peak likelihood $\delta\phi$

$$\delta\phi \sim \begin{cases} 2\pi & n_0 \ll 1 , \\ n_0^{-1} & n_0 \gg 1 . \end{cases} \tag{A.24}$$

• $\langle \hat{n} \rangle = F \to \infty$
the normalization factor behaves asymptotically as follows

$$\mathcal{N}^{-1/2}(F) \sim F^{-1/2} , \tag{A.25}$$

whereas the state coefficients become

$$c_n = \sqrt{\binom{\frac{n_0}{1-F}}{n} (F^{-1}-1)^n} \sim \left(1 - F^{-1}\right)^{n/2} . \tag{A.26}$$

In Eq. (A.26) the following identity has been used

$$\binom{-\alpha}{n} = (-)^n \binom{\alpha + n - 1}{n} , \tag{A.27}$$

which gives

$$\lim_{F\to\infty} \binom{\frac{n_0}{1-F}}{n} = \binom{n}{n} = 1 . \tag{A.28}$$

The asymptotic state is obtained

$$|F; F; 0\rangle \sim F^{-1/2} \sum_{n=0}^{\infty} \left(1 - F^{-1}\right)^{n/2} |n\rangle . \tag{A.29}$$

For the state (A.29) it is possible to evaluate analytically the probability distribution of the phase. Taking the scalar product between the state (A.29) and the SG state

$$|e^{i\phi}\rangle = \sum_{n=0}^{\infty} e^{in\phi} |n\rangle , \tag{A.30}$$

one obtains the probability distribution

$$P(\phi) = \frac{1}{2\pi} |\langle e^{i\phi} | F; F; 0\rangle|^2 \simeq \frac{F^{-1}}{2\pi} \left(1 - 2\sqrt{1 - F^{-1}} \cos(\phi) + 1 - F^{-1}\right)^{-1} , \tag{A.31}$$

which has the peak likelihood $\delta\phi$

$$\delta\phi \simeq \pi F^{-1} \equiv \pi n_0^{-1} . \tag{A.32}$$

References

1. H. P. Yuen and J. H. Shapiro, *IEEE Trans. Info. Theory* **24**, 657 (1978); **IT-25** 197 (1979); **IT-26**, 78 (1980).
2. K. S. Thorne, *Rev. Mod. Phys.* **52**, 285 (1980); see also *Physics Today* **39**, 17 (Feb. 1986).
3. *Quantum Aspects of Optical Communications*, Lecture Notes in Physics 378, ed. C. Bendjaballah, O. Hirota and S. Reynaud, (Springer, 1991).

4. *Squeezed States of the Electromagnetic Field*, ed. H. J. Kimble and D. Walls, *J. Opt. Soc.* **B4** (1987) (special issue).
5. *Squeezed Light*, ed. R. Loudon and P. L. Knight, *J. Mod. Opt.* **34** (1987) (special issue).
6. *Squeezed and Nonclassical Light*, ed. P. Tombesi and E. R. Pike (Plenum, New York, 1989).
7. C. W. Helstrom, *Quantum Detection and Estimation Theory* (Academic Press, New York, 1976).
8. H. P. Yuen, *Phys. Lett.* **51A**, 1 (1975).
9. H. P. Yuen, *Phys. Rev.* **A13**, 2226 (1976).
10. H. P. Yuen, in *Quantum Optics, Experimental Gravitation and Measurement Theory*, ed. P. Meystre and M. O. Scully (Plenum, New York 1983), p.249.
11. P. Carruthers and M. M. Nieto, *Phys. Rev. Lett.* **14**, 387 (1965).
12. R. Jackiw, *J. Math. Phys.* **9**, 339 (1968).
13. Y. Yamamoto, N. Imoto and S. Machida, *Phys. Rev.* **A33**, 3243 (1986).
14. Y. Yamamoto, S. Machida, N. Imoto, M. Kitagawa, and G. Björk, *J. Opt. Soc. Am.* **B4**, 1645 (1987).
15. Y. Yamamoto and H. A. Haus, *Rev. Mod. Phys.* **58**, 1001 (1986).
16. H. P. Yuen, in Ref. 3, p. 333.
17. W. K. Wootters and W. H. Zurek, *Nature* **299**, 802 (1982).
18. A. Hasegawa, *Optical Solitons in Fibers* (Springer-Verlag, 1990).
19. J. H. Shapiro, S. R. Shepard and N. C. Wong, *Phys. Rev. Lett.* **62**, 2377 (1989).
20. R. S. Bondurant and J. H. Shapiro, *Phys. Rev.* **A30**, 2548 (1984).
21. C. M. Caves, *Phys. Rev.* **D23**, 1693 (1981).
22. G. A. Sanders, N. G. Prentiss and S. Ezekiel, *Opt. Lett.* **6**, 569 (1981).
23. K. Kraus, *States, Effects and Operations*, Lecture Notes in Physics 190 (Springer 1983).
24. G. Lindblad, in Ref. 3, p. 71.
25. H. P. Yuen, *Phys. Rev. Lett.* **56**, 2176 (1986).
26. H. P. Yuen, *Phys. Lett.* **A113**, 405 (1986).
27. H. P. Yuen, *Opt. Lett.* **12**, 789 (1987).
28. R. A. Campos, B. E. Saleh and M. C. Teich, *Phys. Rev.* **A40**, 1371 (1989).
29. F. Singer, R. A. Campos, M. C. Teich, and B. E. A. Saleh, *Quantum Optics* **2** 307 (1990).
30. G. D'Ariano, in Ref. 3, p. 325.
31. G. D'Ariano, *Nuovo Cimento B* (1992) (in press).
32. G. D'Ariano, *Phys. Rev.* **D32**, 1034 (1985).
33. J. Katriel, A. Solomon, G. D'Ariano, and M. Rasetti, *Phys. Rev.* **D34**, 2332.
34. G. D'Ariano and M. Rasetti, *Phys. Rev.* **D35**, 1239 (1987).
35. G. D'Ariano, S. Morosi, M. Rasetti, J. Katriel, and A. Solomon, *Phys. Rev.* **D36**, 2399 (1987).
36. J. Katriel, A. Solomon, G. D'Ariano, and M. Rasetti, in Ref. 4, p. 1728.
37. G. D'Ariano, M. Rasetti, J. Katriel, and A. Solomon, in Ref. 6, p. 301.
38. R. A. Fisher, M. M. Nieto and V. D. Sandberg, *Phys. Rev.* **D29**, 110 (1984).
39. S. L. Braunstein and R. I. Mc Lachlan, *Phys. Rev.* **A35**, 1659 (1987).
40. G. D'Ariano, *Phys. Rev.* **A41**, 5239 (1990).
41. R. A. Brandt and O. W. Greenberg. *J. Math. Phys.* **10**, 1168 (1969).
42. T. Holstein and H. Primakoff, *Phys. Rev.* **58**, 1048 (1940).
43. J. Katriel, M. Rasetti and A. Solomon, *Phys. Rev.* **D35**, 1248 (1987).
44. G. D'Ariano and N. Sterpi, *Phys. Rev.* **A39**, 1860 (1989).

45. G. D'Ariano, *Phys. Rev.* **A41**, 2636 (1990).
46. G. D'Ariano, *Phys. Rev.* **A43**, 2550 (1991).
47. G. D'Ariano, in *1990 EPS Conference on Optics, Optical Systems and Applications Inst. Phys. Conf. Ser.* No. 115 (IOP, 1991), p. 73.
48. G. D'Ariano, in *Squeezed States and Uncertainty Relations*, ed. D. Han, J. S. Kim and W. W. Zachary, NASA CP (1991) (in press).
49. G. D'Ariano, *Phys. Rev. A* (1992) (in press).
50. P. A. M. Dirac, *Proc. R. Soc. London* **A114**, 243 (1927).
51. R. Loudon, *The Quantum Theory of Light* (Clarendon Press, Oxford, 1983).
52. L. Susskind and J. Glogower, *Physics* **1**, 49 (1964).
53. A. S. Holevo, *Probabilistic and Statistical Aspects of Quantum Theory* (North-Holland Amsterdam, 1982).
54. D. T. Pegg and S. M. Barnett. *Europhys. Lett.* **6** 483 (1988).
55. M. J. W. Hall, *Quantum Opt.* **3**. 7 (1991).
56. C. W. H. Helstrom, *Int. J. Theor. Phys.* **11**, 357 (1974).
57. M. Ozawa, "Operator algebras and nonstandard analysis" in *Current Topics in Operator Algebras*, ed. H. Araki *et al.* (World Scientific, 1991), p. 52.
58. R. J. Glauber, *Phys. Rev.* **131**, 2766 (1963); *Phys. Rev. Lett.* **10**, 84 (1963).
59. J. V. Schwinger, in *Quantum Theory of Angular Momentum*, ed. L. C. Biedernharn and H. Van Dom (Academic, New York, 1965).
60. J. C. Katriel and D. G. Hummer, *J. Phys.* **A14** 1211. (1981)
61. R. Loudon and P. L. Knight, *J. Mod. Opt.* **34**, 709 (1987); B. L. Schumaker, *Phys. Rep.* **135**, 317 (1986); C. M. Caves and B. L. Schumaker, *Phys. Rev.* **A31**, 3068 (1985); K. Wodkiewicz and J. H. Eberly, *J. Opt. Soc. Am.* **B2**, 458 (1985).
62. V. Buzěk and T. Quang, *J. Opt. Soc. Am.* **B6**, 2447 (1989).
63. M. Reed and B. Simon, *Methods of Modern Mathematical Physics*, Vol. 2, *Fourier Analysis, Self-Adjointness* (Academic, New York, 1975).
64. G. D'Ariano, M. Rasetti and M. Vadacchino, *J. Phys.* **A18**, 1295 (1985).
65. P. Tombesi and A. Mecozzi, *Phys. Rev.* **A37**, 4778 (1988).
66. A. M. Perelomov, *Commun. Math. Phys.* **26**, 222 (1972); for a review on the subject see A. Perelomov, *Generalized Coherent States and Their Applications* (Springer Verlag, 1986).
67. M. Rasetti, *Int. J. Theor. Phys.* **13**, 425 (1973); **14**, 1 (1975).
68. A. Cavalli, G. D'Ariano and L. Michel, *Ann. Ist. Poincaré - Phys. Theor.* **44**, 173 (1986).
69. J. Katriel, M. Rasetti and A. I. Solomon, *Phys. Rev.* **D35**, 2601 (1987).
70. W. P. Schleich, J. P. Dowling and R. J. Horowicz, *Phys. Rev.* **A44**, 3365 (1991).
71. Ts. Gantsog and R. Tanaś, *Phys. Lett.* **A157**, 330 (1991).
72. H. P. Yuen, *Phys. Lett.* **A91**, 101 (1982).
73. E. Arthurs and M. S. Goodman, *Phys. Rev. Lett.* **60**, 2447 (1988).
74. W. F. Stinespring, *Proc. Amer. Math. Soc.* **6**, 211 (1955).
75. E. B. Davies, *Quantum Theory of Open Systems* (Academic Press, 1976).
76. G. M. D'Ariano (unpublished).
77. G. M. D'Ariano and M. Ozawa (unpublished).
78. A. S. Holevo, in Ref. 3, p. 127.
79. I. S. Gradshteyn and I. M. Ryzhik, *Table of Integrals, Series, and Products* (Academic Press, New York 1980).